FUNCTIONAL GENOMICS BASED INTERROGATION OF CELL-FATE DETERMINATION PATHWAYS

APPROVED BY SUPERVISORY COMMITTEE

Lawrence Lum, Ph.D.

Ondine Cleaver, Ph.D.

Eric Olson, Ph.D.

John Abrams, Ph.D.

DEDICATION

To my parents

FUNCTIONAL GENOMICS BASED INTERROGATION OF CELL-FATE DETERMINATION PATHWAYS

by

LENI SUSAN JACOB

DISSERTATION

Presented to the Faculty of the Graduate School of Biomedical Sciences

The University of Texas Southwestern Medical Center at Dallas

In Partial Fulfillment of the Requirements

For the Degree of

DOCTOR OF PHILOSOPHY

The University of Texas Southwestern Medical Center at Dallas

Dallas, Texas

March, 2011

ACKNOWLEDGEMENTS

I must begin by expressing my sincere gratitude to my mentor, Dr. Lawrence Lum. His never waning enthusiasm for scientific discovery is an inspiration. I am truly grateful for the patience, encouragement, guidance, and support that he has provided to me throughout my tenure in his lab.

I would also like to thank the members of my thesis committee, Dr. Ondine Cleaver, Dr. John Abrams, and Dr. Eric Olson, for their mentorship and encouragement.

I offer my appreciation to all the members of the Lum lab, past and present, for their support and friendship. I am especially grateful for the scientific partnership of Dr. Xiaofeng Wu. I must also thank Dr. Wei Tang and Dr. Baozhi Chen for technical instruction and helpful discussions that have contributed to my success.

I have been fortunate to benefit from the generous and collaborative nature of the UT Southwestern community as well as the signal transduction community at large. I am indebted to Dr. James Amatruda, the members of the Amatruda lab, Dr. Thomas Carroll, Dr. Lily Huang, Dr. Kate Luby-Phelps, Dr. Brian Perkins, Dr. Christopher Gilpin, and the members of the Molecular and Cellular Imaging Facility for their collaboration and kind advice. I would also like to thank Drs. Jerry Shay, Diego Castrillon, John Minna, Eric Olson, Massimo Attanasio, Chuo Chen, Nabeel Bardeesy, Jynho Kim, Philip Beachy, Baolin Wang, Aimin Liu, Lawrence Kirschner, Ralph Mazitschek, Stuart Schreiber, Suzie Scales, and members of UT Southwestern High Throughput Screening facility for their generous supply of reagents and access to equipment.

Finally, I would like to thank my family. I am blessed to have the unconditional love and support of my parents, Koshy and Achakutty Jacob, and the encouragement and friendship of my brother, Jeffry Jacob. It would have been impossible to have completed this journey without their unwavering support and belief in me.

FUNCTIONAL GENOMICS BASED INTERROGATION OF CELL-FATE DETERMINATION PATHWAYS

Leni S. Jacob, Ph.D.

The University of Texas Southwestern Medical Center at Dallas, 2011

Supervising Professor: Lawrence Lum, Ph.D.

The Hedgehog (Hh) and Wnt signal transduction pathways are master regulators of embryogenesis and tissue renewal and represent anticancer therapeutic targets. Using genome-wide RNA interference screening in murine cultured cells, I established previously unknown associations between these signaling pathways and genes linked to developmental malformations, diseases of premature tissue degeneration, and cancer. I identified functions in both pathways for the multitasking kinase Stk11 (also known as Lkb1), a tumor suppressor implicated in lung and cervical cancers. Stk11 loss resulted in

disassembly of the primary cilium, a cellular organizing center for Hh pathway components, thus dampening Hh signaling. Loss of Stk11 also induced aberrant signaling through the Wnt pathway. Chemicals that targeted the Wnt acyltransferase Porcupine or that restored primary cilia length by inhibiting the tubulin deacetylase HDAC6 (histone deacetylase 6) countered deviant pathway activities driven by Stk11 loss. My study demonstrates that Stk11 is a critical mediator in both the Hh and the Wnt pathways, and that functional genomics based approaches to dissect cell-fate determination pathways may support the development of targeted therapeutic strategies.

TABLE OF CONTENTS

PRIOR PUBLICATIONS

1. **Jacob LS**, Wu X, Dodge ME, Fan CW, Kulak O, Chen B, Tang W, Wang B, Amatruda JF, Lum L. (2011). Genome-Wide RNAi Screen Reveals Disease-Associated Genes That Are Common to Hedgehog and Wnt Signaling. *Sci Signal* 4, ra4.

2. **Jacob L**, and Lum L. (2007). Deconstructing the hedgehog pathway in development and disease. *Science* 318, 66-68.

3. **Jacob L**, and Lum L. (2007). Hedgehog signaling pathway. *Sci STKE* 2007, cm6.

4. **Jacob L**, and Lum L. (2007). Hedgehog signaling pathway in Drosophila. *Sci STKE* 2007, cm7.

5. Muzny DM, Scherer SE, Kaul R, Wang J, Yu J, Sudbrak R, Buhay CJ, Chen R, Cree A, Ding Y, Dugan-Rocha S, Gill R, Gunaratne P, Harris RA, Hawes AC, Hernandez J, Hodgson AV, Hume J, Jackson A, Khan ZM, Kovar-Smith C, Lewis LR, Lozado RJ, Metzker ML, Milosavljevic A, Miner GR, Morgan MB, Nazareth LV, Scott G, Sodergren E, Song XZ, Steffen D, Wei S, Wheeler DA, Wright MW, Worley KC, Yuan Y, Zhang Z, Adams CQ, Ansari-Lari MA, Ayele M, Brown MJ, Chen G, Chen Z, Clendenning J, Clerc-Blankenburg KP, Chen R, Chen Z, Davis C, Delgado O, Dinh HH, Dong W, Draper H, Ernst S, Fu G, Gonzalez-Garay ML, Garcia DK, Gillett W, Gu J, Hao B, Haugen E, Havlak P, He X, Hennig S, Hu S, Huang W, Jackson LR, **Jacob LS**, Kelly SH, Kube M, Levy R, Li Z, Liu B, Liu J, Liu W, Lu J, Maheshwari M, Nguyen BV, Okwuonu GO, Palmeiri A, Pasternak S, Perez LM, Phelps KA, Plopper FJ, Qiang B, Raymond C, Rodriguez R, Saenphimmachak C, Santibanez J, Shen H, Shen Y, Subramanian S, Tabor PE, Verduzco D, Waldron L, Wang J, Wang J, Wang Q, Williams GA, Wong GK, Yao Z, Zhang J, Zhang X, Zhao G, Zhou J, Zhou Y, Nelson D, Lehrach H, Reinhardt R, Naylor SL, Yang H, Olson M, Weinstock G, Gibbs RA. (2006). The DNA sequence, annotation and analysis of human chromosome 3. *Nature* 440, 1194-1198.

6. Scherer SE, Muzny DM, Buhay CJ, Chen R, Cree A, Ding Y, Dugan-Rocha S, Gill R, Gunaratne P, Harris RA, Hawes AC, Hernandez J, Hodgson AV, Hume J, Jackson A, Khan ZM, Kovar-Smith C, Lewis LR, Lozado RJ, Metzker ML, Milosavljevic A, Miner GR, Montgomery KT, Morgan MB, Nazareth LV, Scott G, Sodergren E, Song XZ, Steffen D, Lovering RC, Wheeler DA, Worley KC, Yuan Y, Zhang Z, Adams CQ, Ansari-Lari MA, Ayele M, Brown MJ, Chen G, Chen Z, Clerc-Blankenburg KP, Davis C, Delgado O, Dinh HH, Draper H, Gonzalez-Garay ML, Havlak P, Jackson LR, **Jacob LS**, Kelly SH, Li L, Li Z, Liu J, Liu W, Lu J, Maheshwari M, Nguyen BV, Okwuonu GO, Pasternak S, Perez LM, Plopper FJ, Santibanez J, Shen H, Tabor PE, Verduzco D, Waldron L, Wang Q, Williams GA, Zhang J, Zhou J, Allen CC, Amin AG, Anyalebechi V, Bailey M, Barbaria JA, Bimage KE, Bryant NP, Burch PE,

Burkett CE, Burrell KL, Calderon E, Cardenas V, Carter K, Casias K, Cavazos I, Cavazos SR, Ceasar H, Chacko J, Chan SN, Chavez D, Christopoulos C, Chu J, Cockrell R, Cox CD, Dang M, Dathorne SR, David R, Davis CM, Davy-Carroll L, Deshazo DR, Donlin JE, D'Souza L, Eaves KA, Egan A, Emery-Cohen AJ, Escotto M, Flagg N, Forbes LD, Gabisi AM, Garza M, Hamilton C, Henderson N, Hernandez O, Hines S, Hogues ME, Huang M, Idlebird DG, Johnson R, Jolivet A, Jones S, Kagan R, King LM, Leal B, Lebow H, Lee S, LeVan JM, Lewis LC, London P, Lorensuhewa LM, Loulseged H, Lovett DA, Lucier A, Lucier RL, Ma J, Madu RC, Mapua P, Martindale AD, Martinez E, Massey E, Mawhiney S, Meador MG, Mendez S, Mercado C, Mercado IC, Merritt CE, Miner ZL, Minja E, Mitchell T, Mohabbat F, Mohabbat K, Montgomery B, Moore N, Morris S, Munidasa M, Ngo RN, Nguyen NB, Nickerson E, Nwaokelemeh OO, Nwokenkwo S, Obregon M, Oguh M, Oragunye N, Oviedo RJ, Parish BJ, Parker DN, Parrish J, Parks KL, Paul HA, Payton BA, Perez A, Perrin W, Pickens A, Primus EL, Pu LL, Puazo M, Quiles MM, Quiroz JB, Rabata D, Reeves K, Ruiz SJ, Shao H, Sisson I, Sonaike T, Sorelle RP, Sutton AE, Svatek AF, Svetz LA, Tamerisa KS, Taylor TR, Teague B, Thomas N, Thorn RD, Trejos ZY, Trevino BK, Ukegbu ON, Urban JB, Vasquez LI, Vera VA, Villasana DM, Wang L, Ward-Moore S, Warren JT, Wei X, White F, Williamson AL, Wleczyk R, Wooden HS, Wooden SH, Yen J, Yoon L, Yoon V, Zorrilla SE, Nelson D, Kucherlapati R, Weinstock G, Gibbs RA; Baylor College of Medicine Human Genome Sequencing Center Sequence Production Team. (2006). The finished DNA sequence of human chromosome 12. *Nature* 440, 346-351.

7. Ross MT, Grafham DV, Coffey AJ, Scherer S, McLay K, Muzny D, Platzer M, Howell GR, Burrows C, Bird CP, Frankish A, Lovell FL, Howe KL, Ashurst JL, Fulton RS, Sudbrak R, Wen G, Jones MC, Hurles ME, Andrews TD, Scott CE, Searle S, Ramser J, Whittaker A, Deadman R, Carter NP, Hunt SE, Chen R, Cree A, Gunaratne P, Havlak P, Hodgson A, Metzker ML, Richards S, Scott G, Steffen D, Sodergren E, Wheeler DA, Worley KC, Ainscough R, Ambrose KD, Ansari-Lari MA, Aradhya S, Ashwell RI, Babbage AK, Bagguley CL, Ballabio A, Banerjee R, Barker GE, Barlow KF, Barrett IP, Bates KN, Beare DM, Beasley H, Beasley O, Beck A, Bethel G, Blechschmidt K, Brady N, Bray-Allen S, Bridgeman AM, Brown AJ, Brown MJ, Bonnin D, Bruford EA, Buhay C, Burch P, Burford D, Burgess J, Burrill W, Burton J, Bye JM, Carder C, Carrel L, Chako J, Chapman JC, Chavez D, Chen E, Chen G, Chen Y, Chen Z, Chinault C, Ciccodicola A, Clark SY, Clarke G, Clee CM, Clegg S, Clerc-Blankenburg K, Clifford K, Cobley V, Cole CG, Conquer JS, Corby N, Connor RE, David R, Davies J, Davis C, Davis J, Delgado O, Deshazo D, Dhami P, Ding Y, Dinh H, Dodsworth S, Draper H, Dugan-Rocha S, Dunham A, Dunn M, Durbin KJ, Dutta I, Eades T, Ellwood M, Emery-Cohen A, Errington H, Evans KL, Faulkner L, Francis F, Frankland J, Fraser AE, Galgoczy P, Gilbert J, Gill R, Glöckner G, Gregory SG, Gribble S, Griffiths C, Grocock R, Gu Y, Gwilliam R, Hamilton C, Hart EA, Hawes A, Heath PD, Heitmann K, Hennig S, Hernandez J, Hinzmann B, Ho S, Hoffs M, Howden PJ, Huckle EJ, Hume J, Hunt PJ, Hunt AR, Isherwood J, **Jacob L**, Johnson D, Jones S, de Jong PJ, Joseph SS, Keenan S, Kelly S, Kershaw JK, Khan Z, Kioschis P, Klages S, Knights AJ, Kosiura A, Kovar-Smith C,

Laird GK, Langford C, Lawlor S, Leversha M, Lewis L, Liu W, Lloyd C, Lloyd DM, Loulseged H, Loveland JE, Lovell JD, Lozado R, Lu J, Lyne R, Ma J, Maheshwari M, Matthews LH, McDowall J, McLaren S, McMurray A, Meidl P, Meitinger T, Milne S, Miner G, Mistry SL, Morgan M, Morris S, Müller I, Mullikin JC, Nguyen N, Nordsiek G, Nyakatura G, O'Dell CN, Okwuonu G, Palmer S, Pandian R, Parker D, Parrish J, Pasternak S, Patel D, Pearce AV, Pearson DM, Pelan SE, Perez L, Porter KM, Ramsey Y, Reichwald K, Rhodes S, Ridler KA, Schlessinger D, Schueler MG, Sehra HK, Shaw-Smith C, Shen H, Sheridan EM, Shownkeen R, Skuce CD, Smith ML, Sotheran EC, Steingruber HE, Steward CA, Storey R, Swann RM, Swarbreck D, Tabor PE, Taudien S, Taylor T, Teague B, Thomas K, Thorpe A, Timms K, Tracey A, Trevanion S, Tromans AC, d'Urso M, Verduzco D, Villasana D, Waldron L, Wall M, Wang Q, Warren J, Warry GL, Wei X, West A, Whitehead SL, Whiteley MN, Wilkinson JE, Willey DL, Williams G, Williams L, Williamson A, Williamson H, Wilming L, Woodmansey RL, Wray PW, Yen J, Zhang J, Zhou J, Zoghbi H, Zorilla S, Buck D, Reinhardt R, Poustka A, Rosenthal A, Lehrach H, Meindl A, Minx PJ, Hillier LW, Willard HF, Wilson RK, Waterston RH, Rice CM, Vaudin M, Coulson A, Nelson DL, Weinstock G, Sulston JE, Durbin R, Hubbard T, Gibbs RA, Beck S, Rogers J, Bentley DR.. (2005). The DNA sequence of the human X chromosome. *Nature* 434, 325-337.

8. McLeod MP, Qin X, Karpathy SE, Gioia J, Highlander SK, Fox GE, McNeill TZ, Jiang H, Muzny D, **Jacob LS**, Hawes AC, Sodergren E, Gill R, Hume J, Morgan M, Fan G, Amin AG, Gibbs RA, Hong C, Yu XJ, Walker DH, Weinstock GM. (2004). Complete genome sequence of *Rickettsia typhi* and comparison with sequences of other rickettsiae. *J Bacteriol* 186, 5842-5855.

LIST OF FIGURES

LIST OF TABLES

LIST OF APPENDICES

LIST OF ABBREVIATIONS

Aaas - Achalasia, adrenocortical insufficiency, alacrimia syndrome

ACC - Acetyl-coA carboxylase

Ac-Tub - Acetylated tubulin

Ago - Argonaute

APC - Adenomatous polyposis coli

Arl13b - ADP-ribosylation factor-like 13B

ATP - Adenosine-5'-triphosphate

α-tub - Alpha tubulin

Aurka - Aurora Kinase A

BTG1 - B-cell translocation gene 1

cDNA - Complementary deoxyribonucleic acid

CDO - Cell adhesion molecule–related/down-regulated by oncogenes

Ci - Cubitus interruptus

CiFL - Cubitus interruptus full length

CiR - Cubitus interruptus repressor

CK1a - casein kinase 1a

CM - Conditioned media

Cmpd - Compound

c-Myc - Myelocytomatosis oncogene

CNOT3 - CCR4-NOT transcription complex, subunit 3

Cos2 - Costal 2

Ctrl - Control

DAG - Diacylglycerol

DAPI - 4',6-diamidino-2-phenylindole

Dgkq - Diacylglyerol kinase theta

Dhh - Desert Hedgehog

Disp - Dispatched

Dlp - Dally-like

DMSO - Dimethyl sulfoxide

DNA - Deoxyribonucleic acid

Dnchc2 - Dynein cytoplasmic heavy chain 2

dsRNA - Double stranded ribonucleic acid

Dvl - Dishevelled

Dyrk1B - Dual-specificity tyrosine-(Y)-phosphorylation regulated kinase 1B

Dyrk2 - Dual-specificity tyrosine-(Y)-phosphorylation regulated kinase 2

E2F1 - E2F transcription factor 1

EIPA - 5-(N-ethyl-n-isopropyl)-amiloride

Endo - Endometrial cells

Eng1a - Engrailed 1a

ENU - N-ethyl-N-nitrosourea

esiRNA - Endoribonuclease-prepared siRNA

FL - Firefly luciferase

Fu - Fused

Fuz - Fuzzy

Fz - Frizzled

Gapdh - Glyceraldehyde-3-phosphate dehydrogenase

GFP - Green fluorescent protein

Gli1 - GLI-Kruppel family member 1

Gli2 - GLI-Kruppel family member 2

Gli3 - GLI-Kruppel family member 3

Gli3R - GLI-Kruppel family member 3 repressor

GliBS - Gli binding site

GliFL - Full length GLI-Kruppel family member 3

GPC1 - Glypican 1

GPI - Glycosyl phosphatidylinositol

GSK3b - glycogen synthase kinase 3b

HBEC - Human bronchial epithelial cells

HDAC 6 - Histone deacetylase 6

HDAC1 - Histone deacetylase 1

Hh - Hedgehog

HhN - N-terminal Hedgehog precursor

hpf - Hours post fertilization

IFT122 - Intraflagellar transport protein 122

IFT57 - Intraflagellar transport protein 57

IFT88 - Intraflagellar transport protein 88

Ihh - Indian Hedgehog

Ihog - Interference hog

Int1 - Integration1

IWP - Inhibitor of Wnt production

IWR - Inhibitor of Wnt response

KD - Kinase dead

Kif11 - Kinesin family member 11

Kif3A - Kinesin family member 3A

LEF - Lymphocyte enhancement factor

LKB1 - Liver Kinase B1 (Stk11)

LRP - Low-density lipoprotein related protein

MBOAT - membrane-bound O-acyltransferase

Med14 - Mediator complex subunit 14

MEF - Mouse embryonic fibroblast

Mef2C - Myocyte enhancer factor 2C

miRNA - Micro ribonucleic acid

MO - Morpholino oligonucleotide

Morph - Morpholino oligonucleotide

mRNA - Messenger ribonucleic acid

MSX1 - Msh homeobox 1

mTOR - Mechanistic target of rapamycin

MyoD - myogenic differentiation 1

Nedd9 - Neural precursor cell expressed, developmentally down-regulated 9

NFATC2 - Nuclear factor of activated T-cells, cytoplasmic, calcineurin-dependent 2

NSCLC - non-small cell lung cancer

OEX - Overexpression

OMIM - Online Mendelian Inheritance in Man database

PA - Phosphatidic acid

PCR - Polymerase Chain Reaction

PKA - Protein Kinase A

Porcn - Porcupine

Prkar1a - Protein kinase, cAMP-dependent, regulatory, type I, alpha

Prkcc - Protein kinase C

Ptc - Patched

Ptch1 - Patched 1 *Drosophila* homolog

qPCR - Quantitative polymerase chain reaction

RISC - RNA-induced silencing complex

RL - *Renilla* Luciferase

Rlbp1 - Retinaldehyde binding protein 1

RLU - Relative light units

RNA - Ribonucleic acid

RNAi - Ribonucleic acid interference

RNase - Ribonuclease

RT-PCR - Reverse transcription polymerase chain reaction

SAG - Smoothened Agonist

SAHA - Suberoylanilide hydroxamic acid

SANT1 - Smo Antagonist

SD - Standard deviation

Shh - Sonic Hedgehog

ShhN - N-terminal Sonic Hedgehog signaling domain lacking cholesterol modification

shRNA - Short-hairpin ribonucleic acid

siRNA - Short interfering ribonucleic acid

SLC9A1 - Solute carrier 9A1

SLC9A5 - Solute carrier 9A5

SLC9A7 - Solute carrier 9A7

SLC9A8 - Solute carrier 9A8

Slmb - Slimb

SMAD7 - SMAD family member 7

Smo - Smoothened

SSMD - Strictly standard mean difference

STF - SuperTopFlash

Stk11 - Serine/threonine kinase 11

Stk22b - Serine/threonine kinase 22B

Sufu - Suppressor of fused

TCF - T cell factor

TGFb - Transforming growth factor, beta

Tnks - Tankyrase

TOFA - 5-(tetradecyloxy)-2-furoic acid

Wg - Wingless

Wnt - Wingless-type MMTV integration site family member

Wnt3A - Wingless-type MMTV integration site family member 3A

WT - Wild-type

CHAPTER ONE

INTRODUCTION AND LITERATURE REVIEW

1.1 The Hedgehog and Wnt signal transduction pathways in development and disease

The complex design of multicellular organisms entails the separation of functionally distinct groups of cells into tissues and organs. During development, the coordinated deployment of a small set of evolutionarily conserved intercellular protein signals, termed morphogens, serves to spatially and temporally sculpt cellular function and organization. Each of these protein signals cues a cascade of intracellular molecular events which alter the transcriptome and ultimately the proteome of individual cells to determine cell fate.

Sparking widespread interest in the mechanisms of developmental signaling, a groundbreaking forward genetic screen in *Drosophila* by Christiane Nüsslein-Volhard and Eric Wieschaus first identified genes whose products were ultimately classified as morphogens. Two of these genes, *hedgehog* (*hh*) and *wingless* (*wg*), bring about severe defects in body patterning when mutated (Nüsslein-Volhard and Wieschaus, 1980). The body of *Drosophila* larvae is organized along the anterior-posterior axis in segments that can be further characterized by the alternating presence or absence of denticle structures on the ventral cuticle surface (Figure 1-1). Null mutations in either gene result in abnormal larval segment polarity marked by the absence of naked cuticle and embryonic lethality (Figure 1-1) (Baker, 1988; Mohler, 1988).

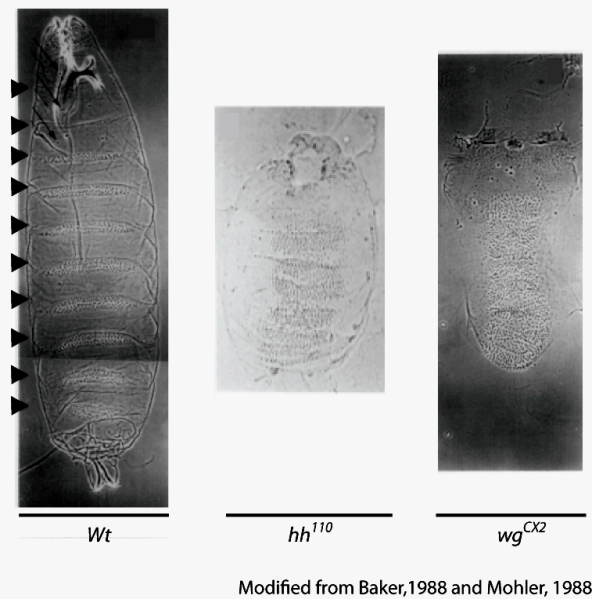

Figure 1-1 *Hedgehog* and *wingless* regulate segment polarity in *Drosophila*. Images display larval cuticular phenotypes of wild-type, *hh110* mutant, *wgCX2* mutant larvae. Black arrowheads indicate segment boundaries. Each segment contains regions of naked and denticulated cuticle. Both *hh* and *wg* mutants lack naked cuticle regions.

Extensive gene duplication in vertebrates produced expanded *hh* and *wg* gene families. The vertebrate family of Hedgehog signaling molecules consists of Sonic hedgehog (Shh), Indian hedgehog (Ihh), and Desert hedgehog (Dhh) (Echelard et al., 1993; Marigo et al., 1995; Tate et al., 2000). These molecules orchestrate, at least in part, the development of most organ systems in the vertebrate body. In mammals, the widely expressed Shh directs patterning of midline structures such as the neural tube (Echelard et al., 1993; Roelink et al., 1994), formation of the limbs and distal structures from the primitive limb bud (Chang et al., 1994; Riddle et al., 1993), and the development of many major organ systems (Barakat et al., 2010; Varjosalo and Taipale, 2008). Ihh is required for bone growth (Lanske et al., 1996; St-Jacques et al., 1999) and formation of certain

extra-embryonic structures such as the yolk-sac vasculature (Byrd et al., 2002). Dhh is expressed in the smallest range of tissues and plays a role in the production of gametes (Bitgood and McMahon, 1995; Bitgood et al., 1996). As a consequence of the extensive requirement of Hh proteins for development, mutations in mammalian Hh or its downstream signaling effectors lead to embryonic lethality or birth defects that vary in severity from polydactyly to holoprosencephaly (Belloni et al., 1996; Lettice et al., 2003; Roessler et al., 1996).

In mammals, nineteen homologues of the *Drosophila wg* gene direct critical steps in development (Chien et al., 2009). The first of these homologues was originally identified as the oncogene, Integration 1 (Int1) (Nusse and Varmus, 1982). When a relationship to *wg* was uncovered, the term "Wnt" was coined as a combination of "Int" and "*wg*" (Rijsewijk et al., 1987). During early vertebrate embryonic development members of the Wnt family of signaling proteins help guide processes such as gastrulation, establishment of an anterior-posterior axis, and convergent extension movements (Haegel et al., 1995; Heisenberg et al., 2000; Liu et al., 1999; van Amerongen and Berns, 2006). Later in development, several organs, including the kidneys, lungs, mammary glands, prostate, bones, and heart, rely on Wnt signals for proper formation (Bennett et al., 2005; Brisken et al., 2000; Carroll et al., 2005; Huang et al., 2009a; Li et al., 2002; Majumdar et al., 2003; Pandur et al., 2002; Roarty and Serra, 2007; Shu et al., 2002; Stark et al., 1994; van Amerongen and Berns, 2006; Yang et al., 2003). Interestingly, Wnt proteins coordinate with Hh proteins in either an antagonistic or synergistic manner in the development of a number of tissues including the neural tube

and limb structures (Akita et al., 1996; Alvarez-Medina et al., 2008; Kawakami et al., 2000a; Kawakami et al., 2000b; Parr and McMahon, 1995). Although there is some genetic redundancy between Wnts in the development of mammals, loss of function mutations in a few family members lead to congenital malformations that manifest as the absence of limbs or dysgenesis of major organ groups (Mandel et al., 2008; Niemann et al., 2004).

The Hh and Wnt developmental regulators also control several important processes in the adult animal. These signaling proteins frequently, but not exclusively, function in self-renewing tissues to govern cell proliferation and differentiation (Beachy et al., 2004; Clevers, 2006). For example, Hh signaling supports stem cell renewal in the subventricular zone (SVZ) of the adult brain. Perturbations to the pathway compromise cell proliferation, neurogenesis, and neuronal migration (Balordi and Fishell, 2007a, b). Hair follicle morphogenesis and hair growth depend on the Hh- and Wnt-mediated maintenance of stem cells that exist in the follicular bulge compartment (Chiang et al., 1999; Jaks et al., 2008; St-Jacques et al., 1998). In the adult colon, Hh and Wnt signals sometimes play opposing roles. At the base of colonic crypts Wnt signaling promotes survival and proliferation of progenitor cells. Outside the stem cell niche, Hh signaling restricts response to Wnt signals while also furthering differentiation (Barakat et al., 2010; van den Brink et al., 2004). Decreased bone mass in regenerating skeletal tissue can result from defects in Wnt signaling, which facilitates osteoblastogenesis and hampers osteoclastogenesis (Bennett et al., 2005; Holmen et al., 2005; Kato et al., 2002).

These examples illustrate the role of Hh and Wnt proteins as master regulators of tissue homeostasis and stem cell renewal in adult animals.

In tissues where Hh and Wnt signal transduction balance the delicate equilibrium between proliferation and differentiation, corruption of these signaling pathways sometimes leads to pathological outcomes, including the initiation and progression of tumors. One theory is that tumor cells hijack these signaling programs to enhance their proliferative and survival capacity (Barakat et al., 2010; Barker and Clevers, 2006; Beachy et al., 2004). Gliomas, medulloblastomas, and basal cell carcinomas are often associated with mutations in Hh pathway components (Gailani et al., 1996; Goodrich et al., 1997; Hahn et al., 1996; Johnson et al., 1996; Kinzler et al., 1987). Malignant melanomas, some leukemias, and greater that eighty percent of spontaneous colorectal cancers can occur as a result of misactivation of the Wnt signaling pathway (Dissanayake et al., 2007; Korinek et al., 1997; Liu et al., 2006; Mazieres et al., 2005; Sjöblom et al., 2006; Weeraratna et al., 2004). Given the importance of Hh and Wnt signal transduction to development and disease a better understanding of cellular responses to these signals would yield clarity into disease progression and novel therapeutic targets.

1.2 Mechanisms of Hedgehog signal transduction

1.2.1 Hedgehog production and distribution

In developing tissues, the localized secretion of Hh protein elicits graded responses in surrounding cells that are dependent upon the distance of the responding cell to the ligand-producing cell. The functional relevance of such a gradient is that the

dosage of Hh serves as a positional cue for the adoption of cell fates (Strigini and Cohen, 1997). For example, during vertebrate neural tube development, notochord and floor plate cells manufacture Shh which travels dorsally to form a concentration gradient along the dorso-ventral axis. In accordance with the local concentration of Shh, progenitor cells differentiate into one of five types of neurons (Briscoe et al., 1999; Ericson et al., 1997; Jessell, 2000; Wijgerde et al., 2002). Perturbations in the size or shape of the gradient result in the expansion, absence, or mislocalization of these neuronal cell types (Yamada et al., 1991). Crucial to the design of such gradients is the conserved dually lipidated structure of Hh which constrains its free diffusion (Porter et al., 1996).

Production of active Hh protein begins with autocatalytic cleavage of a precursor molecule to yield a cholesterol modified amino-terminal signaling domain (HhN) (Lee et al., 1994; Porter et al., 1996). Subsequent palmitoylation of HhN results in a dually lipidated molecule that is restricted to the cell membrane (Chamoun et al., 2001; Pepinsky et al., 1998). Release of Hh from the cell membrane is mediated by Dispatched (Disp), a 12-transmembrane protein that is structurally similar to the Hh receptor, Patched (Ptc) (Burke et al., 1999; Marigo et al., 1996). Both proteins belong to the Resistance Nodulation Division (RND) superfamily of proteins that in prokaryotes function to transport small molecules across membranes. Disp and Ptc likely act as small-molecule transporters, as their activity in the Hh pathway is dependent on residues important to the transporter function of RND protein family members (Ma et al., 2002; Taipale et al., 2002). In *Drosophila*, Hh released by Disp appears to be incorporated into particles scaffolded by the lipid-transporting lipophorin proteins (Panáková et al., 2005). This role

for lipoprotein complexes in Hh signaling may represent a universal mechanism for distributing other lipophilic signaling molecules in animals, such as the Wnt proteins (Panáková et al., 2005).

1.2.2 Hedgehog response in Drosophila

Initiation of the pathway response entails binding of Hh ligand to Ptc (Chen and Struhl, 1996; Marigo et al., 1996), which in turn derepresses the seven-transmembrane protein Smoothened (Smo) (Taipale et al., 2002) (Figure 1-2). A number of receptors facilitate binding of Hh to Ptc (Jacob and Lum, 2007a, b), including members of the Interference hog (Ihog) family. *Drosophila* Ihog, like its mammalian homolog, cell adhesion molecule–related/down-regulated by oncogenes (Cdo), associate with Hh through a fibronectin type III (FnIII) repeat (Tenzen et al., 2006; Yao et al., 2006), a motif with potential for binding sulfate ions (McLellan et al., 2006). Dimerization of Ihog and its conversion from a weak to a high-affinity Hh-binding molecule can be induced by heparin, a protein with sulfated polysaccharide modifications (McLellan et al., 2006). How Ihog and Cdo proteins promote Hh-mediated responses in coordination with Ptc and other Hh receptors, particularly the heparan sulfate–modified Dally-like protein (Dlp), which also contributes to the Hh response (Lum et al., 2003a), remains to be addressed.

Ultimately, the concerted action of these receptors activates Smo by promoting Hh interaction with Ptc. Phosphorylation of cytosolic C-terminal tail of Smo leads to a conformational change (Jia et al., 2004; Zhang et al., 2004; Zhao et al., 2007) thus allowing interactions with a cytoplasmic regulatory complex scaffolded by the kinesin-

like molecule Costal-2 (Cos2) (Hooper, 2003; Jia et al., 2003; Lum et al., 2003b; Ogden et al., 2003) and corresponds with protein accumulation at the plasma membrane (Denef et al., 2000) (Figure 1-2). This complex also contains the serine/threonine kinase Fused (Fu) (Lum et al., 2003b; Robbins et al., 1997; Ruel et al., 2003) and the transcriptional effector Cubitus interruptus (Ci) (Sisson et al., 1997; Wang et al., 2000; Zhang et al., 2005) (Figure 1-2).

In the absence of Smo activation, this cytoplasmic complex functions to mediate the proteolytic processing of Ci through activity of several kinases. Protein kinase A (PKA), glycogen synthase kinase 3b (GSK3b), and casein kinase 1a (CK1a) phosphorylate Ci, targeting the molecule for E3 ubiquitin ligase, Slimb (Slmb), dependent proteasome mediated processing (Chen et al., 1998; Jia et al., 2002; Jia et al., 2005; Jiang and Struhl, 1998; Price and Kalderon, 1999, 2002; Theodosiou et al., 1998). Processing removes the C-terminal activation domain of Ci resulting in a N-terminal, DNA binding fragment, Ci repressor (CiR) (Aza-Blanc et al., 1997) (Figure 1-2). Unprocessed Ci is subject to additional regulation by the poorly characterized Suppressor of Fused (Sufu) protein that may anchor localization of Ci to the cytosol (Lum et al., 2003b; Monnier et al., 1998; Méthot and Basler, 2000; Ohlmeyer and Kalderon, 1998; Wang et al., 2000) (Figure 1-2).

Recruitment of the Cos2 scaffolded cytoplasmic complex by Smo to the plasma membrane stabilizes active Smo and abrogates the proteolytic processing of Ci into CiR (Aza-Blanc et al., 1997; Hooper, 2003; Jia et al., 2003; Lum et al., 2003b; Ogden et al., 2003; Zhang et al., 2005). Genetic evidence for the inhibition of Sufu by Fu exists (Préat,

1992), and while Sufu becomes hyperphosphorylated following Hh stimulation, it is not clear if phosphorylation is directly mediated by Fu (Lum et al., 2003b). Without the regulatory pressures of proteolytic processing and Sufu inhibition full length Ci (CiFL) is free to accumulate in the nucleus and facilitate target gene transcription (Alexandre et al., 1996; Wang et al., 2000) (Figure 1-2). In order to be fully competent to initiate transcription full length Ci may require additional post-translational modifications, however, the exact nature of these modifications is unknown.

The requirement of both transcriptional activators and transcriptional repressors for the regulation of Hh target gene expression provides multiple layers of transcriptional control. Active transcription of some Hh target genes require only the absence of CiR whereas transcription of others cannot commence without the activity of CiFL (Müller and Basler, 2000). Tight regulation of the ratio between CiR and CiFL by Smo, Cos2 and Fu enables the translation of varying Hh doses into meaningful transcriptional responses and ultimately the appropriate cell fate.

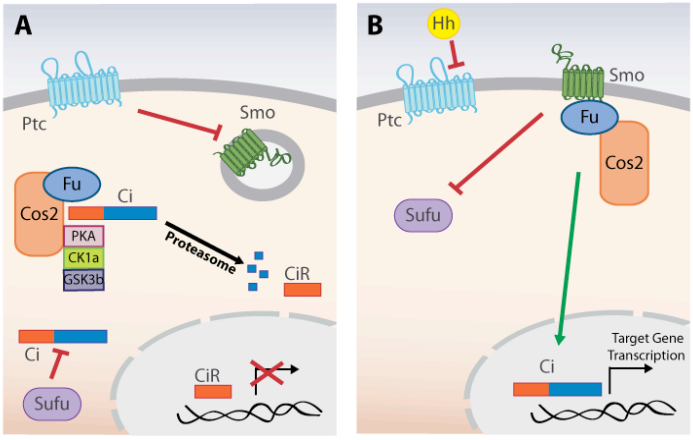

Figure 1-2 The Hedgehog signal transduction pathway in *Drosophila*. A. In the absence of Hh ligand Patched (Ptc) represses the activity of the seven transmembrane

protein Smoothened (Smo) and gates its access to the cell surface. The transcriptional effector Cubitus interruptus (Ci) is phosphorylated by a large cytoplasmic complex consisting of Costal2 (Cos2), Fused (Fu), and several kinases, PKA, Ck1a, and GSK3b. Phosphorylation of Ci targets the protein for proteasome-mediated proteolytic processing resulting in an N-terminal repressor fragment (CiR). Sufu also inhibits full length Ci. **B.** Binding of Hh to Ptc inhibits its repression of Smo. Smo accumulates at the cell surface, recruits the cytoplasmic regulatory complex scaffolded by Cos2, and inhibits Sufu function. Ci processing ceases and full length Ci activates target gene transcription.

1.2.3 Hedgehog response in mammals

Although Hh reception at the cell surface is well conserved among metazoans, mammalian homologues of some *Drosophila* Hh co-receptors remain to be identified. Binding of Hh to its core receptor Patched 1 (Ptch1) ablates the suppression of Smo activity (Figure 1-3). This process may be transduced through a small molecular intermediary because Ptch substoichiometrically inhibits Smo (Taipale et al., 2002). Several candidate small molecules have emerged, including cholesterol biosynthesis metabolites, such as oxysterols, that promote Smo function when exogenously added to cultured cells (Corcoran and Scott, 2006). Considering that the potent Smo antagonist cyclopamine (Taipale et al., 2000), a naturally occurring teratogen, is structurally similar to sterols, there is growing evidence that Ptch gates interactions between Smo and specific sterols to regulate Smo function. The ultimate target of Smo action in mammals is the Gli zinc finger family of proteins composed of three mammalian homologs of Ci (Gli1, Gli2, Gli3) (Bai and Joyner, 2001; Kinzler et al., 1988; Mo et al., 1997; Park et al., 2000), with proteolytically processed Gli3 (Gli3R) predominantly functioning as a transcriptional repressor (Hui and Joyner, 1993; Litingtung and Chiang, 2000) (Figure 1-3). Many studies support the hypothesis that Smo in *Drosophila* and mammals uses

different mechanisms of action to activate Ci or Gli proteins, respectively (Huangfu and Anderson, 2006; Varjosalo et al., 2006).

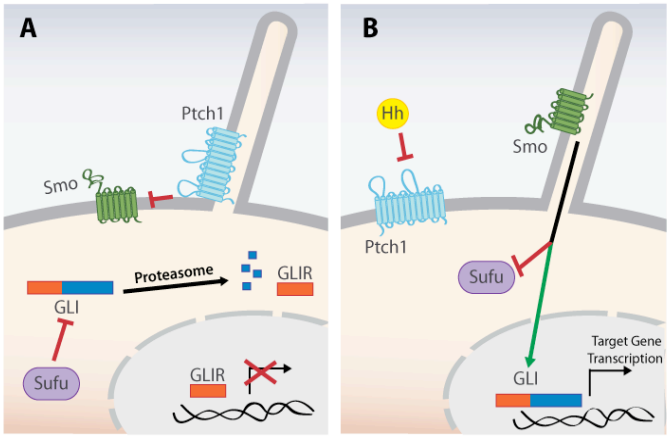

Figure 1-3 The Hedgehog signal transduction pathway in mammals. A. In the absence of the Hh ligand, Patched1 (Ptch1), suppresses the activity of the GPCR-like protein Smoothened (Smo). Under these conditions, Suppressor of Fused (Sufu) suppresses the Gli family of transcriptional effectors. Gli repressor molecule (GliR) is generated from the proteasome-dependent proteolytic processing of full-length Gli protein, silencing target gene transcription. **B.** Binding of Hh ligand to Ptch1 lifts its suppression of Smo that in turn accumulates in the primary cilium, a microtubule-scaffolded organelle that protrudes from the cell surface. Transcription of Hh pathway target genes is initiated by nuclear accumulation of full length Gli, and abrogation of GliR formation.

Insight into the mammalian Hh pathway has come from forward genetic screens in mice with chemically induced mutations that have revealed genes essential to neural tube formation, a Hh dependent process (Kasarskis et al., 1998). Surprisingly, the majority of these genes are involved in the formation of the primary cilium, a microtubule-scaffolded organelle found in most cells (Huangfu et al., 2003) (Figure 1-3). Subsequent studies revealed that components of the cilia, such as intraflagellar transport proteins, are required not only for the activation of Gli proteins but also for the

processing of Gli3 (Haycraft et al., 2005; Huangfu and Anderson, 2005; Liu et al., 2005). In this capacity, ciliary proteins appear to be the functional equivalent of Cos2. Furthermore, almost all the known mammalian Hh components, including Ptch, Smo, Sufu, and Gli proteins, localize to primary cilia (Corbit et al., 2005; Haycraft et al., 2005; Rohatgi et al., 2007). Ptch1 inhibits the localization of Smo to cilia in a Hh dependent manner, suggesting that this compartment is essential to Smo activation (Rohatgi et al., 2007) (Figure 1-3). Though it is conceivable that the cilium may simply represent an assembly point for pathway components, its requirement for both Hh pathway activation and suppression implicates a more direct role.

1.3 Mechanisms of Wnt signal transduction

Similar to Hh molecules, production of mature Wnt proteins is dependent upon lipid modifications. Before Wnt proteins can be secreted, a member of the membrane-bound O-acyltransferase (MBOAT) family of proteins, Porcupine (Porcn) (Kadowaki et al., 1996), adds a palmitate moiety to the N-terminus of Wnt precursor molecules. Modification by Porcn results in a functional Wnt ligand capable of transducing signals to targets in responding cells (Komekado et al., 2007; Kurayoshi et al., 2007; Takada et al., 2006; Willert et al., 2003).

Wnt stimulates multiple downstream pathways, those involving activation of the transcriptional coactivator β-catenin and those independent of β-catenin effector (so called "canonical" or "non-canonical" Wnt pathway responses, respectively) (MacDonald et al., 2009). The mechanisms of β-catenin-dependent Wnt responses have been well

studied and are conserved among metazoans. Briefly, in the absence of Wnt ligands, a large cytoplasmic complex comprised of the scaffolding protein, Axin, the tumor suppressor, the Adenomatous polyposis coli (APC) protein, and several kinases recruit and phosphorylate the transcriptional co-activator β-catenin (Amit et al., 2002; Behrens et al., 1998; Hamada et al., 1999; Itoh et al., 1998; Liu et al., 2002; Yanagawa et al., 2002). Phosphorylation marks β-catenin for ubiquitination by E3 ligases and subsequent proteasome-mediated degradation (Aberle et al., 1997; Jiang and Struhl, 1998; Marikawa and Elinson, 1998). Unable to bind to β-catenin, the T cell factor/lymphocyte enhancement factor (TCF/LEF) family of transcriptional effectors repress target gene transcription (Figure 1-4A) (Cavallo et al., 1998; Roose et al., 1998; Waltzer and Bienz, 1998). Binding of Wnt ligands to their receptors, the seven-transmembrane GPCR-like Frizzled family of proteins (Bhanot et al., 1996; Chen and Struhl, 1999; Rulifson et al., 2000) and the low-density lipoprotein related protein (LRP) family of proteins (Pinson et al., 2000; Wehrli et al., 2000), recruits Dishevelled (Dvl) and members of the β-catenin destruction complex to the cell surface (Bilic et al., 2007; Cliffe et al., 2003; Mao et al., 2001; Schwarz-Romond et al., 2007a; Schwarz-Romond et al., 2007b; Zeng et al., 2008). Abrogation of β-catenin degradation allows accumulation and translocation to the nucleus where binding of β-catenin to TCF/LEF proteins activates target gene transcription (Figure 1-4B) (Behrens et al., 1996; Brunner et al., 1997; Huber et al., 1996; Molenaar et al., 1996; Riese et al., 1997; van de Wetering et al., 1997).

Mechanisms of β-catenin independent Wnt responses are less well understood. In addition to transcriptional responses, these pathways elicit a wide variety non-

transcriptional signaling outcomes including changes in cell polarity, chemotaxis, and reorganization of cytoskeletal components (Gao and Chen, 2010; van Amerongen and Nusse, 2009). Whereas many downstream effectors of β-catenin-independent Wnt pathways have been described, the lack of biochemical tools has limited our ability to understand how signals are transduced to these effectors. Common to the activation of many of the known Wnt pathways, both β-catenin-dependent and –independent, is the engagement of the Dishevelled (Dvl) signaling molecule, which entails redistribution from the cytoplasm to membrane-bound receptors in response to Wnt stimulation (Bilic et al., 2007; Schwarz-Romond et al., 2007a; Schwarz-Romond et al., 2007b; Wallingford and Habas, 2005) (Figure 1-4B, Figure 1-4C). Acting as a molecular switch, Dvl molecules may help to interpret and translate upstream Wnt signals into appropriate cellular responses (Grumolato et al., 2010; Wallingford and Habas, 2005).

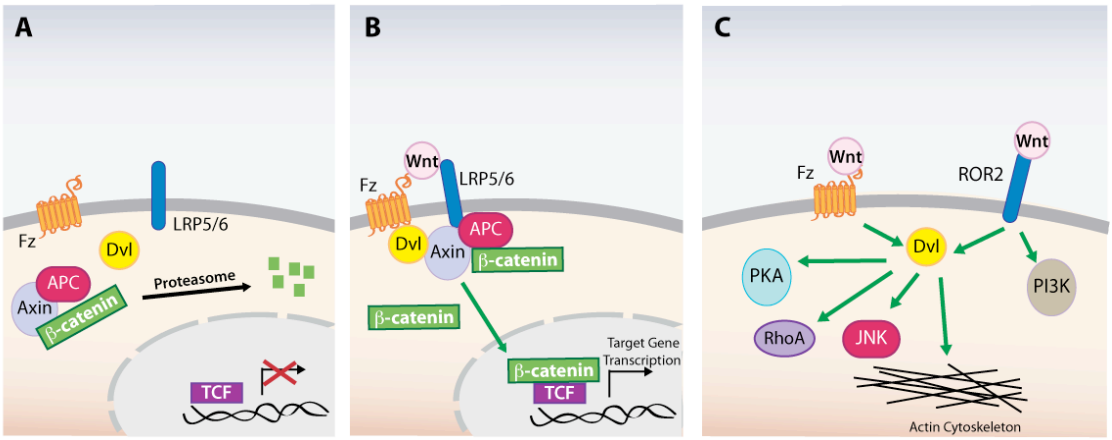

Figure 1-4 The Wnt pathway. A. In the absence of Wnt ligand a cytoplasmic complex that includes Axin, APC, CKI (not shown) and GSK3b (not shown) binds to and phosphorylates the transcriptional co-activator β-catenin, thus marking it for proteasome-mediated degradation. In the absence of β-catenin, members of the TCF/LEF family of transcriptional regulators largely function as transcriptional repressors. **B.** Binding of

Wnt to a member of the Frizzled (Fz) family of G-protein coupled receptors, and LRP5 or 6, members of the LDL-like receptor family recruits Axin and members of the Dishevelled (Dvl) family of signaling molecules to the cell membrane. Sequestration of Axin results in the dissolution of the β-catenin destruction complex thus resulting in accumulation of β-catenin. β-catenin binds to and activates TCF/LEF family members to induce transcription of Wnt/β-catenin pathway target genes. **C.** β-catenin independent (or non-canonical) Wnt responses are often routed through the Dvl family of proteins to down-stream effectors to affect cellular characteristics like cell polarity and cytoskeletal organization. Panel C was modified from Gao, 2010, Grumolato, 2010 and Dodge, 2011.

1.4 Small molecule modulation of cell-fate determination pathways

Given the influence of Hh and Wnt signaling on the pathology of diseases like cancer, tremendous effort has been successfully applied to gaining chemical control of these pathways (Dodge and Lum, 2011). The vast majority of small-molecule regulators of the Hh pathway target the positive effector Smo. The first of these identified, cyclopamine, was derived from a natural source, the wild corn lily plant (*Veratrum californicum*) and inhibits Smo function by direct binding (Chen et al., 2002; Taipale et al., 2000). Recently, in mammals, endogenous derivatives of oxysterols have been shown to influence Smo function (Bijlsma et al., 2006; Corcoran and Scott, 2006; Dwyer et al., 2007) and studies of these molecules may provide insight into the current black box of Smo regulation by Ptch. The most therapeutic promise has come from the identification of synthetic chemical modulators of Smo. In this category, molecules that potentiate Smo function, such as Smo agonist (SAG), in addition to those that restrict Smo function, including Smo antagonists (SANTs) and GDC-0449, have been identified (Rominger et al., 2009; Von Hoff et al., 2009).

Prior to the discovery of several synthetic compounds that target Tankyrase (Tnks) and Porcn (Chen et al., 2009; Huang et al., 2009b), the Wnt pathway was

perceived to be undruggable. Representative of these novel classes of compounds are the inhibitors of Wnt production (IWP) and inhibitors of Wnt response (IWR) (Chen et al., 2009). IWP compounds restrict palmitoylation of Wnt ligands by targeting the aceltransferase, Porcn (Chen et al., 2009). The IWR compounds inhibit the poly-ADP-ribosylating enzymes tankyrase 1 and tankyrase 2 which target Axin proteins for degradation. Inhibition of Tnks enzymes leads to Axin accumulation and subsequent β-catenin destruction (Huang et al., 2009b). In addition to the potential of these molecules as therapeutic agents against disease, the utility of Wnt and Hh chemical modulators is also exemplified by their use as tools for the dissection of signal transduction mechanisms.

CHAPTER TWO

SCREENING AND IDENTIFICATION OF NOVEL HEDGEHOG AND WNT PATHWAY COMPONENTS

2.1 Introduction

Studies spanning nearly half a century have attempted to elucidate the mechanisms of Hh and Wnt signal transduction. Largely powered by genetic studies in the *Drosophila* model organism, understanding of the cellular responses to Hh and Wnt signals has flourished. Whereas the molecular events that occur in response to Wnt signals are highly conserved across metazoans, Hh signal transduction has diverged between *Drosophila* and mammals (Huangfu and Anderson, 2006; Varjosalo et al., 2006). In lieu of homologues to several *Drosophila* Hh pathway components, mammalian cells engage alternative cellular machinery, including the primary cilia, to transduce Hh signals (Huangfu et al., 2003). Many of the evolutionarily divergent events that comprise mammalian Hh signaling have been poorly characterized. Given the integral role that the Hh and Wnt signaling pathways play in many diseases, and their potential as therapeutic targets, gaps in our knowledge of mammalian signal transduction must be filled through further study.

2.1.1 A comparison of two screening strategies in the mammalian system

Classical forward genetic screens offer a robust approach to identify novel regulators of a biological process. Traditionally performed in lower order model organisms, advances in screening protocols have made such strategies feasible in a mammalian system (Kile and Hilton, 2005). Indeed, a murine, phenotype-based, N-

ethyl-N-nitrosourea (ENU) mutagenesis screen to identify developmental regulators first observed that components of primary cilia play a role in mammalian Hh signal transduction (Huangfu et al., 2003; Kasarskis et al., 1998). Advantages of the classical forward genetics approach include the opportunity to relate a gene to a particular biological process without prior knowledge of that gene and the ability to identify several alleles of a gene that may provide insights into its function (Boutros and Ahringer, 2008).

Though mutagenesis screens in mice have proven a viable and attractive option for interrogating biological processes, several drawbacks accompany this screening platform. Phenotypes that are lethal or masked by a contribution of maternal mRNA are difficult to identify. Also, once desired phenotypes have been collected, mapping of causative genetic lesions can be a labor intensive and time consuming process (Boutros and Ahringer, 2008). The use of transposable elements, such as the *piggybac* transposon, instead of chemical mutagens circumvents this obstacle by supplying an anchor of known sequence from which PCR analysis can be used to identify the affected locus (Ding et al., 2005). However, insertional events are not stochastic, as evidenced by one study which produced only 5590 non-redundant insertions from a total of 55,000 *piggybac* insertion events (Rad et al., 2010). Another study estimates that successful insertion of one *piggybac* transposon into at least 15,000 of the roughly 30,000 genes in the mouse genome would require a staggering 57,000 mice and at least one year to generate (Wu et al., 2007). The biased nature of target selection limits insertional mutagenesis methodologies from achieving a truly genome-wide scope.

The completion of genome sequencing projects prompted the design of innovative tools for functional genomics based applications in the dissection of biological processes. Assembly of genome-wide libraries of reagents that can silence gene expression through RNA interference (RNAi) facilitate the systematic analysis of gene function. Screening platforms that take advantage of these reverse genetics based resources are amenable to high-throughput, automated configurations and mammalian cell-culture systems (Mohr et al., 2010). Consequently, they often require less time and manpower than classical genetic screens. Compared to screens that require animal breeding, cell-culture based screens are less likely to miss phenotypes that are lethal or masked by a maternal contribution of mRNA (Boutros and Ahringer, 2008). Allocation of resources for the positional mapping of genes of interest is unnecessary as reagent design for RNAi is based on known gene sequences (Boutros and Ahringer, 2008). The potential to target every known gene also means that genome-wide coverage is a possibility for RNAi based screens. Though cell based RNAi screens offer several advantages, this screening platform does not replace but rather complements classical genetics methodologies.

2.1.2 RNA interference

RNAi has become a widely used approach to generate loss of function phenotypes in some whole animal and cell-culture systems. RNAi was first observed in *Caenorhabditis elegans* when the introduction of exogenous double stranded RNA (dsRNA) resulted in silencing of genes containing similar sequences (Fire et al., 1998). Conserved across eukaryotes, this process endogenously functions to regulate gene

expression and protect cells from invasive nucleic acids (Carthew and Sontheimer, 2009; Hannon, 2002).

Initiation of RNAi entails processing of dsRNA, derived from either endogenous or foreign sources, by the Dicer family of proteins, a sub-class of RNase III enzymes (Figure 2-1) (Bernstein et al., 2001; Ketting et al., 2001; Knight and Bass, 2001). Processing produces a twenty one to twenty five base pair non-coding RNA, however, the exact size of resultant RNA, termed short interfering RNA (siRNA), is species specific (Elbashir et al., 2001a; Elbashir et al., 2001c; Zamore et al., 2000). Subsequent denaturing of the double stranded siRNA leads to loading of one strand onto the RNA-induced silencing complex (RISC) while the other strand is discarded (Hammond et al., 2000; MacRae et al., 2008; Nykänen et al., 2001). Guide strand selection is determined by the strength of base pairings, and the strand that is least stably base paired at the 5' end will be chosen (Khvorova et al., 2003; Krol et al., 2004; Schwarz et al., 2003). Association of RISC complex proteins with the siRNA guide strand directs the complex to messenger RNA (mRNA) targets (Hammond et al., 2000). Argonaute (Ago) protein family members are core components of the RISC complex and execute cleavage of mRNAs with perfect Watson-Crick base pair complementarity to the siRNA guide strand (Figure 2-1) (Matranga et al., 2005; Miyoshi et al., 2005; Rand et al., 2005). Exonucleases further degrade the mRNA fragments resulting in effective post-transcriptional inhibition of gene expression (Orban and Izaurralde, 2005). The RISC complex will tolerate some base pair mismatches between the guide strand and the target mRNA as it is also optimized for inhibition of gene expression through microRNA

(miRNA) mediated RNAi (Jackson et al., 2003). Endogenously encoded miRNAs silence multiple genes with close but not perfect complementarity through inhibition of translation rather than degradation of the mRNA; however, the exact mechanism is highly debated (Carthew and Sontheimer, 2009; Kim et al., 2009b). Suppression of mRNAs with similar but not perfect base pair complementarity to the siRNA guide strand may account for some of the "off-target" effects documented in RNAi based studies (Jackson et al., 2003).

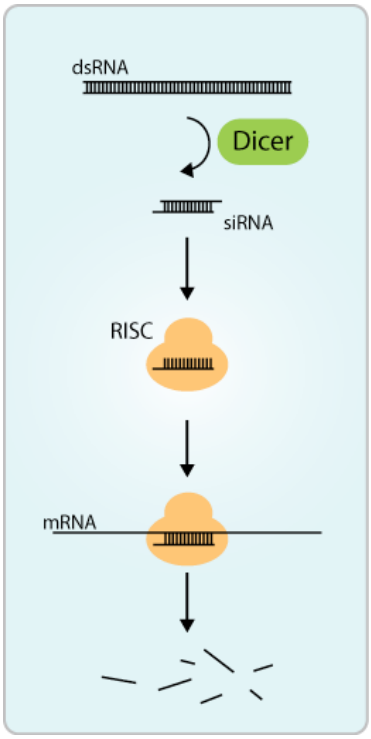

Figure 2-1 Mechanisms of RNA interference. A simplified schematic of RNAi shows that dsRNA is processed by Dicer proteins to form siRNA. RISC-siRNA complexes mediate cleavage of mRNA targets with perfect Watson-Crick complementarity to the siRNA, resulting in post-transcriptional silencing of gene expression. Figure is modified from Hannon, 2002.

The RISC complex derives its specificity from the siRNA guide strand sequence (Hammond et al., 2000) and thus is adaptable for the inhibition of many different RNA targets. This flexibility not only endows cells with a strategy to combat a wide array of foreign threats but also provides investigators with a powerful system for genome-wide inhibition of gene expression. Cellular RNAi machinery can be co-opted for laboratory studies through the introduction of RNA effector molecules. Endoribonuclease-prepared siRNAs (esiRNAs) generated from the *in vitro* cleavage of dsRNA (Yang et al., 2002), chemically synthesized siRNAs (Elbashir et al., 2001b), or dsRNAs are typically introduced into cell culture through transfection and their effects are transient. Short-hairpin RNAs (shRNAs) are introduced as DNA expression constructs which are transcribed to produce a precursor hairpin RNA structure that is subsequently processed by Dicer proteins and loaded onto RISC complexes (Paddison et al., 2002; Sui et al., 2002). Viral packaging of shRNA encoding plasmids facilitates genomic integration and stable expression of the shRNA (Barton and Medzhitov, 2002; Devroe and Silver, 2002). For RNAi based studies in mammalian cells, suitable effector molecules include siRNAs, esiRNAs and shRNAs, whereas long dsRNAs generally evoke an anti-viral apoptotic response (Elbashir et al., 2001a; Kibler et al., 1997).

2.1.3 The utility of RNAi screening platforms for the study of Hh and Wnt signal transduction

Application of RNAi based screening methodologies to the study of mammalian Hh signal transduction is achievable and holds tremendous promise for biomedical discovery. Response to Hh ligands occurs at the level of single cells and thus can be

studied in cell culture. Luciferase reporter systems that faithfully measure Hh pathway response exist (Sasaki et al., 1997) and provide an easily scorable phenotype for screening. Also, identification of several novel Hh pathway components, including the ligand co-receptor Dally-like (Dlp) and the Ci kinase Casein kinase α (CK1α), using genome-wide RNAi in *Drosophila* cell culture (Lum et al., 2003a) predicts that this approach may be useful in other cell types. In mammalian cells, screens using siRNA libraries targeting the mouse kinome have identified several kinases that regulate Hh signal transduction (Evangelista et al., 2008; Varjosalo et al., 2008), however, no RNAi based studies of Hh signal transduction have yet been attempted on a genome-wide scale.

Mechanistic understanding of Wnt signaling in both *Drosophila* and mammals has benefited from RNAi screening technologies (DasGupta et al., 2005; Miller et al., 2009; Tang et al., 2008). Despite the dynamic and sometimes integrative relationship that the Wnt and Hh pathways share *in vivo*, few systematic studies have sought out mutual regulators. Identification of points of integration between signaling pathways would be the first step to deconvolution of signal transduction networks. RNAi screening strategies may yield additional insights into the mechanisms of Wnt signal transduction and its relationship to Hh mediated cellular responses through the discovery of genes that are common to both pathways.

2.1.4 Obstacles and solutions for successful RNAi-based screening

Establishing a useful RNAi screening strategy begins with the development of a robust high-throughput assay platform (Figure 2-2). As with any screening platform, assays to be used with RNAi screens should be specific and clearly distinguish between

true signal and background noise. For cell-based, high-throughput screening platforms, the Z' factor is the most widely calculated coefficient for the assessment of screening quality and indicates whether or not positive controls can be separated from negative controls (Zhang et al., 1999). However, this stringent quality metric was originally optimized to be used with small-molecule based screens where typically the signal to background ratio is high and variability is low, when compared to RNAi screens (Birmingham et al., 2009). In addition, the Z' factor coefficient can be skewed with the use of very strong positive controls, and, in such cases, may not reflect the screen's ability to detect weaker and possibly more realistic phenotypes (Birmingham et al., 2009; Zhang, 2007). A more informative and less conservative alternative to the Z' factor is the Strictly standard mean difference (SSMD) coefficient. The SSMD estimates the difference between positive and negative control groups in relation to the standard deviation of the difference between the two groups (Zhang, 2007). A strong SSMD score denotes a high probability that the positive and negative control groups are different from each other and predicts that the desired phenotypes will be discernable from background noise (Birmingham et al., 2009; Zhang, 2007).

Other parameters that influence the success of an RNAi screening strategy include false positive (or discovery) and false negative (or non-discovery) rates. Once an assay is developed and validated through small-scale pilot screens, the next step is the execution of a primary screen (Figure 2-2). Primary screens should be performed in multiple replicates for statistical strength and include internal controls at the well, plate, screening run, and whole screen levels (Figure 2-2) (Echeverri et al., 2006; Mohr et al.,

2010). Statistical normalization of the data can be performed to correct for the presence systemic artifacts typically associated with high throughput methodologies, such as plate edge-effects (Figure 2-2) (Boutros and Ahringer, 2008). These measures will reduce the contribution of noise from automation and high-throughput formats to false positive and negative rates.

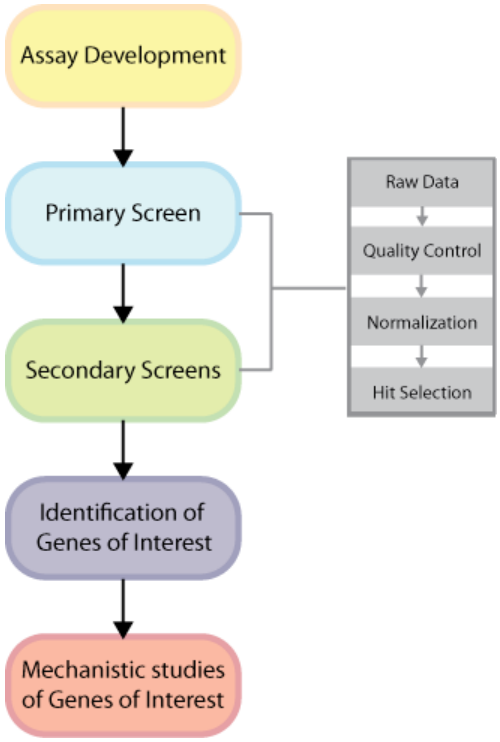

Figure 2-2 Workflow for cell-based RNAi screens. After development of a robust assay, execution of the primary screen will identify candidate genes. The list of candidate genes should be further refined by secondary screens to reduce false positives and identify genes of interest. For both primary and secondary screening strategies raw data must be analyzed to ensure that quality control standards are met. Raw data values are subject to statistical analysis and normalization to provide meaningful comparisons between samples and negative controls before hits can be delineated. Genes of interest identified from primary and secondary screening can be further examined through mechanistic studies. Figure modified from Boutros, 2008.

Sources of false positive and false negatives in an RNAi dataset are not limited to poor assay design or high-throughput techniques, but include characteristics of the RNAi process and the design of silencing molecules. The kinetics of RNAi may contribute to false negative rates for certain genes whose protein products have a long half-life. Completion of the assay or clearing of the siRNA from the cell before the protein has turned over may cause a false negative result (Birmingham et al., 2009; Perrimon and Mathey-Prevot, 2007). Also, RNAi may produce only a partial knockdown of gene expression, yielding a weak phenotype in the experimental assay that may be overlooked (Perrimon and Mathey-Prevot, 2007). Off-target effects, where gene expression of unintended targets is silenced (Jackson et al., 2003), is a common culprit of the presence of false positives and negatives in an RNAi dataset. Often the result of sequence similarities between the RNAi reagent and multiple mRNA targets (Jackson et al., 2006), a theoretical solution would be to make siRNA design more specific. However, no algorithm yet exists to do so (Echeverri et al., 2006).

Secondary screens offer a powerful way to remove false positives from an RNAi dataset. SiRNAs that produce a desired phenotype, termed “hits”, in the primary screen should be further validated with the use of secondary screening strategies (Figure 2-2). Common approaches include repeating the primary screen assay to test hits for reproducibility, using multiple siRNA reagents to confirm hits, validating hits using non-RNAi methods, and testing hits using a different model organism or cell line (Boutros and Ahringer, 2008; Echeverri et al., 2006). The design of a secondary screening strategy depends upon the specific goals of the investigator.

A final challenge for the success of an RNAi screening approach is the selection of genes for further study (Figure 2-2). Historically, RNAi screens produce large lists of candidate genes. Although the majority, if not all, of the results may be true, engaging in mechanistic studies of all the candidate genes identified is typically impractical. Gauging which genes will lead to an interesting story is often difficult. One trend is to base selection on the strength of the phenotype generated by the siRNA in the screening assay. However, the study of genes corresponding to weaker phenotypes may provide the same or greater insights into the biological process in question (Boutros and Ahringer, 2008). Another consideration is the ease with which the candidate gene can be studied immediately. If no reagents exist to examine the function of a gene of interest, the investigator must produce them from scratch, delaying further biological discovery. Application of secondary screens may help to narrow a large gene list and identify candidate genes with characteristics that are appropriate and preferable to the investigator for further mechanistic studies (Figure 2-2).

This chapter focuses on the use of RNAi screening approaches to identify novel regulators of the Hh and Wnt signal transduction pathways. In addition to interrogation of signal transduction biology, methods to improve the design of RNAi screening platforms are discussed and tested. Several secondary screens are employed to identify genes of interest for immediate study and compared.

2.2 Results

2.2.1 Primary screen

2.2.1.1 Assay development

The 3T3-ShhFL cells are derived from NIH-3T3 cells which are capable of forming primary cilia and responding to Hh ligand (Figure 2-3A). These transformant cell lines stably harbor with a firefly luciferase (FL) Hh-responsive reporter (GliBS reporter) (Sasaki et al., 1997), a control *Renilla* Luciferase (RL) reporter, and a plasmid encoding Shh (Figure 2-3B). The constitutively expressed RL reporter serves as an indicator of general cell health. Because stable overexpression of Shh in 3T3-ShhFL cells results in cell-autonomous Hh signaling, targeting of genes encoding proteins involved in Shh production or downstream response can reduce GliBS reporter activity.

3T3-ShhFL cells faithfully report Hh pathway activity. Compared to untreated NIH-3T3 cells, I found that 3T3-ShhFL cells displayed similar abundance of the Ptch1 transcript, a target of the Hh pathway, to NIH-3T3 cells treated with Shh conditioned media (Figure 2-3C). Sensitivity to a small-molecule Smoothened (Smo) antagonist, cyclopamine, indicated that FL production in 3T3-ShhFL cells is dependent upon Smo-mediated Shh signaling (Figure 2-3D).

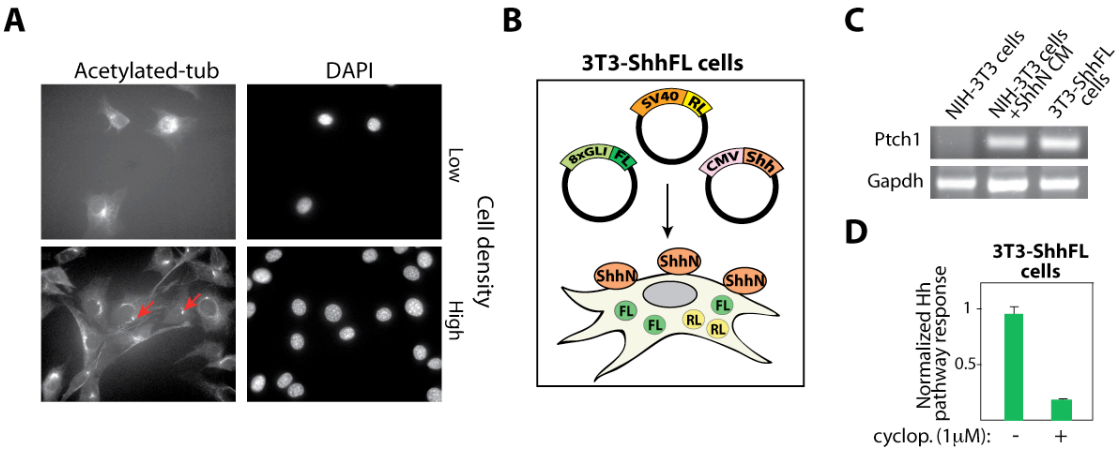

Figure 2-3 Generation of stable cell line to measure Hh response. **A.** NIH-3T3 cells form cilia under high-density conditions. (*Panel A by Wei Tang*). **B.** A cell-autonomous signaling assay for Hh pathway response. NIH-3T3 cells were stably integrated with an Hh-responsive firefly luciferase (FL) reporter (GliBS reporter), a control reporter (*Renilla* luciferase; RL), and an expression construct encoding Shh to generate the 3T3-ShhFL cell line. **C.** 3T3-ShhFL cells exhibit faithful Hh transcriptional response. RT-PCR analysis of the Hh target gene Ptch1 in 3T3-ShhFL cells was compared with wild-type NIH-3T3 cells treated with or without ShhN conditioned medium. **D.** 3T3-ShhFL cells are responsive to cyclopamine.

Optimization of siRNA transfection protocols was achieved by testing the ability of Gli2 and Smo siRNA, transfected using various reagents and conditions, to reliably reduce FL activity in 3T3-ShhFL cells. Transfection of siRNA, at a final concentration of 57nM, using the X-tremeGENE transfection reagent according to the manufacturer's protocol achieved the strongest and most consistent results (data not shown). Assay protocols were modified to permit high-throughput formatting and automated addition of reagents.

To determine the efficacy of an automated assay in the identification of siRNAs that can affect cellular Hh responses I conducted pilot screens. A representative pilot screen is shown in Figure 2-4. SiRNAs from a 96-well plate spiked with six Gli2 siRNA

controls were transfected into 3T3-ShhFL cells in triplicate. Gli2 siRNAs reduced Hh pathway activity by fifty percent when compared to control siRNA. A Z' factor of 0.13 was calculated from this pilot screen. Although, convention states that a minimum Z' factor of 0.5 is necessary to complete a high quality screen (Zhang et al., 1999), a study of nineteen siRNA screens showed that a Z' factor > 0 was sufficient to successfully separate positive controls from background when the samples were screened in duplicate or triplicate (Birmingham et al., 2009). An SSMD coefficient of -4.6 further confirmed the utility of this assay for the identification of Hh pathway regulators. An SSMD coefficient < -3 (or > 3 if positive control values are greater than negative control values) indicates a probability of greater than 99% that the positive and negative control groups are different (Zhang, 2007).

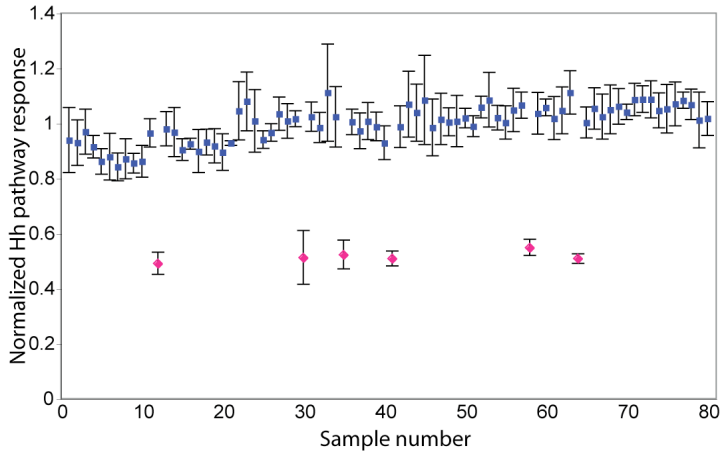

Figure 2-4 A representative pilot screen for genome-wide RNAi screening in 3T3-ShhFL cells. Positive controls, siRNA targeting Gli2, were seeded onto 96-well plates containing negative control siRNA. 3T3-ShhFL cells were plated and transfected using automated and high-throughput methodologies. Columns one and twelve of the 96-well plate left empty to avoid edge effects. Luciferase activity was measured after 72 hours. Blue - Control siRNA. Pink – Gli2 siRNA.

Two commercially available, chemically synthesized siRNA libraries generated by Dharmacon and Qiagen were obtained for screening. Both libraries are arrayed in 96 well plates so that each well contains a pool of four non-redundant siRNAs targeting a single gene. The Dharmacon and Qiagen libraries consist of 16,872 and 22,781 siRNA pools, respectively, with ~15,700 of these mutually targeting the same genes with mostly non-overlapping siRNA sequences (Figure 2-5A) (Tang et al., 2008).

2.2.1.2 Primary screening

To identify previously unknown Hh pathway components, I screened two parallel genome-wide RNAi libraries by transiently introducing gene-specific siRNA pools into 3T3-ShhFL cells (Figure 2-3B, 2-5A). A combined total of 39,698 siRNA pools were screened in triplicate (Figure 2-5A), and targeted 23,995 distinct genes, or approximately 80% of the mouse genome. To assess screening quality, a *z*-score, a measure of the number of standard deviations a value lies from the population mean, was calculated for positive controls on each plate. Plates containing Gli2 positive controls that did not achieve a *z*-score of -2.0 or less ($P < 0.05$) were repeated or discarded. Greater than 95% of the total 1,470 assay plates screened met quality control standards.

Analysis and normalization of raw data assists meaningful comparison of samples to controls. Raw luciferase counts were subject to both well-position-centric normalization, to correct for an observed edge-effect (Figure 2-5B), and plate-centric normalization, to control for plate to plate variation. For each screen, I calculated *z*-scores for the firefly and *Renilla* luciferase values of each siRNA pool tested. siRNA pools that affected general cell health, determined by an RL *z*-score of greater than 2.5 or

less than -2.5, or that produced inconsistent results (SD > 0.1) were removed from further evaluation. Screens of both the Qiagen and Dharmacon libraries produced datasets resembling a normal distribution of results (Figure 2-5C).

2.2.1.3 Identification of Hh pathway activators

Focusing on the identification of positive pathway regulators, I selected siRNAs that reduced Hh reporter activity by two standard deviations from the mean signal ($P < 0.05$) or more for further study. Using this criterion, 535 genes of interest were identified (Figure 2-5A). Recovery of known Hh pathway activators such as Smo, the seven-transmembrane pathway effector, and components of the primary cilium was improved with the use of both siRNA libraries (Figure 2-5D), suggesting an advantage in employing multiple siRNA libraries in RNAi-based screening strategies.

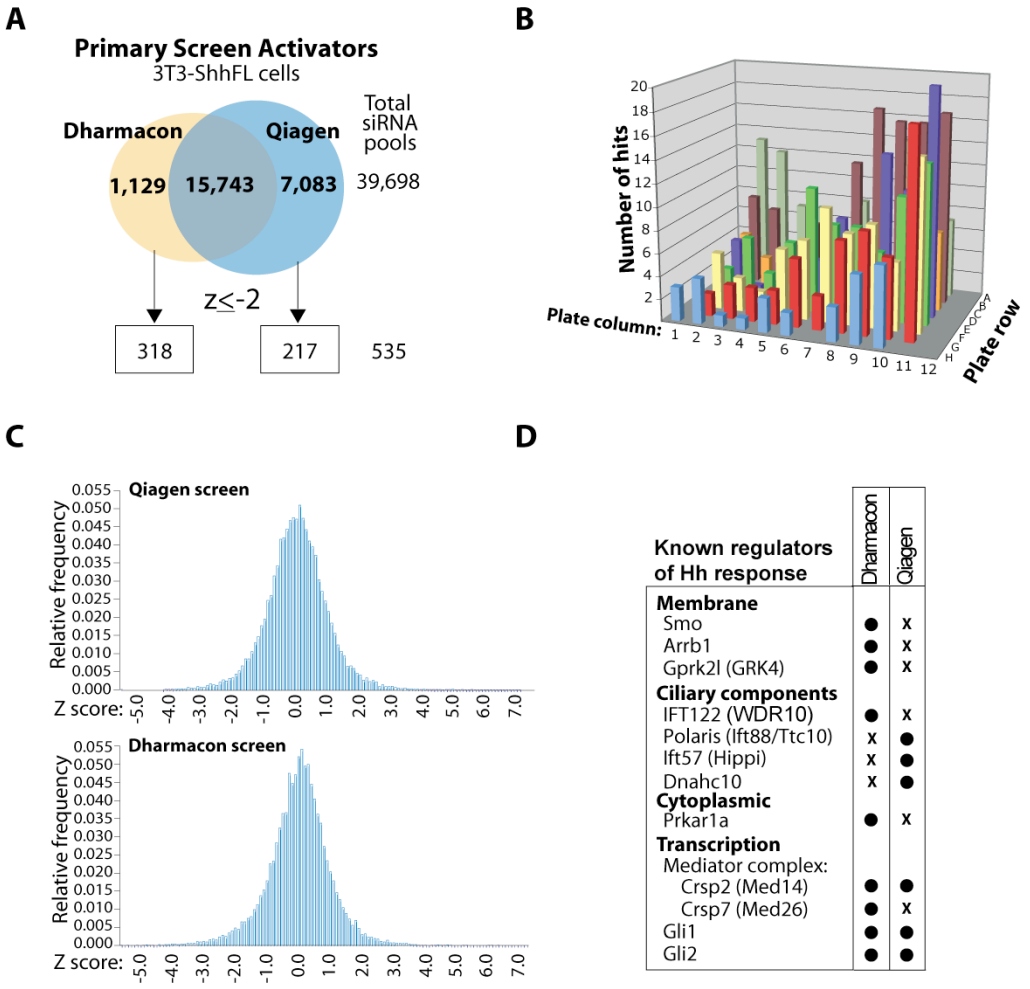

Figure 2-5 Characteristics of the primary screen and identification of Hh pathway activators. **A.** siRNA libraries designed by Dharmacon or Qiagen were screened in triplicate using the 3T3-ShhFL cells. **B.** Summary of hits identified from various well positions in 96 well plates from the primary screen without well-position based normalization procedure. An edge effect is apparent from the skewed well distribution of hit frequencies. **C.** Frequency of *z* score assignment to genes reveals a Gaussian-type distribution of results. **D.** Many known Hh pathway components were identified with siRNAs from a single library.

2.2.1.4 Identification of Hh pathway suppressors

In 3T3-ShhFL cells, given high basal level of GliBS reporter activity brought on by the stable overexpression of Shh (Figure 2-3B, 2-3C, 2-3D), the identification of Hh pathway suppressors by siRNAs that could further increase the Hh reporter activity seemed unlikely. However, the Gaussian-type distribution of primary screening results (Figure 2-5C) demonstrated the utility of this assay system for the discovery of negative as well as positive regulators of Hh signaling. From the primary screen, I found 209 candidate Hh pathway suppressors from siRNAs that increased Hh reporter activity by two and a half standard deviations or more from the mean signal (z >/= 2.5, P < 0.05) (Figure 2-6, Appendix A). The successful detection of several known Hh pathway suppressors, including Suppressor of Fused (Sufu) (Svärd et al., 2006) and Dual-specificity tyrosine-(Y)-phosphorylation regulated kinase 1B (Dyrk1B) (Varjosalo et al., 2008) (Figure 2-6), provided further validation of the dataset as well as the approach to suppressor discovery.

Of interest is the identification of Protein kinase C gamma (Prkcc) as a candidate Hh suppressor from siRNA pools in both libraries. Corroboration by multiple siRNAs increases confidence in the siRNA result (Echeverri et al., 2006). The ability of siRNAs designed by different algorithms to produce similar results will be empirically tested and discussed later in this chapter. Mechanistic interrogation of candidate Hh suppressors will be reserved for future studies.

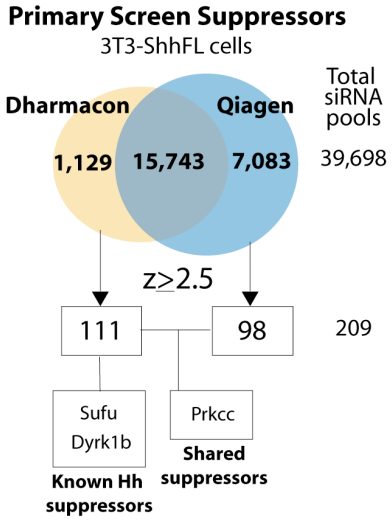

Figure 2-6 Identification of Hh pathway suppressors. SiRNA libraries designed by Dharmacon or Qiagen were screened in triplicate in 3T3-ShhFL cells. Samples that increased reporter activity greater than or equal to 2.5 standard deviations from the mean signal were designated as Hh pathway suppressors. Known pathway suppressors identified from the screens are listed. Also, one gene, Prkcc, was identified by siRNA pools from both libraries.

2.2.2 Secondary screens

Secondary screening approaches further refined the group of 535 candidate Hh pathway activators identified in the primary screen. In order to identify genes of interest, I designed secondary screens to validate primary screening results, discover shared Hh and Wnt pathway components, identify Hh and Wnt regulators with medical relevance, and biochemically assay potential transcriptional co-effectors of Gli1. Secondary screening strategies not only supplied insights into Hh and Wnt signal transduction biology, but also revealed sources of false negatives in high-throughput RNAi screening platforms.

2.2.2.1 Exogenous Hedgehog test

I retested the 535 siRNAs targeting candidate Hh pathway activators identified from the primary screen in ShhLightII cells stimulated with exogenous Shh to enrich for genes that act downstream of Shh protein production (Figure 2-7A). ShhLightII cells are NIH-3T3 cells do not endogenously produce Shh and are stably transfected with the GliBS reporter (Taipale et al., 2000). By identifying genes with characteristics that were consistent with the goals of future studies and by providing validation of the reproducibility of siRNA results in a second assay, the exogenous Hh test proved useful in two ways. I found a total of 351 siRNAs that reduced Hh pathway activity at the level of cellular response (Figure 2-7A, Appendix B, Appendix C).

2.2.2.2 Wnt test

To identify shared regulators of the Hh and Wnt pathways, I counter-screened siRNAs targeting the 351 validated Hh activators against the Wnt/β-catenin pathway using a Wnt-responsive luciferase reporter [SuperTopFlash (STF)] in NIH-3T3 cells. Based on the ability of siRNAs to increase or decrease Wnt reporter activity, I further categorized the Hh activators as Wnt suppressors, Wnt activators, or dedicated Hh pathway activators (Figure 2-7A, 2-7B, Appendix C). Genes when targeted with siRNAs that decreased activities of both pathways may influence cell viability and thus, Hh and Wnt co-activators were not considered for further testing.

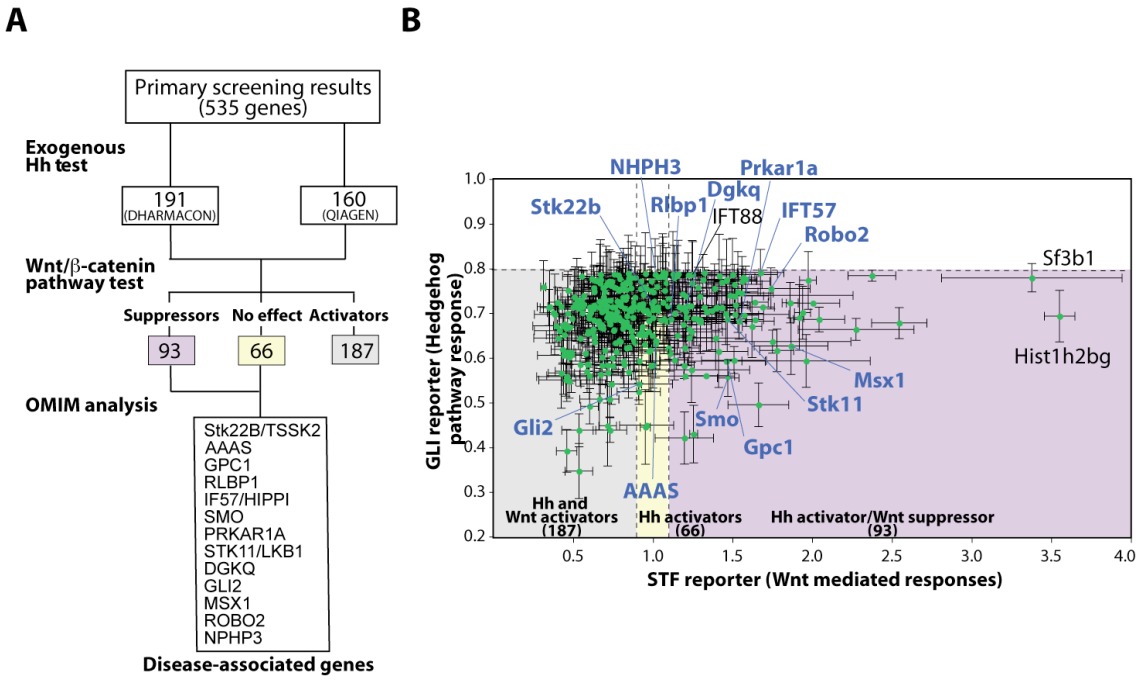

Figure 2-7 Secondary screens identify Hh activators that are important for Wnt signal transduction and associated with disease. **A.** Activators identified from the primary screen (Figure 2-5A) were retested using NIH-3T3 cells stably harboring the GliBS reporter (ShhLightII cells) in the presence of culture medium containing ShhN ("Exogenous Hh test"). siRNAs that retained their activity in this assay were tested with the SuperTopFlash (STF) reporter in NIH-3T3 cells transfected with Wnt3A cDNA to assign function in Wnt/β-catenin pathway response. Genes with no activity or suppressor function in this pathway were cross-referenced with the OMIM database to identify disease-associated genes (see Table 2-1). Multiple names for a single gene are separated by a slash. **B.** Graphical summary of gene function in the Hh (Y axis) and Wnt/β-catenin (X-axis) pathways. Disease-associated genes (blue) are noted along with other genes of interest (black).

2.2.2.3 Identification of disease associated Hh and Wnt regulators

I employed an *in silico* approach to select genes of interest consistent with another goal of future studies, to uncover potentially unknown relationships between disease and Hh and Wnt signal transduction. The 93 Hh activators found to suppress Wnt signaling and the 66 Hh activators with no Wnt function were cross-referenced with the

Online Mendelian Inheritance in Man (OMIM) database (Figure 2-7A, Figure 2-7B). Thirteen genes were identified with alleles that contribute to disease states.

To confirm the specificity of siRNA pools targeting the disease-associated genes, I evaluated the ability of individual siRNAs from the pool to recapitulate the original observation (Figure 2-8; Appendix D). Genes already validated by identification from two siRNAs pools in previous rounds of screening were not re-tested (Appendix B). Using a minimum threshold of three distinct siRNAs inducing a shared phenotypic outcome as the criteria for high confidence genes with minimal influence from RNAi off-targeting (Evangelista et al., 2008), I retained a total of 10 genes associated with either malformation, degenerative disease, or cancer (Table 2-1).

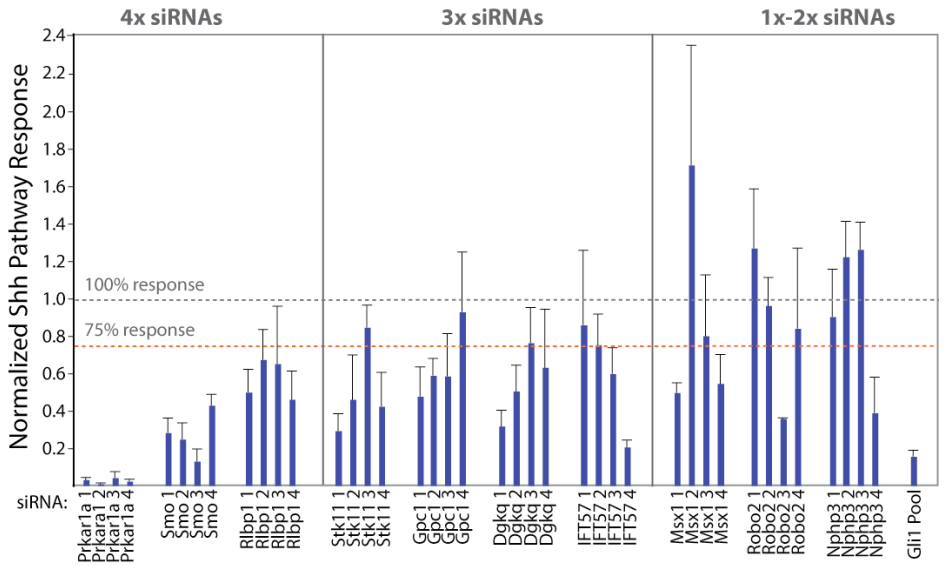

Figure 2-8 Confirmatory siRNA assays for gene function in Hh pathway response. Disease-associated genes identified in Figure 2-7 were re-evaluated using non-redundant siRNAs from each siRNA pool. Gene function in Hh pathway response confirmed by only one or two siRNAs was no longer considered. Data are represented as mean +/− SEM.

	Gene	Function	Associated disease	RNAi specificity test
Malformation	Gli2	Transcription	Holoprosencephaly	2xpools
	Stk22B/Tssk2	Kinase	DiGeorge Syndrome candidate gene (velocardiofacial syndrome)	2xpools
	Dgkq	Kinase	Wolf-Hirschhorn syndrome candidate gene (midline fusion defect)	3
	Gpc1	Receptor	Albright hereditary osteodystrophy (AHO)-like syndrome candidate gene (obesity, brachydactyly, and ectopic ossifications)	3
Degenerative disease	Rlbp1	Signaling	Retinitis pigmentosa (retinal degeneration)	4
	Aaas	Nuclear pore	Triple A syndrome (adrenal insufficiency, alacrima, achalasia)	2xpools
	Ift57/Hippi	Signaling	Bardet-Biedl type 3 syndrome candidate gene (renal failure)	3
Cancer	Smo	Signaling	Gorlin's syndrome (basal cell carcinoma, medulloblastoma, rhabdomyosarcoma)	4
	Prkar1a	Kinase	Carney Complex, Type 1 (myxomas of the heart and skin; endocrine tumors; lentiginosis)	4
	Stk11/Lkb1	Kinase	Peutz-Jeghers syndrome (pancreatic cancer, melanoma, testicular cancer, endocrine tumors; lentiginosis)	3

Table 2-1 Disease-associated genes with potential roles in Hh and Wnt signaling. Disease-associated genes that were confirmed by siRNA re-testing (either by two non-redundant siRNA pools or >/= 3x individual siRNAs; see Figure 2-8, Appendix D) were grouped based on disease-type. Multiple names for a single gene are separated by a slash.

2.2.2.4 cDNA overexpression test

A sequence verified library of 62 cDNA expression plasmids was generated, in collaboration with Xiaofeng Wu, a post-doctoral fellow in the Lum lab, for genes selected from primary screening results. Selection criteria included, but was not limited to, association with disease or primary cilia biology, transcription factor or kinase function, and availability of cDNA clones. Using the GliBS reporter as a readout of Hh pathway activity, I screened the cDNA library by transient overexpression in NIH-3T3 cells (Figure 2-9A, 2-9B). Comparison of overexpression data with RNAi results revealed 3 classes of Hh pathway effectors (2-9C, 2-9D). I was able to identify genes that potentially have dual regulatory roles in the Hh pathway as both activator and

suppressor from cases where overexpression and knockdown of a gene both significantly reduced Hh reporter activity. For the remaining two classes of genes, overexpression and RNAi produced opposite effects on Hh reporter activity and thus these genes were identified as having solely activator function or solely suppressor function.

Known Hh pathway activators, Smo, Gli1, and Gli2, increased Hh pathway activity when overexpressed, whereas overexpression of known Hh pathway suppressors decreased Hh pathway activity as expected (Figure 2-9A, 2-9B). Components of the primary cilia have both negative and positive roles in Hh cellular responses as they are required both for the production of the Gli3 transcriptional repressor (Gli3R) and activation of the Gli1 and Gli2 transcriptional activators (Huangfu and Anderson, 2005). Consistent with this role, intraflagellar transport proteins 88, 122, and 57 (IFT88, IFT122, and IFT57) decreased Hh reporter activity when overexpressed (Figure 2-9A, 2-9B) and when targeted by siRNAs (Figure 2-5, Appendix C). Interestingly, I identified Dual-specificity tyrosine-(Y)-phosphorylation regulated kinase 2 (Dyrk2) as a Hh pathway activator in the primary screen (Appendix C) despite previous studies demonstrating that Dyrk2 has suppressor function (Varjosalo et al., 2008). Comparison of primary screening results with overexpression results indicated that Dyrk2 might in fact play dual roles in Hh signaling (Figure 2-9B, 2-9D, Appendix C). In addition to supplying functional information, the use of cDNAs in this assay provided non-RNAi based confirmation of a role in Hh signaling for the genes tested.

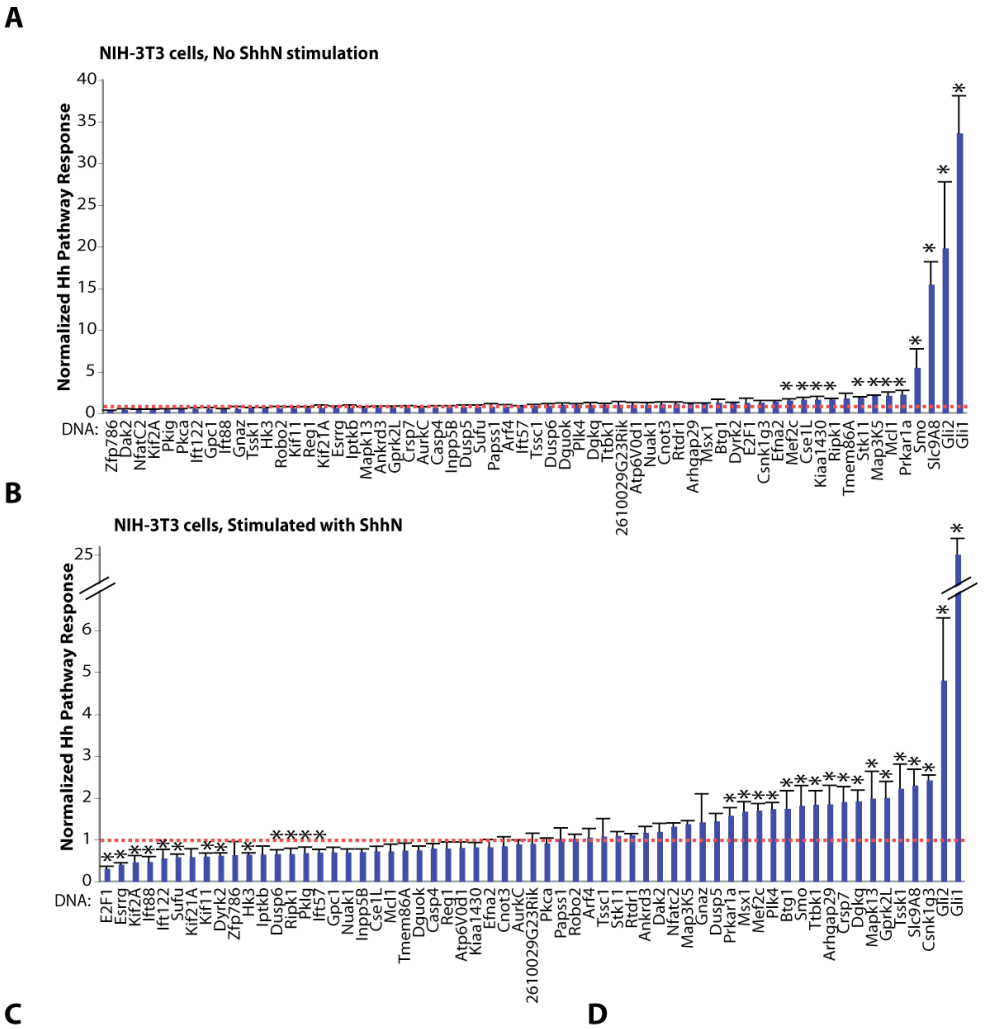

C

Result on Hh pathway		Interpretations
RNAi	OEX	
suppression	activation	**Class I genes**: Gene that functions solely as an activator
suppression	suppression	**Class II genes**: Gene has dual functions in pathway (activator and suppressor)
activation	suppression	**Class III genes**: Gene that functions soley as a suppressor

D

CLASS I		CLASS II	CLASS III
Arhgap29	Mcl1	Dusp6	Kif2A
Btg1	Mef2c	Dyrk2	Sufu
Crsp7	Msx1	E2F1	
Cse1L	Plk4	Esrrg	
Csnk1g3	Prkar1a	Hk3	
Dgkq	Ripk1	Ift122	
Gli1	Slc9A8	Ift57	
Gli2	Smo	Ift88	
Gprk2L	Stk11	Kif11	
Kiaa1430	Tssk1	Pklg	
Map3K5	Ttbk1	Ripk1	
Mapk13			

Figure 2-9 cDNA overexpression screen. A. 62 cDNA clones encoding genes identified as Hh pathway activators were overexpressed in NIH-3T3 cells without Shh stimulation. Dotted red line denotes the level of Hh pathway response when an empty

vector was overexpressed. Asterisks indicate $P < 0.05$ when sample is compared with empty vector controls. **B.** Same as "A" except in the presence of Shh stimulation. **C.** Comparison of overexpression results with RNAi results reveals three classes of Hh effectors. **D.** Genes are categorized by their potential roles in Hh signal transduction described in "C".

2.2.2.5 Transcription factor test

In an attempt to identify co-activators of Gli-mediated transcription, candidate Hh activators with known transcription effector function identified from the primary screen were tested for Gli1 binding. Using a biotinylated DNA oligonucleotide containing Gli binding sequences, I pulled down Gli1 from lysate generated from cells overexpressing Gli1 and a candidate gene (Figure 2-10). Endogenous Sufu, which co-precipitated with Gli1, served as a positive control. None of the transcription factors included in this test were found to bind to Gli1.

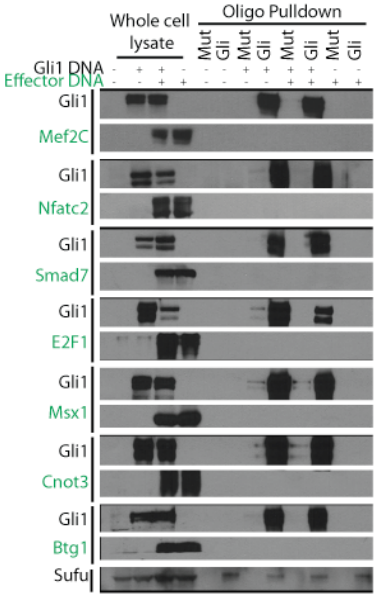

Figure 2-10 Testing the interaction between Gli proteins and other transcriptional regulators identified by genome-wide RNAi. Transcription factors were overexpressed

with Gli1 in NIH-3T3 cells. Gli1 was pulled down using a biotinylated oligonucleotide containing Gli binding sequences. Samples were analyzed by Western blot.

2.2.2.6 Cross-library test

Although the two siRNA libraries that were initially screened in parallel target many of the same genes (Figure 2-5A), only five genes (Gli1, Gli2, Kif11, Med14, and Mef2C) were identified as hits by siRNA pools from both libraries (Figure 2-11, Appendix B). The sparseness of overlapping hits between the screens of the Dharmacon and Qiagen siRNA libraries inspired additional RNAi-based studies. Novel Hh pathway activators, that do no affect Wnt response, identified in previous rounds of screening by siRNA pools from only one library (Figure 2-7, 2-11, Appendix C) were chosen as test subjects. Two known Hh pathway components, Smo and IFT88 (Ttc10), also identified by siRNA pools from only one library (Dharmacon and Qiagen, respectively) were included as controls. In an assay measuring Hh pathway response, the genes were targeted for silencing by siRNA pools from the library that failed to identify them as hits. For example, because the Aaas gene was identified to be required for Hh signaling by an siRNA pool in the Qiagen but not Dharmacon library, the Dharmacon siRNA pool targeting Aaas was selected for testing. Genes for which a corresponding siRNA pool was not arrayed in both libraries could not be retested.

I transfected the selected 46 siRNA pools into ShhLightII cells stimulated with Shh conditioned media, using conditions that minimize inherent noise associated with high-throughput screening platforms. The use of non-automated, low throughput techniques improved the overlap of hits between siRNA libraries by 10 genes or 22% for

this small dataset (Figure 2-11, Appendix C), highlighting the contribution of noise from high-throughput methodologies to the rates of false negatives in RNAi screens. Although, factors related to assay design cannot be ruled out, the inability of this approach to improve the overlap among the remaining 78% of genes in this dataset including the known Hh pathway regulators, Smo and IFT88 (Appendix C), may point to the major difference between the siRNA libraries, siRNA design (Tang et al., 2008), as a source of false negatives in RNAi screens.

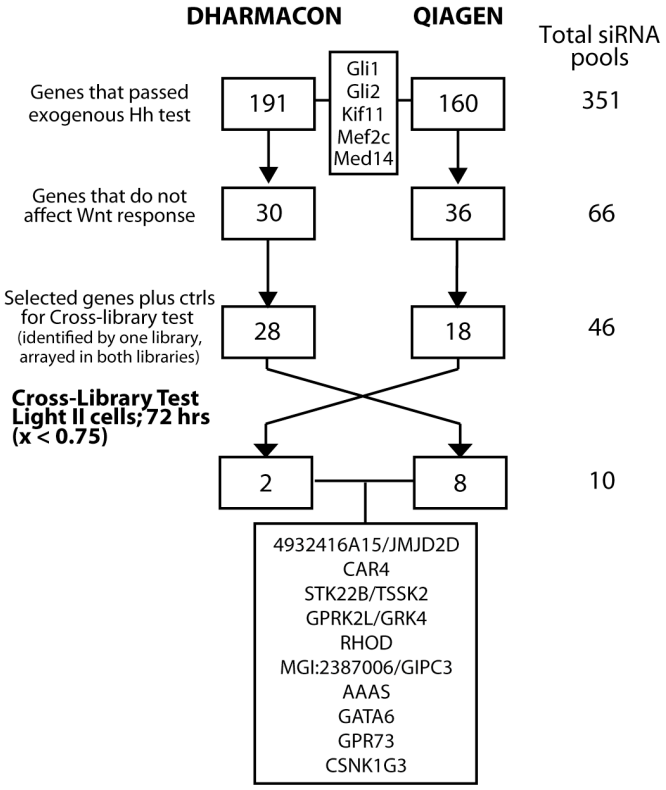

Figure 2-11 Cross-library test. From initial parallel screening of the Dharmacon and Qiagen siRNA libraries, 5 genes (Gli1, Gli2, Kif11, Mef2C, Med14) were identified by siRNA pools in both libraries. Hh pathway activators that to not affect Wnt pathway response identified by siRNAs from only one library were manually re-tested in 96 well plates avoiding wells on the edge of the plate using siRNAs targeting the same gene from the other library. A total of 18 genes could not be re-tested given a corresponding siRNA

set was not arrayed in the library. Ten additional genes were confirmed by two siRNA pools using this approach.

2.3 Discussion

2.3.1 Improvement of RNAi screening platforms

From this multi-pronged approach I have demonstrated strategies useful for coping with large datasets typically associated with RNAi screening. Whereas these large datasets may contain a great many insights into the biological process in question, the challenge lies in classifying the data in ways that allow useful information to become apparent. The application of well designed secondary screens can not only reduce unreproducible false positives in later studies but also discern additional characteristics of screening hits helpful for the selection of genes for mechanistic studies. Using secondary screening strategies I was able to identify genes that were amenable to future studies including those that co-regulate the Wnt pathway and those that are involved in disease.

These additional studies also revealed that the integration of RNAi-derived datasets is limited by the effectiveness of siRNA design and current high-throughput screening formats. Interestingly, had either of the two siRNA libraries been screened alone, many of the known pathway components would have been missed (Figure 2-5D). This fact coupled with the low overlap of hits between the parallel screens of both libraries indicated the presence of false negatives. Using the cross-library secondary screen I estimated that approximately one-fifth of the potential false negatives in my dataset were derived from noise due to high throughput technologies (Figure 2-11). The remaining four-fifths of potential false negatives could be due to other factors like siRNA

design. Poor siRNA design resulting in inefficient knockdown of the target gene or off-target effects that mask the desired phenotype may have contributed to the false negative rate. The cross-library test would have benefited from qPCR of target genes to confirm silencing of gene expression. Because vetting of the silencing efficiencies of all of the individual siRNAs (or pools) in siRNA libraries is not practical, I found that screening of multiple libraries of RNAi reagents reduces false negatives and increases genomic coverage in RNAi screens.

2.3.2 Identification of novel Hh and Wnt pathway regulators

From this screening strategy I identified several categories of genes that regulate Hh pathway activity. Discovery of co-regulators of Hh and Wnt signal transduction may not only yield exciting insights into the mechanisms of Hh and Wnt signaling but also increase our understanding of signal transduction networks and points of integration. In developing tissues, cells may encounter many concurrent or even conflicting signals. Identification of genes that regulate responses to more than one signal can shed light on how cells translate these signals into cell-fate decisions. Although a cell may be exposed to a variety of signals that coincide with Hh signals (TGFβ, Notch) I chose to study Wnt signaling due to similar modes of signal transduction between the two pathways. The shared requirement for lipid modified ligands (Porter et al., 1996; Willert et al., 2003), dynamic redistribution of pathway components upon initiation of pathway response (Corbit et al., 2005; Schwarz-Romond et al., 2007b), and proteasome-dependent regulation of transcriptional effectors (Aberle et al., 1997; Aza-Blanc et al., 1997) increases the likelihood that shared pathway components could be uncovered.

Another category of genes of interest for future studies includes novel Hh and Wnt pathway components that are associated with disease. The heparan sulfate proteoglycan, glypican 1 (Gpc1), is a homolog of the Dally-like protein (Dlp) that functions as part of the receptor complex for Hh in *Drosophila* (Lum et al., 2003a). Prkar1a, the regulatory subunit of protein kinase A (PKA), was previously identified as critical to Hh pathway response in a kinome-wide RNAi screen (Evangelista et al., 2008). Two gene products linked to ciliopathies were also identified, retinaldehyde binding protein 1 (Rlbp1) and intraflagellar transport 57 (Ift57) (Krock and Perkins, 2008; Maw et al., 1997). With the exception of Smo and Gli2, the Hh-related functions of the remaining genes [the serine-threonine kinase Stk22b, diacylglyerol kinase theta (Dgkq), and the achalasia, adrenocortical insufficiency, alacrimia syndrome (Aaas) gene] are unknown. The Stk11 tumor suppressor controls microtubule dynamics, metabolism, and cell polarity (Hezel and Bardeesy, 2008) but has not been previously implicated in Hh-mediated signaling. Given chemical tractability of the Hh and Wnt signaling pathways, identification of Hh and Wnt pathway components associated with disease broadens the number of diseases that potentially may be managed with chemical modulators of these pathways.

CHAPTER THREE

MECHANISTIC STUDIES OF HEDGEHOG PATHWAY COMPONENTS IDENTIFIED BY RNAI SCREENING

3.1 Introduction

The role of the primary cilium in the activation of the Hh pathway has been well validated but poorly understood. In the absence of Hh ligand, the Hh receptor Patched1 (Ptch1) localizes to the base of the cilia (Rohatgi et al., 2007). Upon pathway activation the positive Hh effector Smoothened (Smo) moves into the cilia (Corbit et al., 2005) and Ptch is shuttled away from the cilia (Rohatgi et al., 2007). Gli molecules have been shown to localize to the cilia (Haycraft et al., 2005) and components of the primary cilia are required for both the activator and repressor functions of Gli proteins (Huangfu and Anderson, 2005; Liu et al., 2005). The dual requirement for cilia in both the activation and repression of the pathway confounds attempts to dissect the mechanisms involved in each. Inhibition or knockdown of the proteins that facilitate transport of proteins within in the primary cilia reduces Hh pathway activity while also restricting production of repressors (Huangfu and Anderson, 2005; May et al., 2005). The identification of novel ciliary regulators may facilitate a mechanistic understanding cilia function with respect to Hh signal transduction.

In this chapter, the roles in the Hh pathway of three genes identified from RNAi screening (Chapter 2) are carefully examined. I found that Stk11, a serine/threonine kinase that influences cell polarity and microtubule dynamics (Hezel and Bardeesy, 2008), functions to maintain primary cilia length and to control abundance of the Gli3

transcriptional repressor. Prkar1a has been previously identified to regulate Hh signaling (Evangelista et al., 2008), however, its mode of action has not been verified. I show that Prkar1a is required for Hh signaling by restricting the abundance of the Gli3R. The Na+/H+ exchanger solute carrier 9A8 (SLC9A8) (Goyal et al., 2003; Zhang et al., 2007) has with no previous association with the Hh pathway. The studies presented here suggest that the ion exchange function of SLC9A8 is important for its role in Hh signaling and that localization of Smo to the primary cilia may be dependent on this activity by SLC9A8.

3.2 Results

3.2.1 Stk11 influences Hh pathway response through control of GliR abundance and regulation of primary cilia length

3.2.1.1 Stk11 is required for Hh response

Analysis of the transcriptional response to Shh in mouse embryonic fibroblasts (MEFs) null for STK11, by examination of GliBS reporter activity and Ptch1 expression, confirmed that loss of Stk11 decreased Hh pathway response (Figure 3-1A, 3-1B, 3-1C). Because Stk11 has been reported to have a nutrient sensing function (Shaw et al., 2004b), it is possible that the low serum conditions typically used to test Hh pathway activity contributed to the previous observations. However, knockdown of STK11 in NIH-3T3 cells under both high and low serum conditions were shown to reduce Hh pathway response (Figure 3-1D).

I also investigated the role of Stk11 *in vivo* by analyzing zebrafish embryos treated with morpholino oligonucleotides (MOs) targeting *stk11*. Consistent with reduced Hh signaling (Lewis et al., 1999), the Stk11 morphants exhibited U-shaped somites when analyzed at 24 hours post fertilization (hpf) (Figure 3-2A). A subset of Stk11 morphants exhibited shortened tails, a phenotype that may arise from altered non-canonical Wnt-mediated responses (Marlow et al., 2004) (Figure 3-2A). *Engrailed 1a* (*eng1a*) expression, which is associated with high levels of Hh response (Wolff et al., 2003), was also reduced in the Stk11 morphants in the midbrain-hindbrain boundary and muscle pioneers (Figure 3-2B). *Ptch1* expression appeared unaffected in Stk11 morphants (Figure 3-2C), suggesting that Stk11 may not be required for low levels (Wolff et al., 2003) of Hh response *in vivo*.

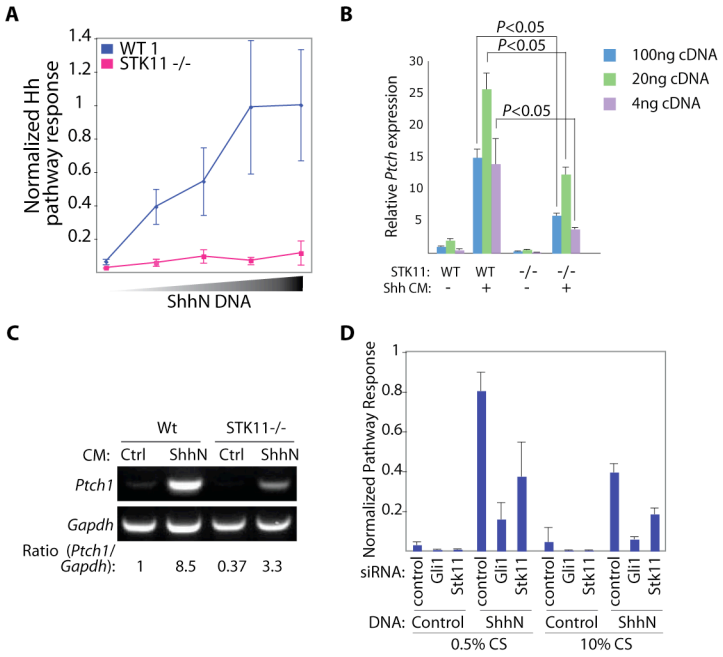

Figure 3-1 Hh pathway response requires Stk11. A. MEFs null for STK11 fail to achieve normal levels of Hh pathway response. MEFs were transfected with the GliBS

reporter, control reporters, and increasing amounts of ShhN cDNA. Mean and SD are shown. The experiment was performed in triplicate. **B.** STK11−/− MEFs have dampened transcriptional response to exogenous ShhN. qPCR analysis of *Ptch1* expression in wild-type (WT) and STK11−/− MEFs in the presence or absence of Shh stimulation. PCR was performed from different concentrations of total cDNA generated from RNA samples, analyzed, and compared to test reproducibility. *Ptch1* transcript abundance was normalized to *Gapdh* (glyceraldehyde-3-phosphate dehydrogenase). Graph shows mean and SD from three samples. (*Panel B by Ozlem Kulak*) **C.** RT-PCR–based confirmation of qPCR results. *Ptch1* RT-PCR results from WT and STK11−/− cells in the presence and absence of Shh-conditioned medium (CM) also show reduced responsiveness of STK11−/− cells to Shh. **D.** The role of STK11 in Hh response does not appear to be dependent upon nutrient availability. NIH-3T3 cells were co-transfected with reporters, plasmids encoding Shh or control, and siRNAs under low and high serum conditions. Experiment was performed in triplicate.

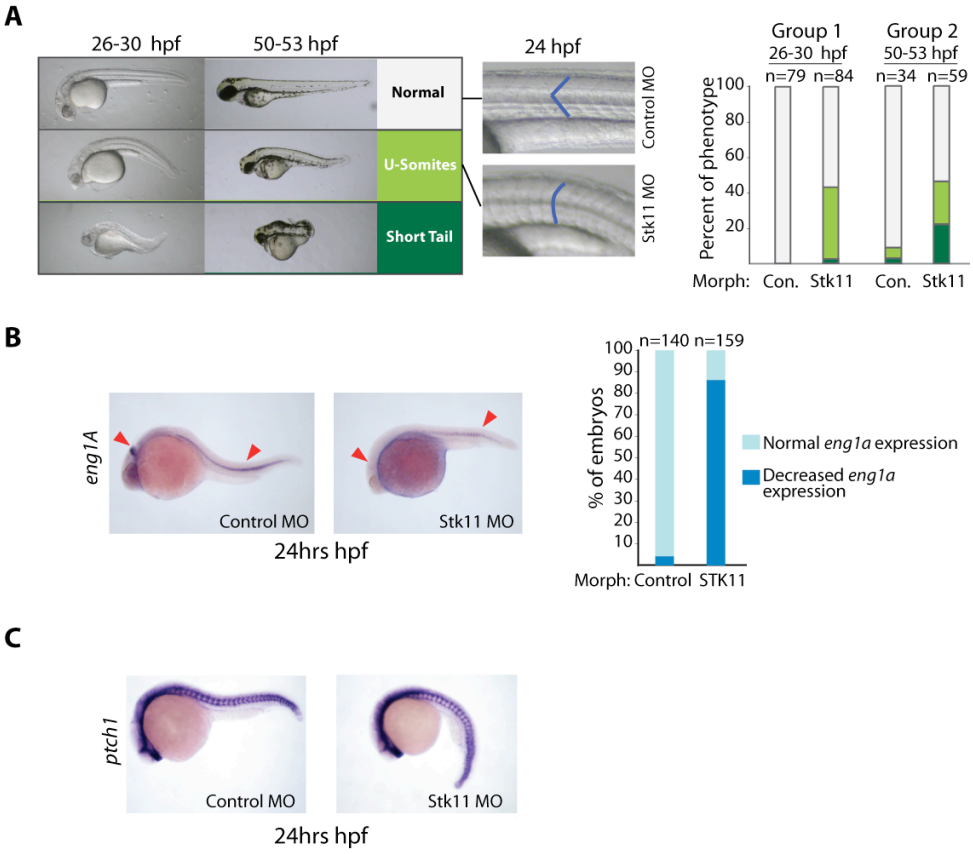

Figure 3-2 Knockdown of *stk11* in zebrafish embryos yields phenotypes consistent with Hh and Wnt signaling defects. A. Zebrafish injected with MO against *stk11* show

U-shaped somites, shortened tails, or no detectable change in body patterning. Phenotypic analysis was performed at two different developmental stages (groups 1 and 2) in separate experiments. The left side shows representative embryos of each phenotype and the right side shows quantification. hpf, hours postfertilization. **B.** Loss of *stk11* reduces expression of *Engrailed 1A* (*eng1a*), a target gene induced by Hh signaling. Quantification of embryos with decreased *eng1a* expression at the midbrain-hindbrain boundary and muscle pioneers. In situ hybridization with digoxigenin-labeled antisense probes against *eng1a* mRNA was performed at 24 hpf. More than 100 animals were scored in each condition. **C.** Knockdown of *stk11* does not produce a detectable change in *ptch1* expression. In situ hybridization with digoxigenin-labeled antisense probes against *ptch1* mRNA was performed at 24 hpf. Images are representative of more than 100 animals scored in each condition.

3.2.1.2 Stk11 controls the abundance of the Gli3 transcriptional repressor

STK11-/- MEFs also exhibited increased Gli3R abundance relative to WT MEFs that cannot be accounted for by changes in the Gli3 expression (Figure 3-3A, 3-3B). Rather than an overall increase in Gli3 protein, I found that the proteolytically processed form was selectively increased as noted by the difference in the ratio of Gli3R to full length Gli3 (Gli3FL) between WT and STK11-/- MEFs (Figure 3-3A). The abundance of Gli3R in STK11-null cells was reduced in the presence of Shh protein ligand or a Smo agonist (SAG), suggesting that Smo function was intact (Figure 3-3A).

Using pulse-chase analysis, following either addition of SAG or Hh-conditioned medium, I confirmed that the rate of Gli3R formation was increased by nearly three fold in STK11-null MEFs relative to that in wild-type MEFs (Figure 3-4A). Furthermore, in the presence of a proteasome inhibitor, which blocks Gli3R production (Wen et al., 2010), the stability of Gli3R does not appear to be increased in STK11-null MEFs when compared to WT MEFs (Figure 3-4B). Thus, alteration of Gli3R turnover rate does not appear to contribute to the accumulation of Gli3R observed in STK11-null MEFs.

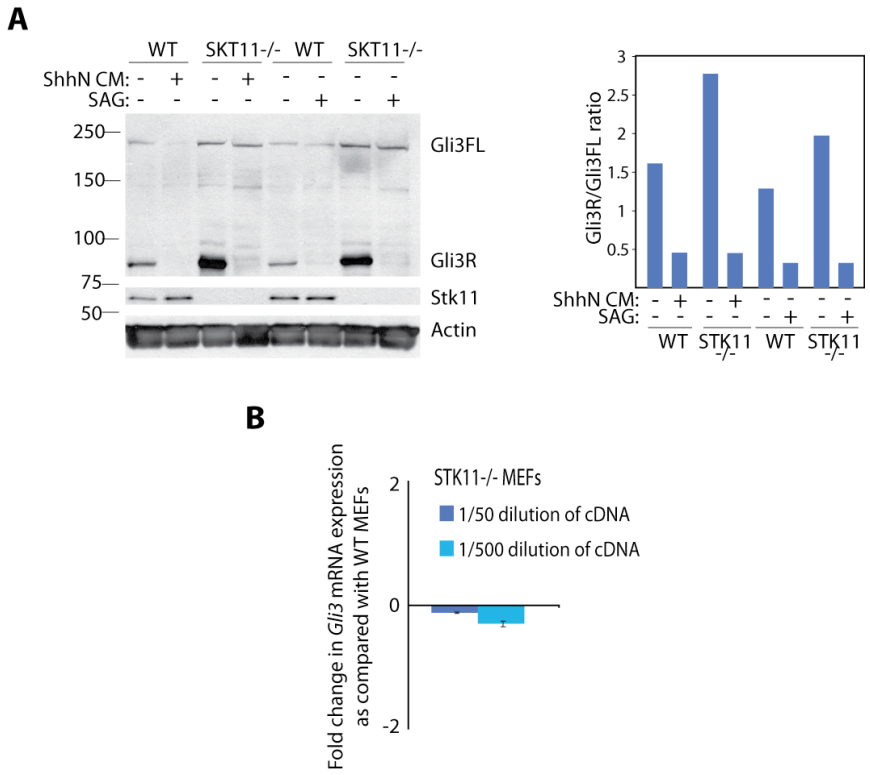

Figure 3-3 Loss of Stk11 increases the abundance of GliR. **A.** Stk11 regulates Gli3R abundance. STK11−/− MEFs exhibit increased abundance of Gli3R that is inhibited by Hh pathway activation. Graph shows quantification of results by densitometry. A representative of three independent experiments is shown. **B.** WT and STK11-/- MEFs express comparable levels of *Gli3*. PCR was performed from different dilutions of total cDNA generated from RNA samples, analyzed, and compared to test reproducibility. *Gli3* transcript abundance cells is normalized to *Gapdh*. Values are shown as the fold change between Stk11-/- cells and WT cells. Graph shows average and SD from 3 samples. (*Panel B by Ozlem Kulak*).

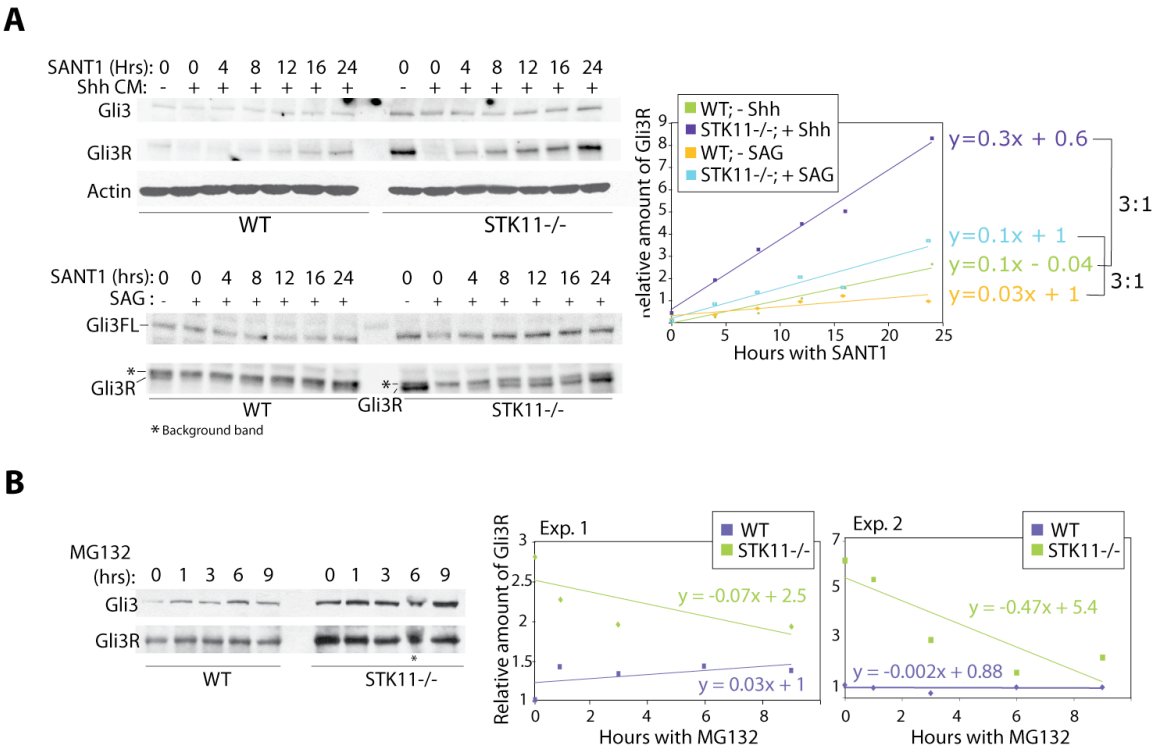

Figure 3-4 Kinetics of Gli3 formation and destruction in the absence of Stk11. A. STK11−/− MEFs exhibit an accelerated rate of Gli3R accumulation. WT or STK11−/− MEFs were treated with Shh CM or Smo agonist (SAG) overnight to inhibit Gli3 processing. Shh CM or SAG was then removed and replaced with the Smo inhibitor SANT1 to allow processing to proceed. Cells were lysed at indicated time points. Quantification (right) indicates that the rate of Gli3R accumulation is three times faster in the absence of Stk11 as calculated from two independent experiments. Rate of Gli3R formation was calculated from the slope of each line. Gli3R abundance is calculated relative to abundance of Gli3R in WT cells at 0 hours of SANT1 treatment in the absence of Shh CM or SAG. **B.** Gli3R destruction is accelerated rather than slowed in STK11−/− MEFs. WT or STK11−/− MEFs were treated with the proteasome inhibitor MG132 for various time periods to restrict new formation of Gli3R by proteasome-dependent proteolytic processing. Gli3R abundance was determined by Western blot analysis and quantified by normalizing to Gli3R in WT cells in the absence of MG132. The asterisk indicates result not used for quantification. Data shown are representative of two experiments.

3.2.1.3 Stk11 regulates primary cilia length

To further understand the mechanism underlying the Stk11-induced increase in the abundance of Gli3R, the primary cilium, an organelle essential for proteolytic processing of Gli molecules into transcriptional repressors (Haycraft et al., 2005; Huangfu and Anderson, 2005), was examined. The cilia in STK11-/- cells were on average one-half the length of their counterparts in wild-type cells, suggesting a defect in achieving the normal length of this organelle in STK11-/- cells (Figure 3-5A). Examination of cilia in STK11-/- cells by transmission electron microscopy confirmed the establishment of a basal body, the cellular anchor of cilia, and the ability of STK11-/- cells to elaborate rudimentary cilia (Figure 3-5B). Because the dynamics of cilia formation and disassembly are influenced by the cell cycle and STK11-/- MEFs double more rapidly than do WT MEFs (Bardeesy et al., 2002) (Figure 3-5C), I analyzed the propensity of the WT and STK11-/- MEFs to exhibit growth arrest under conditions typically used to examine primary cilia (low serum, high cell density). Both cell lines achieved cell cycle arrest at confluency, suggesting that the differences in primary cilium length are not attributable to changes in the duration of cell cycle phases (Figure 3-5D).

To determine if shortened cilia length perturbed the ability of Hh pathway components to accumulate in the primary cilium in response to Shh (Corbit et al., 2005; Rohatgi et al., 2007), Smo and Gli2 localization were analyzed by immunofluorescence. Consistent with the ability of Hh and SAG to block Gli3 processing (see Figure 3-3A), the translocation of Smo into the cilium and accumulation of Gli2 protein at the tip of the cilium in response to Shh appeared normal in the STK11-/- cells (Figure 3-6A, 3-6B).

Thus, the excessive accumulation of Gli3R in STK11-/- cells is not likely due to altered subcellular localization of Smo or Gli proteins.

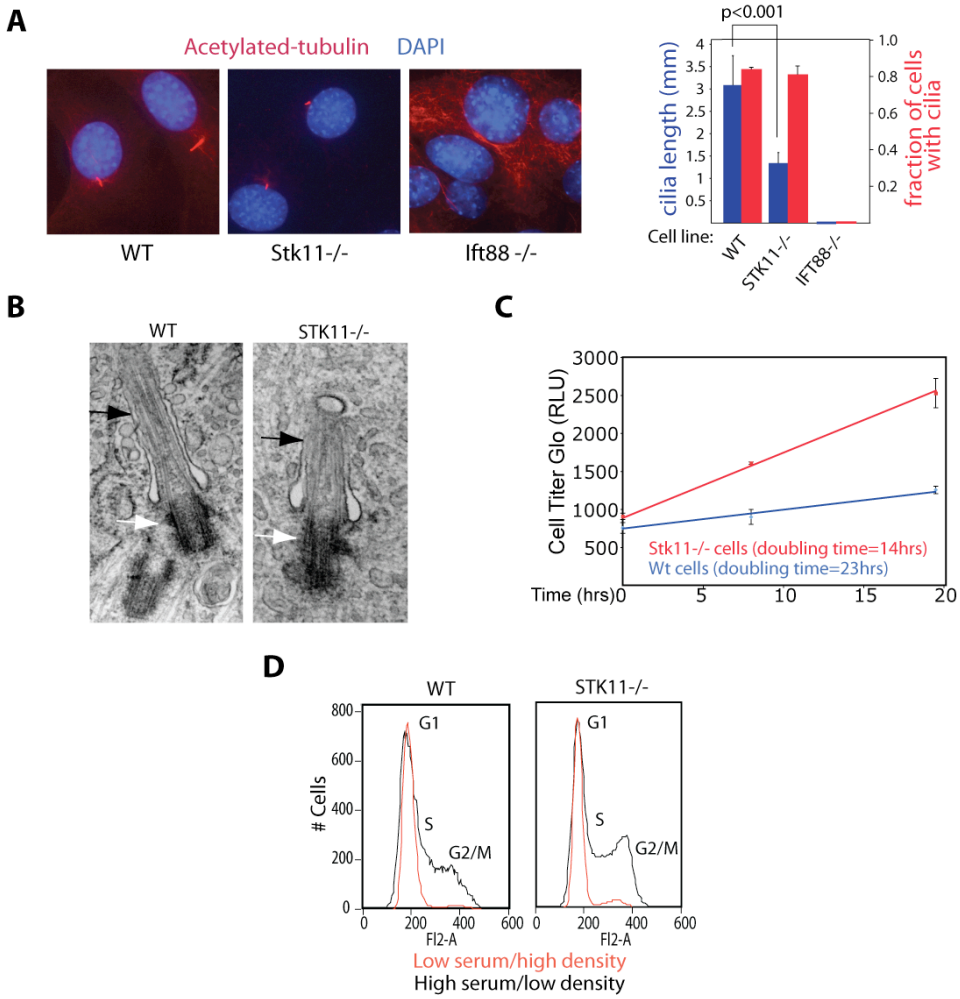

Figure 3-5 Stk11 is required for primary cilia maintenance in embryonic fibroblasts. **A.** MEFs were immunostained for acetylated tubulin to detect the primary cilium. Unlike cells lacking the ciliary component IFT88, a rudimentary primary cilium is observed in STK11−/− cells. Cells lacking Stk11 do not have a defect in establishing cilia. MEFs of the indicated genotype were scored for the presence of cilia and cilia length by immunofluorescence. Data show the mean and SD of >35 cells per condition. (*Panel A by Xiaofeng Wu*). **B.** Ultrastructural analysis of the primary cilium in STK11−/− cells by transmission electron microscopy. No gross defects in the basal body (white arrows) and axoneme (black arrows) are observed in STK11−/− cells. Image of STK11−/− cilia is

representative of four samples. **C.** STK11-/- MEFs exhibit increased rate of doubling time as compared to WT MEFs. Cell number was measured using Cell Titer Glo assay that determines levels of ATP produced by cells. This experiment was performed in triplicate. **D.** WT and STK11−/− MEFs show comparable cell cycle response to serum and cell density. Cells were grown in either high-serum/low-density conditions or low-serum/high-density conditions for 24 hours, stained with propidium iodide, and subjected to FACS (fluorescence-activated cell sorting) analysis.

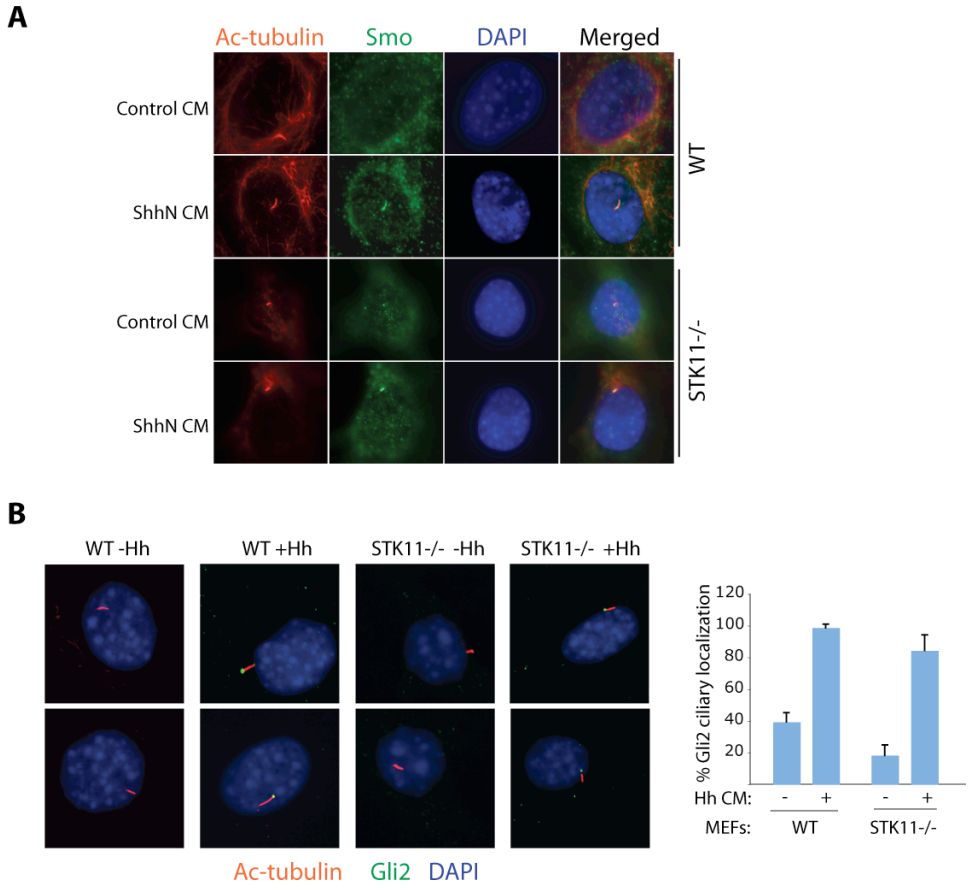

Figure 3-6 Hh-induced Smo or Gli protein accumulation in the primary cilium is not affected in STK11-/- cells. **A.** Endogenous Smo protein and acetylated tubulin were detected by immunofluorescence in the presence and absence of Shh conditioned media. **B.** Gli2 protein localizes to the tip of the primary cilium in STK11-/- MEFs treated with Hh conditioned medium. (*Panel B by Chih-Wei Fan*).

The tubulin deacetylase HDAC6 promotes ciliary disassembly and thus influences cilia length (Pugacheva et al., 2007). Addition of suberoylanilide hydroxamic acid (SAHA), an inhibitor of deacetylases including HDAC6 (Carey and La Thangue, 2006; Finnin et al., 1999; Richon et al., 1998), increased the abundance of acetylated tubulin which is otherwise decreased in STK11-/- cells as compared to WT cells (Figure 3-7A, 3-7B). Concomitantly, I found that SAHA increased cilia length in STK11-/- cells but not in WT cells, suggesting that STK11-/- cells undergo excessive cilia disassembly (Figure 3-7C, 3-7D). Consistent with this model, the HDAC6 inhibitor tubacin, but not the HDAC1 inhibitor MS-275, restored cilia length in STK11-/- cells (Figure 3-7D). The extension of primary cilia in SAHA-treated cells also correlated with restoration of Gli3R to an amount similar to that in WT cells (Figure 3-7E). Considering that Gli proteins must cycle through the primary cilium to acquire PKA-dependent phosphorylation prior to proteolytic processing in the cytoplasm (Humke et al., 2010; Huntzicker et al., 2006; Kim et al., 2009a; Pan et al., 2006) the increased abundance of the GliR molecules may be due to decreased transit time of full-length Gli molecules in the shortened cilia. However, the contribution of other Stk11-dependent mechanisms that may directly influence Gli processing cannot be discounted.

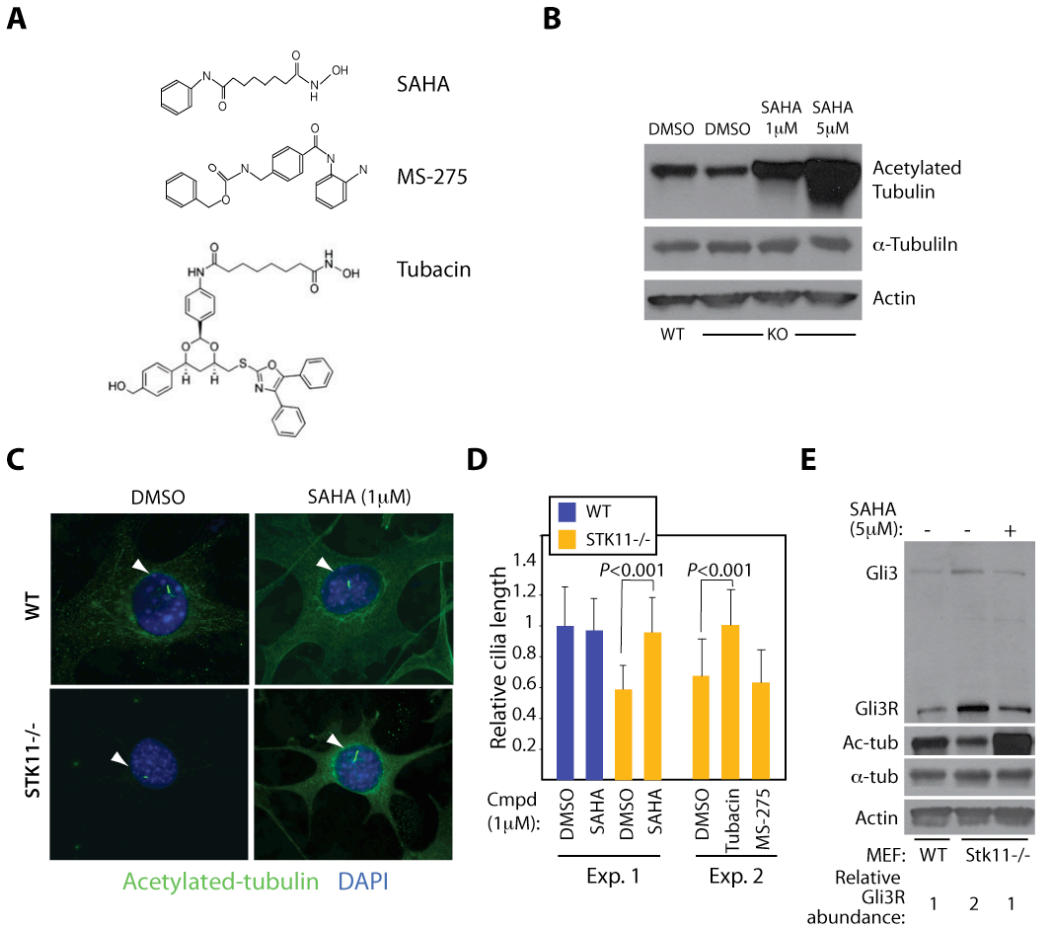

Figure 3-7 HDAC inhibitors rescue defects in Hh signal transduction caused by Stkll loss. **A.** Chemical structures of several classes of HDAC inhibitors. Tubacin and MS-275 exhibit selectivity for HDAC6 and HDAC1, respectively. **B.** Acetylated tubulin abundance is decreased in Stk11-/- MEFs compared to WT. HDAC inhibitors increase the abundance of acetylated tubulin. Cells were treated with SAHA for 24 hours before analysis by western blot. **C.** HDAC inhibition restores primary cilium length in STK11−/− cells. MEFs treated with the nonselective HDAC inhibitor SAHA were stained for acetylated tubulin. DMSO, dimethyl sulfoxide. **D.** HDAC6 inhibition restores primary cilium of STK11−/− cells to normal length. Quantification of results in "C" (Exp. 1) and analysis of the specific HDAC6 inhibitor tubacin and the HDAC1 inhibitor MS-275 on cilia length in STK11−/− cells (Exp. 2). Fifty cells were counted in each experiment. **E.** SAHA treatment of STK11−/− MEFs reduces the abundance of Gli3R. Abundance of Gli3R relative to actin was quantified by Western blot analysis and normalized to WT sample. Acetylated tubulin abundance serves as a positive control for SAHA activity. Data are representative of three experiments.

3.2.2 Prkar1a regulates the abundance of Gli3 transcriptional repressor

By analyzing Hh pathway response in mouse embryonic fibroblasts (MEFs) null for PRKAR1a, I confirmed that loss of PRKAR1a decreased Hh pathway response (Figure 3-8A). Whereas the requirement for Prkar1a in Hh-induced expression of Ptch1 has been reported (Evangelista et al., 2008), its mechanism of action within the pathway has not been well interrogated. In accordance with the role of PKA in Gli processing (Huntzicker et al., 2006; Pan et al., 2006), I found that loss of PRKAR1a results in an increase in the amount of Gli3 repressor (Gli3R) presumably as a result of unregulated PKA activity (Figure 3-8B).

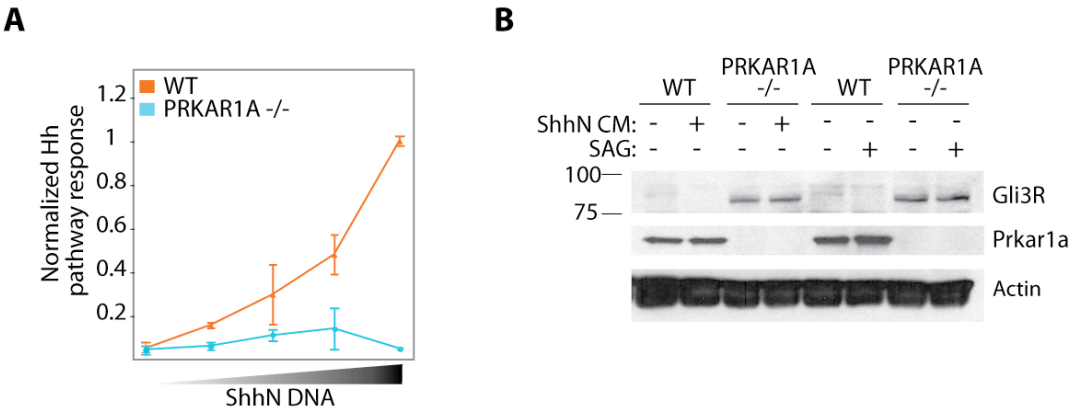

Figure 3-8 Decreased Hh pathway response induced by compromised Prkar1a function is associated with increased abundance of GliR. A. MEFs null for PRKAR1a fail to achieve normal levels of Hh pathway response. MEFs were transfected with the GliBS and control reporters and increasing amounts of ShhN cDNA. Mean and SD are shown. The experiment was performed in triplicate. **B.** MEFs deficient in PRKAR1a exhibit increased formation of Gli3R, even in the presence of Hh signaling mediated by addition of ShhN CM or SAG, as measured with Western blot analysis. Data shown are representative of two experiments.

3.2.3 The ion exchange function of SLC9A8 may contribute to Hh pathway regulation

Solute carrier 9A8 (SCL9A8) is a Na+/H+ exchanger (Goyal et al., 2003; Zhang et al., 2007) that I identified as a Hh pathway activator by RNAi screening and cDNA overexpression studies (Chapter 2). I found that the ability of SLC9A8 to activate the Hh pathway was not shared by other SLC9A family members. SLC9A1, SCL9A5 and SLC9A7 were unable to reduce Hh reporter activity when knocked down in the RNAi screen or increase Hh reporter activity when overexpressed (Figure 3-9A). Mutation of a residue critical for the ion exchange function of SLC9A8 (Khadilkar et al., 2001) hindered SLC9A8 mediated Hh pathway activation (Figure 3-9B). Along with Xiaofeng Wu, a post-doctoral fellow in the Lum lab, a small molecule inhibitor of Na+/H+ exchangers including SLC9A8, 5-(N-ethyl-n-isopropyl)-amiloride (EIPA) (Zhang et al., 2007), was found to inhibit movement of Smo to the primary cilia in a dose dependent manner (Figure 3-9C). Taken together this data suggests that SLC9A8 may play an important role Hh signal transduction and that regulation of Smo localization may involve in the maintenance of a homeostatic pH gradient across the cell membrane.

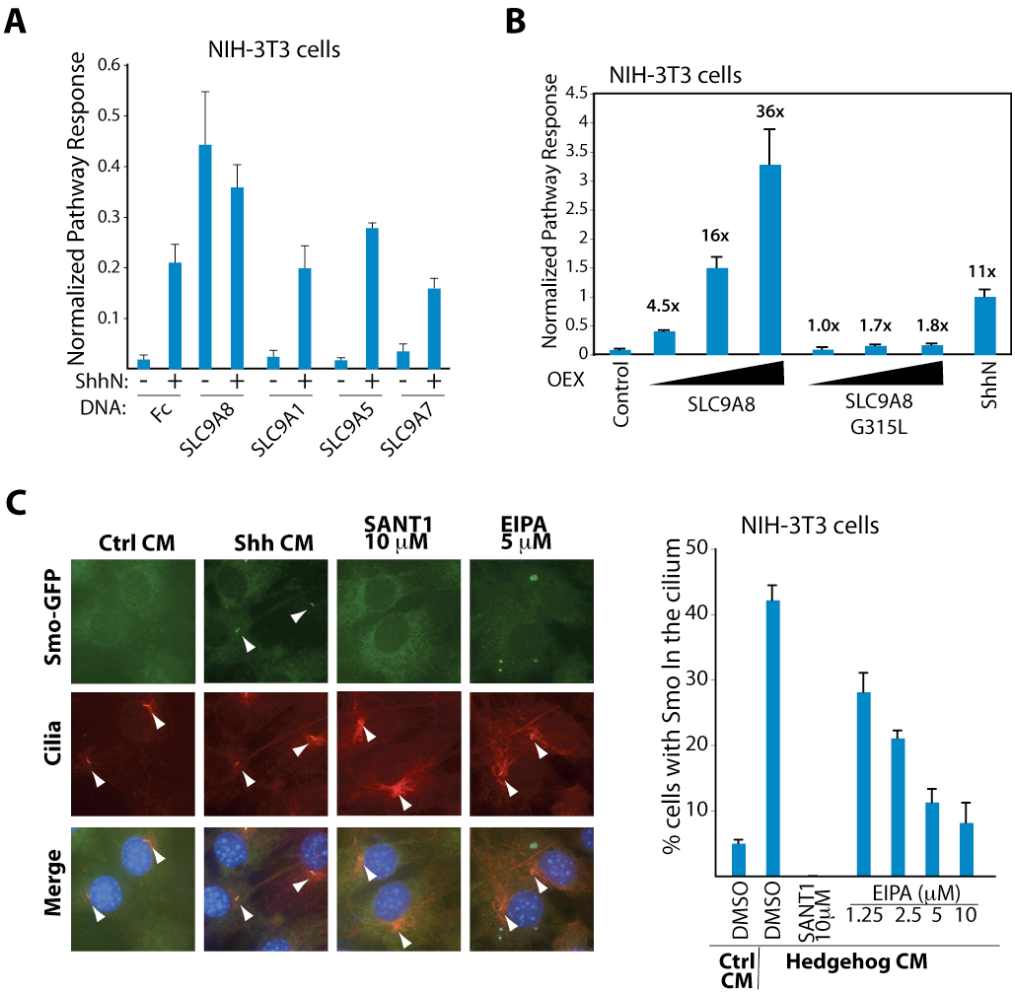

Figure 3-9 SLC9A8 positively regulates Hh pathway activity. **A.** Overexpression of SLC9A8 but not other SLC9A family members is sufficient to activate Hh pathway response. NIH-3T3 cells were transfected with reporters, plasmids encoding control or Shh, and SLC9 family members. The experiment was performed in triplicate. Mean and SD are shown. **B.** Activation Hh pathway response by SLC9A8 is dependent on its ion exchange function. Transfection of increasing amounts of WT SLC9A8 DNA, but not mutant SLC9A8 (G315L) DNA, induces a dose dependent increase in Hh pathway activity. The experiment was performed in triplicate. Mean and SD are shown. **C.** The SLC9A8 inhibitor EIPA blocks Smo accumulation in the primary cilium. Accumulation of GFP-tagged Smo in cells treated with Hh conditioned medium (CM) can be abrogated by addition of EIPA. SANT1, a Smo antagonist, serves as a positive control. Primary cilium is visualized using an acetylated tubulin antibody. (*Panel C by Xiaofeng Wu*).

3.3 Discussion

Proteolytic processing of Gli proteins entails their cycling through the primary cilium to acquire PKA-dependent phosphorylation (Humke et al., 2010; Huntzicker et al., 2006; Kim et al., 2009a; Pan et al., 2006). However, this process has been difficult to study given that genetic approaches to disrupt intraciliary trafficking through targeted deletion of intraflagellar trafficking (IFT) complex components typically results in disruption of ciliogenesis, as well as Gli processing (Huangfu and Anderson, 2005; Liu et al., 2005; Tran et al., 2008). My observations in STK11-null cells suggest that the length of the primary cilium controls the rate of Gli processing. The ability of the tubulin deacetylase inhibitors SAHA and tubacin to influence cilia length in STK11-/-, but not wild-type, MEFs argues that Stk11 plays an important regulatory role in limiting ciliary disassembly and that chemicals targeting HDAC6 maybe useful in restoring some aspects of Stk11-induced pathology (Figure 3-10).

Whereas the requirement of Protein Kinase A (PKA) for the proteolytic processing of Gli proteins has long been known (Huntzicker et al., 2006; Pan et al., 2006), the influence of the regulatory subunit of PKA (Prkar1a) on Gli repressor production has not been previously addressed. I show that Prkar1a is required for Hh signal transduction through its role in restricting production of GliR (Figure 3-10B). Analysis of a third gene identified by genome-wide RNAi screening, SLC9A8, indicated that the transport of ions is important for Hh pathway response (Figure 3-10C). Future studies of this phenomenon may provide interesting clues into the mechanisms of Smo regulation.

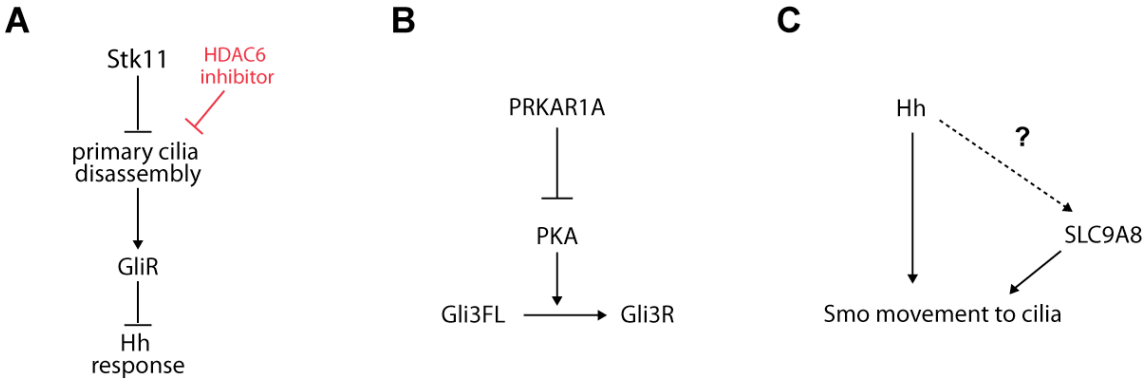

Figure 3-10 Mechanistic roles of Hh activators identified from RNAi screening. A. Stk11 regulates Hh signaling by maintenance primary cilia integrity that in turn controls levels of GliR. In the absence of Stk11 derangements in molecular events important for Hh signaling can be chemically countered by inhibitors of HDAC6. **B.** PRKAR1A control levels of the GliR by regulating PKA function. **C.** SLC9A8 ion exchanger function is required for Smo movement to the primary cilia, however it is unknown if SLC9A8 is regulated in a Hh dependent manner.

CHAPTER FOUR

THE TUMOR SUPPRESSOR STK11 NEGATIVELY REGULATES WNT SIGNALING THROUGH CONTROL OF DVL FUNCTION

4.1 Introduction

Several classes of cancers arise from mutations of the tumor suppressor Stk11 (also known as LKB1) including thirty percent of lung cancers (Ji et al., 2007; Sanchez-Cespedes et al., 2002) as well as endometrial and cervical cancers (Contreras et al., 2008; Wingo et al., 2009). Downstream transcriptional and kinase targets of Stk11 have been implicated in the pathogenesis these cancers (Carretero et al., 2010; Contreras et al., 2010; Ji et al., 2007), however, the molecular mechanisms that drive cell proliferation in the absence of Stk11 have not been well defined. In the present study I show that Stk11, which is required for Hh signal transduction (Chapter 2, Chapter 3), negatively regulates cellular responses to Wnt ligands. Loss of Stk11 results in misactivation of Dvl. The requirement of Stk11 to regulate Dvl activity can be extended into cancerous cells. I show that cervical and lung cancers cell lines lacking Stk11 exhibit aberrant Dvl phosphorylation that translates into increased Wnt pathway responses in a cell context dependent manner. Also, I demonstrate that small molecules targeting Wnt pathway response can counter some of the deviant Wnt pathway activity associated with Stk11 loss.

4.2 Results

4.2.1 Loss of Stk11 induces a gain of Dvl protein function

By examining the biochemical changes associated with Wnt/β-catenin pathway activity in STK11-/- MEFs, I found that the amount of phosphorylated Dvl2 was increased compared to that in WT MEFs (Figure 4-1A, 4-1B). This phosphorylation was not sensitive to HDAC6 inhibitors, suggesting that in MEFs, acetylated tubulin abundance does not affect Dvl protein phosphorylation (Figure 4-1C). Altered pathway activity was interrogated with a synthetic Wnt pathway inhibitor that targets the pathway at the level of Wnt production [Inhibitor of Wnt Production (IWP), an inhibitor of the acyltransferase Porcupine] (Chen et al., 2009) (Figure 4-1D). The IWP compound restored the ratio of phosphorylated to unphosphorylated Dvl proteins in STK11-/- MEFs to that observed in WT MEFs suggesting that the increased Dvl activity is dependent upon production of endogenous Wnt protein (Figure 4-1E). Dvl phosphorylation in Stk11-/- cells can also be disrupted with 5-(tetradecyloxy)-2-furoic acid (TOFA), an inhibitor of acetyl CoA-carboxylase (ACC) which catalyzes an essential step in the production of palmitoyl-CoA (Halvorson and McCune, 1984; McCune and Harris, 1979), the substrate in Porcn-mediated protein acylation (Figure 4-1F) (Kadowaki et al., 1996; Takada et al., 2006). The inability of the mTOR pathway inhibitor rapamycin to do the same suggests that the misregulation of Dvl is independent of this pathway commonly associated with Stk11 (Figure 4-1G) (Shaw et al., 2004a). Phosphorylation of Dvl2 by casein kinase 1 (CK1) family members at consensus CK1 phosphorylation sites contributes to both β-catenin-dependent and noncanonical Wnt signal transduction (Bryja

et al., 2007). Consistent with the ligand-dependent activity of Dvl in STK11-/- MEFs, inhibition of CK1, reduced Dvl phosphorylation (Figure 4-1H); whereas an inhibitor of PKA had little effect on Dvl phosphorylation (Figure 4-1I).

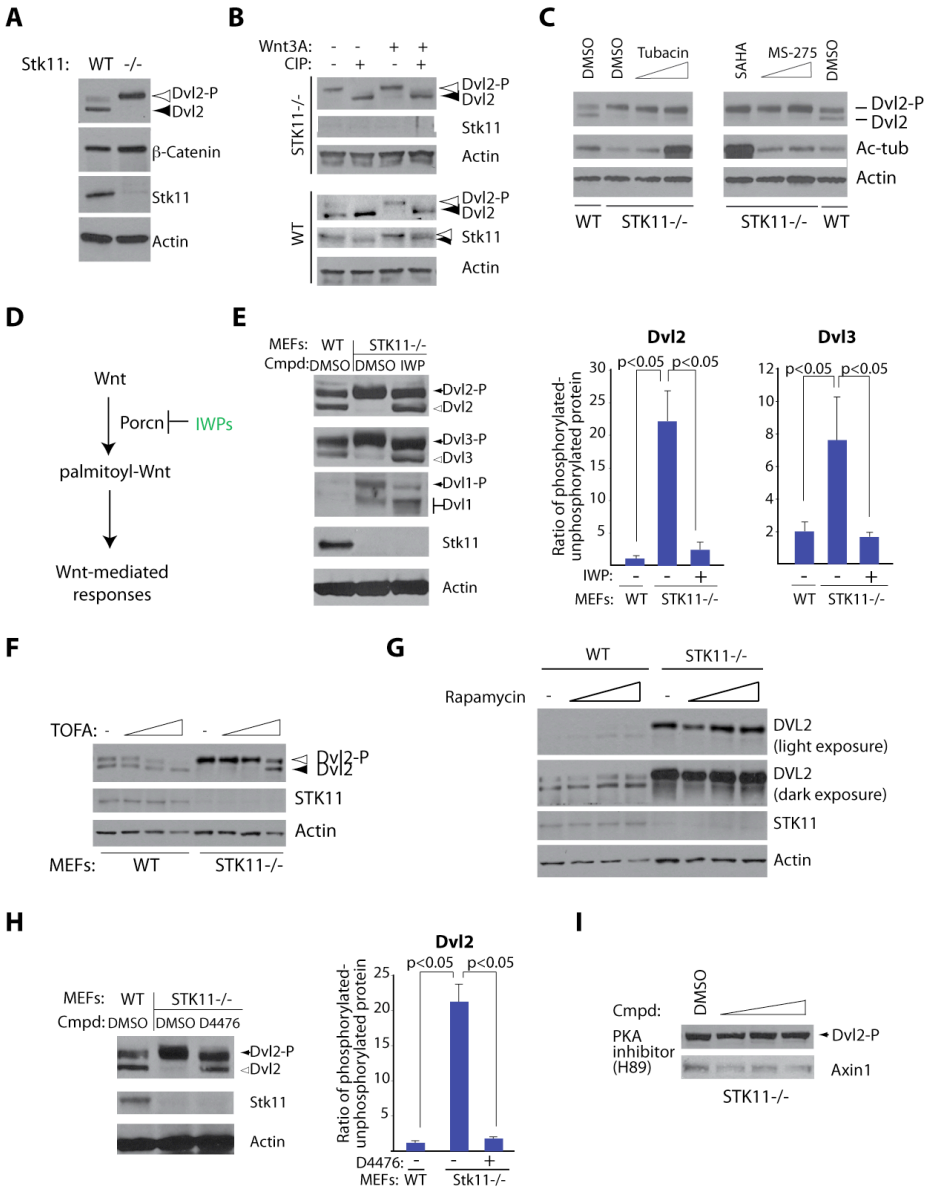

Figure 4-1 Loss of Stk11 increases Dvl phosphorylation. A. Phosphorylated Dvl2 is abundant in MEFs lacking Stk11. In the absence of Stk11 a slower migrating form of

Dvl is enriched. Data are representative of three experiments. **B.** Dvl2 is phosphorylated in STK11-/- cells. Phosphatase treatment of cell lysates derived from STK11-/- cells confirms the slower migrating band recognized by the Dvl2 antibody as phosphorylated Dvl protein. CIP= calf intestinal phosphatase. **C.** Inhibition of HDAC6 does not alter Dvl protein phosphorylation. Tubacin and SAHA, but not MS-275, an inhibitor HDAC1-3, induces accumulation of acetylated tubulin in agreement with their relative activity against HDAC6. **D.** The IWP compound inhibits Porcupine (Porcn), an acyltransferase essential for Wnt protein production (Chen et al., 2009). **E.** Increased Dvl2 and Dvl3 phosphorylation in STK11−/− cells is inhibited by IWP (2.5 μM), indicating that Dvl phosphorylation is dependent on production of Wnt. Results performed from three independent experiments are quantified. The abundance of Dvl1 is increased in STK11−/− cells compared to WT cells, and the relative abundance of phosphorylated to unphosphorylated proteins was not quantified. **F.** The acetyl-coA (ACC) enzyme inhibitor TOFA mimics the effects of IWP on Dvl2 phosphorylation in wild-type and STK11-/- MEFs. Given the role of ACC in the production of palmitoyl-CoA, a co-factor essential to Wnt protein production, this observation further supports previous conclusions that the IWP compounds to inhibit Wnt protein production. **G.** Dvl regulation by Stk11 does not appear to be dependent on mTOR pathway activity. Phosphorylation patterns of Dvl2 in WT and Stk11-/- MEFs do not change with Rapamycin treatment, an inhibitor of mTOR pathway activity. **H.** Application of the CK1 inhibitor D4476 (0.2 mM) to STK11−/− cells inhibits Dvl2 phosphorylation. Data are representative of three experiments. **I.** Inhibition of PKA does not block Dvl2 phosphorylation in STK11-/- cells. STK11-/- MEFs were treated with increasing concentrations of the PKA inhibitor H89 up to 10μM. Axin1 serves as a loading control.

Dvl proteins function as cytoplasmic routers that can transduce both β-catenin-dependent and -independent Wnt-mediated responses (Gao and Chen, 2010; Grumolato et al., 2010; Wallingford and Habas, 2005). RNAi targeting of Dvl2 reduced the rate of growth in STK11-/- MEFs, suggesting that Dvl2 plays a key role in promoting aberrant cell proliferation (Figure 4-2). In response to Wnt, Dvl adopts a diffuse cytoplasmic distribution that contrasts with its localization to punctate structures in the absence of Wnt (Bilic et al., 2007; Schwarz-Romond et al., 2007b). I found that there was abundant diffusely localized Dvl2 [fused to green fluorescent protein (GFP)] in STK11-/- MEFs even in the absence of added Wnt, and this contrasted with the distribution of a GFP-

tagged Axin1, a binding partner of Dvl (Bilic et al., 2007; Schwarz-Romond et al., 2007b), which retained its typical punctate cellular distribution (Figure 4-3). Although IWP restored ratios of phosphorylated to unphosphorylated Dvl2 in the STK11-/- cells to that observed in WT MEFs (Figure 4-1E), it failed to restore punctate Dvl distribution (Figure 4-3). Taken together, these findings suggest that loss of Stk11 results in altered Dvl protein distribution that may facilitate Wnt-dependent Dvl phosphorylation.

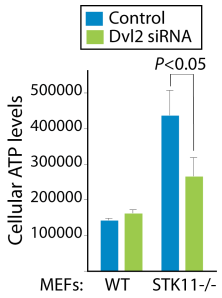

Figure 4-2 Loss of Dvl2 inhibits growth of STK11−/− cells. MEFs transfected with Dvl2 siRNAs were plated at clonal density, and CellTiter-Glo assay was performed after 6 days. Data show the mean and SD of three samples.

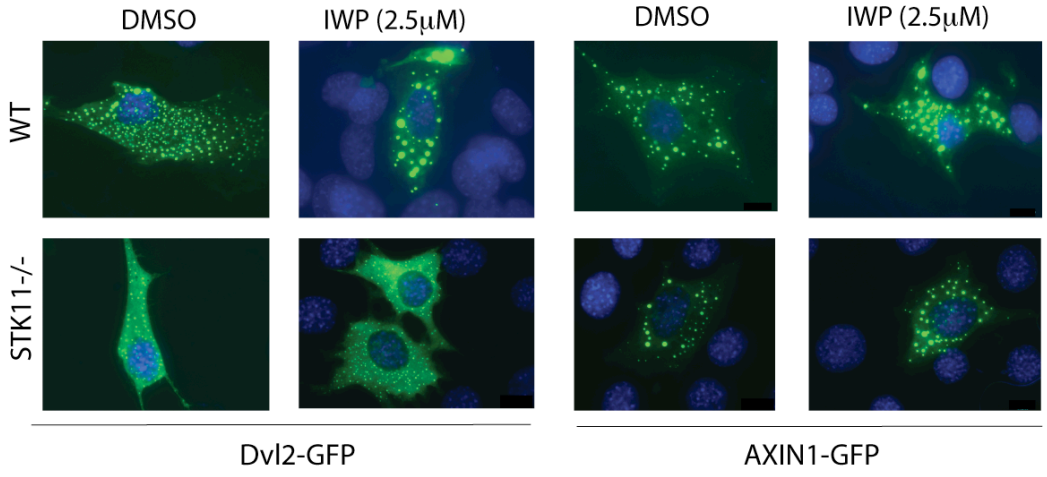

Figure 4-3 Loss of Stk11 is associated with mislocalization of Dvl2. MEFs, transfected with either Dvl2-GFP or Axin1-GFP DNA, were treated with DMSO or IWP. Green,

GFP; blue, DAPI (4′,6-diamidino-2-phenylindole). Images were taken at 40x magnification.

4.2.2 Stk11 regulation of Wnt responses in vivo

To investigate the role of Stk11 in Wnt responses in vivo, I performed in situ hybridization using digoxigenin labeled probes targeting *axin2*, a transcriptional target gene of β-catenin-dependent Wnt signaling (Jho et al., 2002). I noted little change in *axin2* expression in zebrafish, suggesting potential differences in Stk11-mediated regulation of Wnt/β-catenin signaling across species or between developing and adult tissues (Figure 4-4A). Posterior body morphogenesis in zebrafish is dependent upon intact β-catenin-independent Wnt responses (Marlow et al., 2004). The abnormal posterior body development displayed by Stk11 morphants (Figure 3-2A, Figure 4-4B) is consistent with defects non-canonical Wnt responses. This data supports the possibility of a role for Stk11 in the regulation of β-catenin-independent Wnt signaling in *vivo*, but does not rule out the prospect that other functions of Stk11, such as its activity in maintaining cell polarity, also contribute to the observed developmental defects.

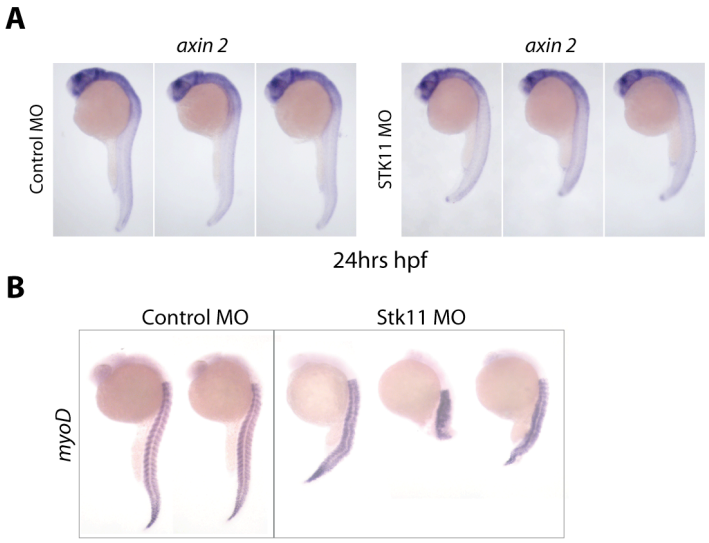

Figure 4-4 Knockdown of *stk11 in vivo* does not appear to affect canonical Wnt responses but may have a role in non-canonical Wnt responses. A. Stk11 morphants exhibit little change in *axin2* expression when compared to control animals. *In situ* hybridization with digoxigenin-labeled antisense probes against *axin2* mRNA was performed at 24 hpf embryos that had been injected with control MO or Stk11 MO. Representative embryos from 30 animals analyzed in each group are shown. **B.** The defect in posterior morphogenesis and somite development is apparent in Stk11 morphants stained for *myoD* expression, which labels somitic tissue. >25 embryos at 24 hrs post fertilization were analyzed in each group.

4.2.3 Stk11 regulation of the primary cilia is independent of Wnt signaling

Given that Dvl proteins control some aspects of cilia biology (Park et al., 2008), it is possible that defects in cilia length in cells lacking Stk11 (Figure 3-5A) stem from misactivation of Dvl (Figure 4-1A). To test this hypothesis, I treated WT and STK11-/- MEFs with the IWP compound to inhibit aberrant Dvl phosphorylation caused by Stkll loss and examined cilia length. Treatment with IWP compound did not affect cilia length in STK11-/- MEFs (Figure 4-5) suggesting that Stk11 maintains cilia integrity independently from Wnt ligand mediated activation of Dvl proteins.

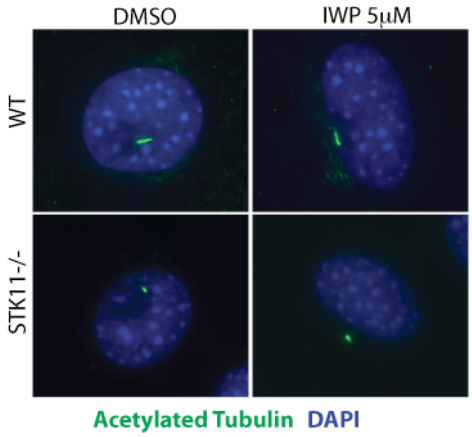

Figure 4-5 IWP does not rescue cilia length in cells lacking Stk11. WT and STK11-/- MEFs were treated with IWP in conditions that promote cilia assembly (low serum, high density) for two days. Cells were stained using antibodies against acetylated tubulin to detect cilia.

4.2.4 Cancerous cells lacking Stk11 engage deviant Wnt-mediated responses

Whereas the Stk11-associated Peutz-Jeghers hereditary tumor syndrome is a relatively rare disease (Hemminki et al., 1997; Jeghers H, 1949), sporadic cancers, such as those from lung and cervix, frequently harbor mutations in STK11 (Sanchez-Cespedes et al., 2002; Wingo et al., 2009). I investigated the relevance of Stk11 loss in Wnt signaling in a panel of cells derived from cervical carcinoma. Consistent with the findings in MEFs, cervical carcinoma cell lines, previously described as lacking Stk11 (Wingo et al., 2009), all exhibited enhanced Dvl2 phosphorylation relative to normal endometrium-derived cells (Endo cells) (Figure 4-6A). A similar link between Stk11 status and Dvl phosphorylation was also present in cell lines derived from another Stk11-associated cancer, non-small cell lung cancer (NSCLC) (Figure 4-6B). The sensitivity of Dvl phosphorylation to the IWP compound, but not a chemical that inhibits Wnt/β-

catenin pathway activity by stabilizing Axin, a negative regulator of β-catenin [the Inhibitor of Wnt Response (IWR)] (Chen et al., 2009), suggests that as in STK11-/- MEFs Dvl phosphorylation in cancerous cells lacking Stk11 is dependent on endogenous Wnt production (Figure 4-6B). Despite the observation that the STK11-null cervical carcinoma cell lines uniformly exhibited an increase in Dvl phosphorylation, only a subset are positive for c-Myc protein (Figure 4-6A), which is encoded by a target gene of the Wnt/β-catenin pathway (He et al., 1998). For example, HeLa and SiHa cells both lack Stk11, but in only HeLa cells was c-Myc detected. This data suggests that the outcome of STK11 loss is context specific with respect to aberrant engagement of Wnt signaling.

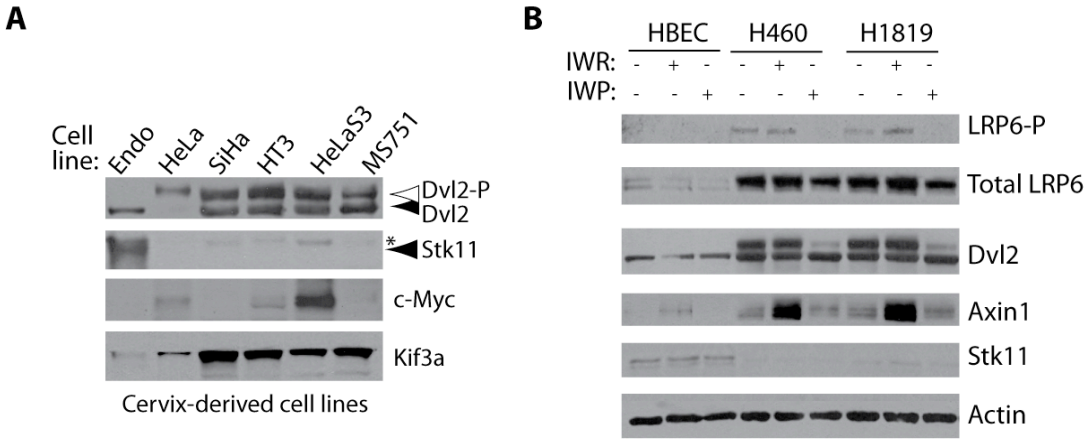

Figure 4-6 Dvl is aberrantly phosphorylated in cancerous cells lacking Stk11. A. Cervical carcinoma cells lacking Stk11 exhibit increased abundance of phosphorylated Dvl2 but not necessarily activation of the canonical Wnt/b-catenin pathway. Lysates from cervical carcinoma cell lines or normal endometrial cells (Endo cells) were Western-blotted for Dvl2, Stk11, or c-Myc, the product of a Wnt/β-catenin target gene. Kif3a is a loading control. The asterisk denotes a background band. **B.** NSCLC cell lines lacking Stk11 exhibit increased abundance of phosphorylated Dvl protein that can be lowered with IWP compound but not IWR compound. Cells expressing Stk11, Human bronchial epithelial cells (HBEC), served as a negative control.

I confirmed the role of Stk11 in controlling Wnt/β-catenin pathway activity in HeLa cells. Consistent with the presence of c-Myc in these cells, I observed increased activity of the STF reporter in HeLa cells relative to that in Endo and SiHa cells (Figure 4-7A). This reporter activity was sensitive to the IWP compound as well as the IWR compound (Figure 4-7A). I also noted in HeLa, but not SiHa cells, the presence of Axin2 and phosphorylated Lrp6 (Figure 4-7B), both hallmarks of Wnt/β-catenin pathway activity (Jho et al., 2002; Zeng et al., 2005).

Introduction of Stk11 into HeLa cells reduced the Wnt-mediated transcriptional response (Figure 4-7C), partially restored the distribution of Dvl2 to punctate structures similar to the localization of its binding partner Axin (Figure 4-7D, Figure 4-7E), and promoted the appearance of nonphosphorylated Dvl2 (Figure 4-7F). Expression of a kinase-dead (KD) form of Stk11 did not increase the abundance of unphosphorylated Dvl2, suggesting that kinase activity of Stk11 is essential to its ability to restrain Dvl activity (Figure 4-7F). These observations, together with the ability of Stk11 to reduce cell growth (either by stalling proliferation or inducing cell death) in HeLa cells (Figure 4-7G), support a role for Stk11 in controlling cell growth or viability possibly by influencing Wnt/β-catenin pathway activity. This cell growth regulation is not likely to involve Hh signaling, given that HeLa cells rarely form primary cilia (Alieva et al., 1999). Interestingly, engagement of Dvl as a consequence of Stk11 loss in cancerous cells may thus give rise to β-catenin-dependent or -independent Wnt-mediated responses, or both. Furthermore, the type of response is likely dictated by the expression pattern of Wnt family members and their receptors (van Amerongen and Nusse, 2009).

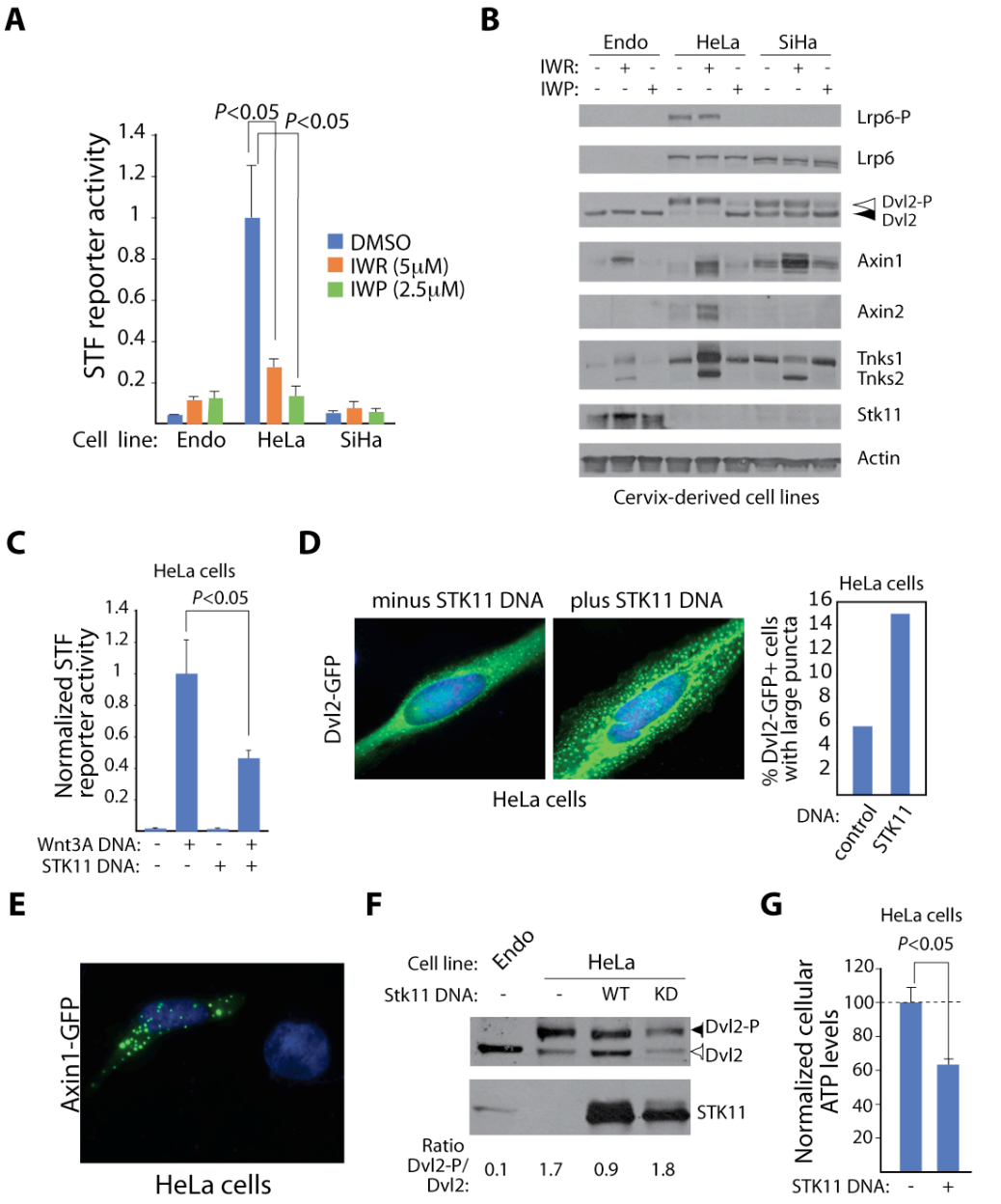

Figure 4-7 Loss of Stk11 results in deviant Wnt-mediated responses in cancer cell lines. A. Wnt/β-catenin pathway activity in HeLa cells is sensitive to disruption of Wnt production or inhibition of the canonical Wnt pathway. Endo, HeLa, or SiHa cells transfected with the STF reporter were treated with either IWP or IWR compounds. Data show the mean and SD of three samples. **B.** Cell line-dependent responses to Wnt ligand in cervical carcinoma cells lacking Stk11. Lysates from Endo, HeLa, or SiHa cells were

Western blotted for various Wnt pathway components. As before, HeLa but not SiHa cells exhibit Wnt/β-catenin pathway response (measured by expression of Axin2) that is sensitive to the IWR and IWP compounds. In addition, HeLa cells exhibit phosphorylation of Lrp6, a receptor for mostly canonical Wnt proteins. Dvl phosphorylation and Tankyrase (Tnks) protein levels are used to measure activity of IWP and IWR compounds, respectively. IWR compounds stabilize Axin proteins through the inhibition and stabilization of Tnks proteins, which facilitate Axin degradation. **C.** Stk11 disrupts Wnt/β-catenin response in HeLa cells. STF reporter was transfected with or without Wnt3A and Stk11 DNA into HeLa cells. Data show the mean and SD of three samples. **D.** Introduction of Stk11 increases the number of HeLa cells with punctate Dvl2 localization. Dvl2-GFP protein in HeLa cells shows a diffuse localization pattern, similar to that observed in STK11−/− MEFs. Cells were transfected with Dvl2-GFP DNA with or without Stk11 DNA. n = 50 for each condition. **E.** Axin1 forms punctate structures in HeLa cells. In contrast to the diffuse localization of Dvl2 in HeLa cells, its binding partner Axin1 is found in punctate structures. (*Panel E by Ozlem Kulak*). **F.** Kinase activity of Stk11 is required for suppression of Dvl2 activity. Expression constructs encoding wild-type or a K78M mutant (kinase-dead, KD) form of Stk11 were transfected into HeLa cells, and effects on Dvl2 phosphorylation were analyzed by Western blotting. Data are representative of three independent experiments. **G.** Introduction of Stk11 in HeLa cells inhibits cell growth. Transfected cells were seeded at clonal density. The amount of cellular ATP was determined as a measure of cell number after 5 days. Data show the mean and SD of three samples. (*Panel G by Michael Dodge*).

4.3 Discussion

The mislocalization of Dvl, increased phosphorylation of Dvl, and aberrant Wnt pathway activity exhibited in cells lacking Stk11 together suggest that sequestration of Dvl away from Wnt receptors represents an important checkpoint in Wnt pathway responses and that this checkpoint may be lost in Stk11-associated tumors. Interestingly, a high percentage of cervical carcinomas and non-small cell lung cancers exhibit increased abundance of Dvl protein (Okino et al., 2003; Uematsu et al., 2003), and this phenomenon correlates with poor prognosis (Zhao et al., 2010). Given the role of Dvl in mediating a diverse array of Wnt-dependent responses, my findings reveal a mechanistic basis underlying deviant Wnt-dependent transcriptional response, and possibly other

Wnt-associated cellular derangements in cancerous cells lacking Stk11. Thus, inhibitors of Wnt production, such as the Porcn inhibitors, may be useful in some Stk11-associated cancers; whereas inhibitors of canonical Wnt responses, such as those that induce Axin stability, may be additionally relevant in a subset of such cancers (Figure 4-8). The identification of chemical means to counter some of the effects resulting from loss of a multitasking gene product, such as Stk11, suggests that screening additional signal transduction pathways with the disease-centric approach discussed in Chapter 2 would further facilitate the deconstruction and ultimately management of complex diseases.

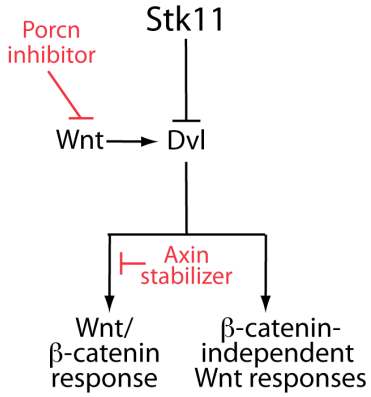

Figure 4-8 Chemically tractable mechanisms underlying aberrant Wnt pathway responses in STK11-null cells. Porcn and Axin stabilizers that respectively inhibit Wnt protein production and induce β-catenin destruction could be used to counter the effects of excess Dvl activation.

CHAPTER FIVE

CONCLUSIONS AND FUTURE DIRECTIONS

Despite intense efforts to uncover the mechanisms of Hh and Wnt signaling in mammals, many questions still remain. Using a functional genomics based approach I discovered novel components of the mammalian Hh and Wnt signal transduction pathways. Further characterization of this set of novel pathway effectors yielded several classes of genes of interest for future studies.

Much of my studies concentrated on the disease associated Hh and Wnt regulators identified in Chapter 2. Of the ten genes that comprise this group, three are known to affect Hh response (Smoothened, Gli2, and IFT57) (Alcedo et al., 1996; Huangfu et al., 2003; Mo et al., 1997; Taipale et al., 2002), while the mechanistic relevance of the last five are unknown. Glypican1 (GPC1) appears to be a mammalian homologue to the *Drosophila* co-receptor Dally-like, a heparan-sulfate modified, glycosyl phosphatidylinositol (GPI) anchored protein. Further study is necessary to assess whether GPC1 plays a receptor role for Hh signaling in mammals. Diacylglycerol kinase theta (Dgkq) is a kinase that mediates the conversion of diacylglycerol (DAG) into phosphatidic acid (PA) (Houssa et al., 1997; van Blitterswijk and Houssa, 2000). Though it is possible that Dgkq directly regulates one of the many phosphorylation events required for Hh or Wnt signal transduction, another attractive model is that the chemically susceptible Smo protein may be influenced by either the substrate (DAG) or product (PA) of Dgkq activity. A third disease related gene, Achalasia, adrenocortical insufficiency, alacrimia syndrome (Aaas) regulates nuclear transport (Cronshaw et al.,

2002) and may be involved in shuttling of the Gli transcriptional regulators to and from the nucleus. It will be interesting to determine if the Retinaldehyde binding protein (RLBP1), which is associated with retinal degeneration (Maw et al., 1997), has roles in maintenance of the primary cilia as mutations in other cilia regulators can also cause retinal degeneration (Krock and Perkins, 2008). Phosphorylation controls signal transduction in the Hh pathway at many levels including Smo activation and Gli processing and thus the candidate Hh pathway regulator Stk22B, a serine threonine kinase, may potentially function at the level of Smo or Gli. Further tests are needed to confirm the role of these genes in the Hh and Wnt pathways.

I performed focused mechanistic studies of the remaining two candidates, Stk11 and Prkar1a. Prkar1a had been previously identified to be important for Hh signal transduction (Evangelista et al., 2008) however its mechanism of action had not been demonstrated. I show that Prkar1a, the regulatory subunit of PKA (Amieux and McKnight, 2002), is required to restrict Gli3 processing (Figure 3-8). In addition, I demonstrated the tumor suppressor, Stk11/LKB1, is important for Hh response. Knockout of STK11 does not eliminate, but significantly dampens response to Hh signals (Figure 3-1). This effect can also be seen in Zebrafish morphants. Knockdown of *stk11* resulted in reduced expression of a transcriptional target that responds to high levels of Hh signaling whereas expression of a gene that requires lower levels of Hh signaling remained unchanged (Figure 3-2). In this way, Stk11 may set thresholds of response to Hh signals within cells. This type of regulation may be relevant to cell-fate decisions during development as transcriptional response is graded by Hh dosage. I found that

Stk11 mediates the level of Hh response through the control of the ratio of transcriptional repressors to activators. Loss of Stk11 results in excessive production of Gli3R (Figure 3-3, 3-4). In addition to regulation of Gli3, Stk11 maintains primary cilia length (Figure 3-5). I found that Stk11 may regulate Hh response ultimately by inhibition of primary cilia disassembly, through control of the abundance of acetylated tubulin, the building blocks of the cilia axoneme. Small molecule targeting tubulin deacetylases in cells lacking Stk11 restored primary cilia length as well as levels of Gli3R to those seen in wild-type cells (Figure 3-7).

My findings further our understanding of Hh signal transduction and cilia biology but also present new questions. It is unclear how Stk11 influences levels of acetylated tubulin in cells. HDAC6 has been shown to localize to the tip of the primary cilia where it deacetylases tubulin resulting in primary cilia disassembly (Pugacheva et al., 2007). This process is initiated by the Neural precursor cell expressed, developmentally down-regulated 9 (Nedd9/HEF1) protein which activates Aurora Kinase A (Aurka) and in turn promotes HDAC6 phosphorylation and activity (Pugacheva et al., 2007). A study of lung cancer cell lines lacking Stk11 showed that expression of Nedd9 is upregulated in Stk11 associated tumors (Ji et al., 2007). Whether Stk11 influences cilia length through regulation of Nedd9 must be determined by future genetic and epistatic experiments.

Another mystery to be examined is how the shortened cilia in cells lacking Stk11 lead to an increased abundance of Gli3R. Mutations of genes that cause a loss of cilia (IFT proteins) or shorter and often deformed cilia [Fuzzy (Fuz), Dynein cytoplasmic

heavy chain 2 (Dnchc2), ADP-ribosylation factor-like 13B (Arl13b), and Tetratricopeptide repeat–containing hedgehog modulator-1 (THM1)] typically lead to a reduction in Gli3 processing (Caspary et al., 2007; Heydeck et al., 2009; Huangfu and Anderson, 2005; Tran et al., 2008). Cells lacking Stk11 have shorter cilia but no observable deformation. In the absence of Hh ligand active PKA molecules localize to the base of the primary cilium (Barzi et al., 2010) and Gli proteins cycle through the cilia (Haycraft et al., 2005; Kim et al., 2009a), presumably, to be targeted for degradation by PKA mediated phosphorylation (Huntzicker et al., 2006; Pan et al., 2006). One possibility for the increase in Gli3 processing is that the shorter cilia give rise to decreased transit time for Gli cycling through the cilia before processing. Perhaps advanced microscopy techniques such as fluorescence recovery after photo-bleaching (FRAP) using labeled Gli molecules may further our understanding of this phenomenon.

From the RNAi screen I also identified Stk11 as a negative regulator of the Wnt pathway (Chapter 2). Biochemical studies of cells lacking Stk11 confirmed this role by revealing phosphorylation and mislocalization of Dvl proteins (Figure 4-1, 4-3). Misactivation of Dvl drives aberrant cell growth in these cells as evidenced by a reduction in cell growth when Dvl was knocked down (Figure 4-2). Interestingly, I found that cancer cells display an increase in Dvl activity in strong correlation with an absence of Stk11 expression (Figure 4-6). In a cell-type dependent manner the increased activity of Dvl translated into β-catenin dependent Wnt response that could be countered by small molecules that inhibit Wnt production or promote β-catenin destruction through Axin stabilization (Figure 4-7). It is unclear if the aberrant Dvl activity in these cancerous cells

also leads to β-catenin independent Wnt responses. My studies in zebrafish show that Stk11 morphants display phenotypes that are associated with misregulation of non-canonical Wnt signals (Figure 4-4), however further studies are necessary to fully dissect the downstream pathways affected by deviant Dvl function in the absence of Stk11. Together these studies highlight the possibility that Wnt pathway activity may play a role in the pathogenesis of Stk11 deficient tumors and that small-molecules inhibiting Wnt pathway activity may prove to be a useful therapeutic strategy.

Further studies are also necessary to identify the target of Stk11 function within the Wnt pathway. As inhibition of Wnt production effectively inhibits aberrant Wnt pathway activity associated with Stk11 loss (Figure 4-1, 4-6, 4-7), one possibility is that Stk11 promotes increased production of Wnt ligands. Preliminary studies in the Lum lab show that cells lacking Stk11 secrete a greater quantity of overexpressed tagged Wnt molecules than WT cells (data not shown). Even if this is the case, persistent Dvl mislocalization in the absence of Wnt production and Dvl phosphorylation (Figure 4-3) argues that Stk11 may regulate Dvl in a different manner. One hypothesis is that loss of Stk11 produces a pool of "free" Dvl protein that is hypersensitive to upstream Wnt pathway activity and that sequestration of Dvl into punctate structures with Axin is necessary to restrict Dvl misactivation. Further studies of the nature of Dvl misactivation would be needed to confirm this model. Regardless of the mechanism of Dvl regulation by Stk11, it appears that much like Stk11 regulation of the Hh pathway, Stk11 is important for defining thresholds of cellular response to Wnt ligands.

Although Stk11 appears to regulate Wnt and Hh through different mechanisms, further studies identifying the cellular substrates of Stk11 kinase activity would be necessary to identify any shared mechanisms of Hh and Wnt regulation. The inverse regulation of Hh and Wnt signal transduction by Stk11 may be relevant in the development and diseases of tissues where Wnt and Hh play opposing roles, such as the gastrointestinal tract. During development, it has been shown that Hh signaling inhibits response to Wnt signals outside the base of the intestinal crypts resulting in restriction of cell proliferation (Barakat et al., 2010; van den Brink et al., 2004). It would be interesting to determine whether recurrent intestinal polyposis exhibited by Peutz-Jehgers syndrome patients (Jeghers H, 1949) is dependent upon on a loss of Hh cellular response and an increase in Wnt signaling caused by loss of Stk11 function. Confirmation of a role for Hh and Wnt signaling in the pathogenesis of Peutz-Jehgers syndrome through further study may indicate the utility of small molecules that modulate Hh and Wnt pathway activity as therapeutics.

In conclusion, using a genome-wide RNAi based screening platform, I identified a number of genes that hold promise for novel regulatory roles in Hh and Wnt signal transduction. My studies highlight the potential obstacles of genome-scale functional genomics based screens and provide practical solutions. I determined the role of Stk11 in regulation of the Hh and Wnt pathways and formulated chemically based approaches to impede the altered cell signaling in cancerous cells lacking Stk11. The use of small molecule modulators of Hh and Wnt signaling may prove useful as molecularly targeted therapeutic strategies for cancers associated with Stkll loss.

CHAPTER SIX

MATERIALS AND METHODS

6.1 Reagents

6.1.1 Cell lines

3T3-ShhFL cells, used in the primary screen, were generated by the stable transfection of NIH-3T3 cells expressing Shh protein (generously provided by Philip Beachy) with a Hh responsive reporter [8x-Gli-BS-Luc] (Sasaki et al., 1997), and a *Renilla* luciferase reporter, pRL-SV40 (Promega). ShhLightII cells (Taipale et al., 2000), HeLa cells, NIH-3T3 cells, and DLD-1 cells were purchased from ATCC. Wild-type MEFs and STK11-/- MEFs were provided by Nabeel Bardeesy. IFT88-/- MEFs were provided by Aimin Liu. PRKAR1A-/- MEFs were provided by Lawrence Kirschner. HBEC cells were provided by Jerry Shay. Lung cancer cell lines, H1819 and H460 were provided by John Minna. Endo and SiHa cells were provided by Diego Castrillon.

6.1.2 Expression constructs

The human STK11 expression construct was purchased from Origene and the human SLC9A8 expression construct was obtained from Open Biosystems. Kinase dead STK11 (STK11 K78M) and mutant SLC9A8 G315L were engineered using PCR-based cloning and mutagenesis strategies. The MEF2C expression construct was provided by Eric Olson. cDNAs encoding SLC9 family members were provided by Massimo Attanasio. Plasmids encoding NFATC2, SMAD7, E2F1, MSX1, CNOT3, and BTG1 were purchased from either Origene or Open Biosystems and cloned into the pcDNA3 vector containing sequence for a C-terminal myc tag using standard molecular cloning

techniques. The SuperTopFlash (STF) reporter plasmid was provided by Randall T. Moon. The pRK5-ShhN and Wnt3A plasmids were provided by Philip A. Beachy. Axin1-GFP and Dvl2-GFP plasmids were provided by Mariann Bienz. All other expression constructs were purchased from Origene or Open Biosystems and sequence verified.

6.1.3 Chemicals

SAG was purchased from Alexis Biochemicals and cyclopamine was purchased from Logan Natural Products. Sant1, MG132, H89, and EIPA were purchased from Sigma. D4476 and Rapamycin were purchased from Calbiochem. IWP and IWR compounds targeting the Wnt pathway components Porcupine and Tankyrase, respectively, were synthesized de novo as previously described (Chen et al., 2009). The HDAC inhibitor SAHA was provided by Chuo Chen. Tubacin (a specific HDAC6 inhibitor) and MS-275 (HDAC1-3 inhibitor) were provided by Ralph Mazitschek and Stuart Schreiber. 5-(tetradecyloxy)-2-furoic acid (TOFA) was purchased from Cayman Chemicals.

6.1.4 Antibodies

Gli3 antibodies were obtained from Genentech (6F5), Baolin Wang, or R&D Systems. Anti-Prkar1a antibody was purchased from BD Biosciences. Smo antibody was provided by Jynho Kim and Philip A. Beachy. Antibodies against acetylated tubulin, β-catenin, Kif3A, and β-actin were purchased from Sigma. Antibodies against Stk11, Dvl2, Dvl3, Axin1, Axin2, p-LRP6, LRP6, c-Myc, and alpha-tubulin were purchased

from Cell Signaling Technologies. Dvl1, Tnks1/2 and 9E10 myc antibodies were purchased from Santa Cruz Biotechnology. GFP antibody was purchased from MBL.

6.1.5 RNAi reagents

Mouse genome-wide siRNA libraries and all other siRNAs targeting specific genes were purchased from either Qiagen or Dharmacon. Non-silencing siRNAs (AllStars Negative Control siRNA) were purchased from Qiagen. Sequences of siRNAs used in secondary tests are described in Appendix D.

6.2 Screening

6.2.1 Primary Screen

Mouse genome wide siRNA libraries produced by Dharmacon and Qiagen, were screened by transfecting siRNA pools targeting a single gene into 3T3-ShhFL cells in 96 well format using the X-tremeGENE transfection reagent (Roche) according to the manufacturer's protocol. The final siRNA concentration was 57nM. 24 hrs after transfection cells were placed under low serum conditions (0.5% calf serum). 72 hrs after transfection, firefly and *Renilla* luciferase activities were assessed using the Dual Luciferase kit (Promega). To account for edge effects and variation across plates, luciferase measurements were normalized to the average luciferase value for each well position across all plates and to the average luciferase measurement of each plate. Samples for which the triplicate data was inconsistent (SD>0.1) were removed from consideration. *Z* scores were calculated by determining the number of standard deviations luciferase measurements for each siRNA pool fell away from the mean values

for all the siRNA pools in each primary screen. siRNA pools that affected the *Renilla* luciferase control reporter (RL, $z<0.5$, $z>2.5$) were removed from consideration. siRNA pools for which FL $z <= -2.0$ (97.73% confidence) were further evaluated by secondary screens.

6.2.2 Secondary Screens

The exogenous Shh secondary screen was performed essentially as above by the transfection of Shh Light II cells with siRNAs and, 24 hrs later, the addition of ShhN conditioned media, collected from Hek293-ShhN cells. Screening quality of assay plates was monitored using siRNAs targeting Gli2 that were added to each assay plate. Average FL measurements less than or equal to 75% of FL for non-silencing siRNA controls and SD<0.15 were considered for further testing.

The Wnt counterscreen was performed by transfection of NIH-3T3 cells with the STF reporter, the *Renilla* luciferase reporter, the Wnt3A plasmid, and siRNAs using the Effectene transfection reagent (Qiagen) according to the manufacturer's protocol. Final siRNA concentration was 25nM. Quality of assay plates was determined by the ability of an siRNA pool targeting β-catenin spiked onto each plate to reduce STF reporter activity by at least 50% when compared to control.

The low throughput counterscreen (Cross-library test) was performed in the same manner as the exogenous Shh secondary test except by hand in 96 well format using only the center wells of the plate. High assay quality was confirmed by the ability of Gli2 siRNA that was spiked onto each assay plate to reduce GliBS reporter activity by at least 50%.

The RNAi specificity test was performed in the same manner as the exogenous Shh secondary test using individual siRNAs (Appendix D).

The cDNA overexpression test was performed in NIH-3T3 cells. Cells were transfected with reporters and either an empty vector or plasmid encoding ShhN. Gli1 cDNA and empty vector were spiked onto every assay plate as controls. Luciferase activity was measured after 48 hours.

To screen for transcription factors that bind to Gli, expression constructs were transfected into NIH-3T3 cells. Forty-eight hours later cells were lysed in PBS/1%NP40 with protease inhibitors. Gli1 was pulled down using biotinylated oligonucleotides containing Gli binding sequences (Sasaki et al., 1997) on Neutravidin agarose resin (Thermo Scientific). Samples were analyzed by western blot.

6.3 RT-PCR and qPCR

RT-PCR primer design was as follows: GapDH F – ATCCTGCACCACCAACT, GapDH R – TGCCTGCTTCACCACCTT, Ptch1 F – ACTGTCCAGCTACCCCAATG, Ptch1 R – CATCATGCCAAAGAGCTCAA. qPCR analysis primers: GapDH F – ACATCGCTCAGACACCATG, GapDH R- TGTAGTTGAGGTCAATGAAGGG, Gli3 F – GGGATTCCGACAGTTCTGAACC, Gli3 R – CTGGGGAGGTCTTCATCAGGC, Ptch F – CGTCAGAAGATAGGAGAAGAGGC, Ptch R – GTAGCACAAATGTTCCAACTTCC.

6.4 Analysis of GliR formation and degradation

Gli3R formation was inhibited by addition of either Shh conditioned medium or a Smo agonist (SAG, 0.2μM) for 24 hours. Conditioned medium or SAG was then removed and replaced with a medium containing Smo antagonist (SANT, 2.5μM) to inhibit Shh pathway response and to allow re-initiation of Gli3R formation. Cellular lysate was then collected at indicated timepoints. To examine the rate of Gli3R turnover, cells were treated with MG132 to inhibit proteasome dependent Gli processing. Cellular lysate was then collected at various timepoints. Samples were analyzed by western blot and Gli3R protein quantified using Image J or Gene Tools software.

6.5 Zebrafish experiments

Wild-type zebrafish embryos were injected with 3pmoles of morpholino targeting STK11 (sequence: GAGATCCGCGCCCACGCTCATCTTT) or standard control at the one to two cell stage. Whole-mount in situ hybridization was performed at 24hpf using digoxygenin-labeled antisense RNA probes generated against Eng1A (BC080209) (bp 3-1433), Axin2 (BC045281) (bp 341-1144), or MyoD (NM_131262) (bp 316-927). RNA probes were generated against Ptch1 using an expression construct encoding Ptch obtained from Philip Ingham. All morpholino oligonucleotides were purchased from Gene Tools.

6.6 Transmission electron microscopy

Cells were fixed in 2.5% glutaraldehyde in 0.1 M sodium cacodylate buffer, post-fixed in buffered 1% osmium tetroxide, en bloc stained in 2% uranyl acetate, dehydrated with a graded series of ethanol, and embedded in EMbed-812 resin. Thin sections were cut on a Leica Ultracut UCT ultramicrotome, then stained with 2% uranyl acetate and lead citrate. Images were acquired on a FEI Tecnai G2 Spirit electron microscope equipped with a LaB6 source and operating at 120 kV.

6.7 RNAi and overexpression studies in cultured cells

For studies involving transfection of siRNAs, Dharmafect3 (Dharmacon) or X-tremeGENE (Roche) reagent was utilized per manufacturer's protocol. For studies involving transfection of cDNAs, Fugene HD (Roche) or Effectene (Qiagen) was used according to manufacturer's instructions.

6.8 Western Blot analysis and immunofluorescence

Cells lysates for Western blot analysis was generated with either PBS/1%NP40 or RIPA buffer (for detection of Gli proteins). Western blot results were quantified using Image J or Gene Tools software. For imaging of cilia, cells were plated at high density and low serum on poly-lysine coated coverslips (BD Biosciences). In experiments using SAHA or IWP cells were treated for 24 hours. For Smo localization experiments cells were treated with ShhN conditioned media for four hours before fixation. Cells were fixed in either 4% formaldehyde or ice cold methanol and incubated with anti-acetylated

tubulin antibody and then secondary antibodies (anti-mouse FITC or Alexa 488) diluted in PBS, 0.2% Triton, 5% goat serum. Cilia were imaged and measurements were taken using Adobe Photoshop.

6.9 Cancer cell growth studies

Cells were transfected with siRNAs or cDNAs in 96 well format. Twenty-four hours later cells were trypsinized and reseeded at clonal density (1,500 cells in 24-well format). Cellular ATP levels were measured 6 days later using the Cell Titer Glo reagent (Promega).

APPENDIX A

Primary Screen Suppressors

LIBRARY	SUB LIBRARY	GENE ID	SYMBOL	Z score
DHARMACON	GENOME	403202	**A430093F15RIK**	7.4
DHARMACON	GENOME	353204	**4921524E03RIK**	6.3
DHARMACON	GPCR	18166	**NPY1R**	6.1
DHARMACON	KINASE	105278	**CCRK**	5.3
DHARMACON	GENOME	319738	**A730020M07RIK**	5.2
DHARMACON	DRUGGABLE	14618	**GJB1**	5.2
QIAGEN		544968	**LOC544968**	4.9
QIAGEN		50995	**Uble1b**	4.8
DHARMACON	DRUGGABLE	12540	**CDC42**	4.7
DHARMACON	KINASE	75678	**1810043M15RIK**	4.6
DHARMACON	KINASE	19252	**Dusp1**	4.5
QIAGEN		327872	**4932416E17**	4.4
DHARMACON	GPCR	84111	**GPR87**	4.4
DHARMACON	GPCR	54214	**GOLGA4**	4.4
DHARMACON	DRUGGABLE	16323	**INHBA**	4.4
DHARMACON	DRUGGABLE	56456	**Actl6a**	4.3
QIAGEN		218993	**Gm534**	4.3
DHARMACON	KINASE	69718	**IMPK**	4.2
QIAGEN		29845	**Olfr155**	4.2
DHARMACON	DRUGGABLE	17217	**MCM4**	4.0
QIAGEN		328573	**4930407I10Rik**	4.0
QIAGEN		52123	**Agpat5**	4.0
QIAGEN		71240	**Osbpl7**	4.0
QIAGEN		76866	**4930417P05Rik**	3.9
DHARMACON	DRUGGABLE	333329	**GM1959**	3.8
QIAGEN		212052	**Gm497**	3.8
QIAGEN		433569	**LOC433569**	3.7
DHARMACON	GENOME	2885	**A930037J23RIK**	3.7
DHARMACON	GENOME	241452	**DHRS9**	3.7
DHARMACON	DRUGGABLE	12010	**B2M**	3.7
QIAGEN		101613	**Nalp6**	3.7
QIAGEN		70458	**2610318N02Rik**	3.6
QIAGEN		60532	**Wtap**	3.6
QIAGEN		545477	**LOC545477**	3.5
DHARMACON	DRUGGABLE	12626	**CETN3**	3.5
QIAGEN		545394	**LOC545394**	3.5
DHARMACON	KINASE	66588	**0610011D08RIK**	3.4
QIAGEN		104836	**Cbll1**	3.4
DHARMACON	KINASE	26420	**MAPK9**	3.4
QIAGEN		60611	**Foxj2**	3.4
DHARMACON	DRUGGABLE	56349	**NET1**	3.4
DHARMACON	GPCR	259071	**OLFR166**	3.4

DHARMACON	KINASE	235604	**BC017634**	3.4
QIAGEN		435919	**LOC435919**	3.4
DHARMACON	GENOME	20479	**VPS4B**	3.3
DHARMACON	DRUGGABLE	17979	**NCOA3**	3.3
DHARMACON	KINASE	13549	**DYRK1B**	3.3
DHARMACON	GENOME	68073	**A930016P21RIK**	3.3
DHARMACON	KINASE	18752	**PRKCC**	3.3
QIAGEN		13823	**Epb4.1l3**	3.3
QIAGEN		19707	**Reps1**	3.3
DHARMACON	KINASE	240752	**C330011J12RIK**	3.3
QIAGEN		380893	**Gm908**	3.3
DHARMACON	GPCR	84112	**Gpr91**	3.2
DHARMACON	GENOME	54673	**SH3GLB1**	3.2
DHARMACON	GENOME	72508	**Rps6kb1**	3.2
QIAGEN		14629	**Gclc**	3.2
DHARMACON	GENOME	270135	**BC038156**	3.2
DHARMACON	GENOME	246104	**RHBDL4**	3.2
DHARMACON	GENOME	22083	**SH2BP1**	3.1
DHARMACON	GENOME	73230	**BMPER**	3.1
QIAGEN		258318	**NM_146321**	3.1
DHARMACON	KINASE	20293	**CCL12**	3.1
QIAGEN		433281	**LOC433281**	3.1
QIAGEN		54484	**Mkrn1**	3.1
QIAGEN		66460	**2610042O14Rik**	3.1
DHARMACON	KINASE	211347	**PANK3**	3.1
DHARMACON	GENOME	140492	**KCNN2**	3.1
QIAGEN		71985	**Acad10**	3.1
DHARMACON	GPCR	319200	**GPR82**	3.1
QIAGEN		102791	**Tcta**	3.1
DHARMACON	DRUGGABLE	27419	**NAGLU**	3.0
DHARMACON	DRUGGABLE	16656	**HIVEP3**	3.0
QIAGEN		218460	**Wdr41**	3.0
QIAGEN		68917	**Hint2**	3.0
DHARMACON	DRUGGABLE	19125	**PRODH**	3.0
DHARMACON	GPCR	15565	**HTR6**	3.0
DHARMACON	GENOME	232023	**AW146242**	3.0
DHARMACON	DRUGGABLE	20926	**SUPT6H**	3.0
QIAGEN		76412	**1700019J19Rik**	3.0
DHARMACON	GENOME	211922	**A630054L15RIK**	3.0
QIAGEN		381126	**Gm944**	3.0
DHARMACON	DRUGGABLE	16363	**IRF2**	3.0
QIAGEN		52202	**D8Ertd233e**	3.0
DHARMACON	GENOME	75284	**4930556P03RIK**	3.0
DHARMACON	KINASE	224105	**PAK2**	2.9
QIAGEN		28042	**D5Wsu178e**	2.9
DHARMACON	GENOME	237636	**NPC1L1**	2.9
QIAGEN		53625	**B3gnt1**	2.9
DHARMACON	DRUGGABLE	243853	**FKRP**	2.9
DHARMACON	KINASE	20872	**STK16**	2.9
QIAGEN		78244	**4930461P20Rik**	2.9

QIAGEN		545691	**LOC545691**	2.9
QIAGEN		21908	**Tlx1**	2.9
QIAGEN		546535	**LOC546535**	2.9
QIAGEN		241634	**Gm355**	2.9
DHARMACON	KINASE	105787	**Prkaa1**	2.9
DHARMACON	KINASE	16150	**Ikbkb**	2.9
QIAGEN		234988	**Mbd3l2**	2.9
QIAGEN		66011	**Ranbp17**	2.9
DHARMACON	DRUGGABLE	70233	**CD2BP2**	2.9
DHARMACON	GENOME	258711	**OLFR432**	2.9
DHARMACON	GENOME	64337	**GNG13**	2.9
QIAGEN		69401	**1700015M15Rik**	2.9
QIAGEN		258859	**Olfr161**	2.9
QIAGEN		231051	**Mll3**	2.8
DHARMACON	DRUGGABLE	16391	**ISGF3G**	2.8
DHARMACON	GENOME	258627	**OLFR1504**	2.8
DHARMACON	GENOME	320321	**9430077A04RIK**	2.8
DHARMACON	DRUGGABLE	229663	**D3JFR1**	2.8
QIAGEN		383981	**LOC383981**	2.8
DHARMACON	DRUGGABLE	74156	**CACH**	2.8
QIAGEN		381142	**Gm949**	2.8
QIAGEN		13663	**Ei24**	2.8
QIAGEN		13875	**Erf**	2.8
DHARMACON	KINASE	13842	**EPHA8**	2.8
DHARMACON	KINASE	269209	**1700112N14RIK**	2.8
DHARMACON	DRUGGABLE	16563	**KIF2A**	2.8
DHARMACON	GENOME	18689	**PHXR4**	2.8
QIAGEN		66713	**ACTR2**	2.8
DHARMACON	DRUGGABLE	110075	**BMP3**	2.8
QIAGEN		110959	**D7Rp2e**	2.8
DHARMACON	GENOME	66489	**RPL35**	2.8
DHARMACON	GENOME	329260	**BC042698**	2.8
QIAGEN		66074	**0610041E09Rik**	2.8
DHARMACON	GENOME	270757	**BPIL2**	2.8
DHARMACON	GENOME	241636	**A030011P16**	2.8
DHARMACON	DRUGGABLE	18032	**NFIX**	2.8
QIAGEN		18752	**Prkcc**	2.7
QIAGEN		114666	**A030001H12Rik**	2.7
QIAGEN		72569	**2700023J09Rik**	2.7
QIAGEN		59053	**Brp16**	2.7
DHARMACON	KINASE	56399	**AKAP8**	2.7
DHARMACON	GENOME	66264	**1810010N17RIK**	2.7
QIAGEN		65105	**Arl6ip4**	2.7
DHARMACON	GENOME	231999	**BC052360**	2.7
DHARMACON	GENOME	14702	**GNG2**	2.7
DHARMACON	GPCR	14608	**GPR83**	2.7
QIAGEN		432610	**LOC432610**	2.7
DHARMACON	KINASE	192185	**BC004012**	2.7
DHARMACON	GENOME	12044	**BCL2A1A**	2.7
DHARMACON	KINASE	23969	**PACSIN1**	2.7

DHARMACON	GENOME	66761	**4933417A18RIK**	2.7
QIAGEN		67073	**Pi4k2b**	2.7
QIAGEN		18231	**Nxph1**	2.7
DHARMACON	DRUGGABLE	217980	**D13WSU64E**	2.7
QIAGEN		14991	**H2-M3**	2.7
QIAGEN		12366	**Casp2**	2.7
QIAGEN		14783	**Grb10**	2.7
QIAGEN		320299	**Iqcb1**	2.6
DHARMACON	GENOME	246081	**DEFB11**	2.6
QIAGEN		52589	**Ncald**	2.6
QIAGEN		13590	**Lefty1**	2.6
QIAGEN		214685	**D930017K21Rik**	2.6
QIAGEN		22256	**Ung**	2.6
DHARMACON	KINASE	245038	**Dcamkl3**	2.6
QIAGEN		26908	**Eif2s3y**	2.6
QIAGEN		208372	**Asb18**	2.6
DHARMACON	DRUGGABLE	11911	**ATF4**	2.6
DHARMACON	GENOME	171429	**SLC26A6**	2.6
QIAGEN		66050	**0610009B22Rik**	2.6
QIAGEN		67922	**2510049I19Rik**	2.6
QIAGEN		233532	**Hbxap**	2.6
DHARMACON	GENOME	56519	**DEFB4**	2.6
DHARMACON	DRUGGABLE	93692	**GLRX1**	2.6
DHARMACON	DRUGGABLE	12647	**CHAT**	2.6
DHARMACON	GENOME	26940	**SITPEC**	2.6
QIAGEN		19719	**Rfng**	2.6
QIAGEN		433001	**LOC433001**	2.6
DHARMACON	GPCR	258387	**OLFR720**	2.6
DHARMACON	GENOME	58176	**RHBG**	2.6
QIAGEN		20269	**Scn3a**	2.5
QIAGEN		244144	**Gm493**	2.5
QIAGEN		83993	**Tbx19**	2.5
DHARMACON	DRUGGABLE	11848	**RHOA**	2.5
QIAGEN		385024	**LOC385024**	2.5
DHARMACON	DRUGGABLE	24069	**SUFU**	2.5
QIAGEN		16841	**Lect2**	2.5
DHARMACON	GENOME	26961	**RPL8**	2.5
QIAGEN		14873	**Gsto1**	2.5
QIAGEN		212772	**2700007P21Rik**	2.5
DHARMACON	GENOME	241568	**6430556C10RIK**	2.5
DHARMACON	GENOME	242669	**4933429I20RIK**	2.5
QIAGEN		218035	**Vps41**	2.5
DHARMACON	DRUGGABLE	12491	**CD36**	2.5
DHARMACON	DRUGGABLE	106389	**EAF2**	2.5
QIAGEN		26430	**Parg**	2.5
QIAGEN		57261	**BRD4**	2.5
QIAGEN		98752	**BB219290**	2.5
QIAGEN		67669	**0610007P06Rik**	2.5
QIAGEN		58200	**Ppp1r1a**	2.5
QIAGEN		228712	**LOC228712**	2.5

QIAGEN		71458	**Bcor**	2.5
QIAGEN		243574	**MGI:2661430**	2.5
DHARMACON	DRUGGABLE	11852	**RHOB**	2.5
DHARMACON	GENOME	16426	**ITIH3**	2.5
QIAGEN		328222	**9130430E04**	2.5
DHARMACON	GENOME	19820	**RNF12**	2.5
DHARMACON	GPCR	108073	**GRM7**	2.5
QIAGEN		216877	**Dhx33**	2.5
QIAGEN		545413	**LOC545413**	2.5
QIAGEN		14782	**Gsr**	2.5
DHARMACON	GENOME	53878	**SVS2**	2.5
DHARMACON	DRUGGABLE	69581	**RHOU**	2.5
DHARMACON	GENOME	215409	**5930437A14RIK**	2.5
QIAGEN		67046	**Tbc1d7**	2.5
DHARMACON	KINASE	117229	**STK33**	2.5
QIAGEN		72821	**2810451E09Rik**	2.5
DHARMACON	GENOME	12859	**COX5B**	2.5

APPENDIX B

Activators identified by two siRNA pools from the primary screen

Library Information					Primary Screen	Exogenous Shh Test	
LIBRARY	GENE NAME	AKA	GENE ID	Sub Library	L *Z*	L AVG	L SD
DHARMACON	CRSP2	Med14	26896	DRUGGABLE	**-3.2**	**0.44**	**0.07**
QIAGEN	Crsp2	Med14	26896		**-2.5**	**0.51**	**0.07**
DHARMACON	GLI		14632	DRUGGABLE	**-4.3**	**0.62**	**0.03**
QIAGEN	Gli1		14632		**-3.3**	**0.48**	**0.05**
DHARMACON	GLI2		14633	DRUGGABLE	**-3.1**	**0.35**	**0.12**
QIAGEN	Gli2		14633		**-4.3**	**0.62**	**0.08**
DHARMACON	KIF11	Eg5	16551	DRUGGABLE	**-2.7**	**0.63**	**0.09**
QIAGEN	Kif11	Eg5	16551		**-2.1**	**0.67**	**0.07**
DHARMACON	MEF2C		17260	DRUGGABLE	**-2.0**	**0.63**	**0.08**
QIAGEN	Mef2c		17260		**-2.4**	**0.60**	**0.05**

APPENDIX C

Counterscreen results

Cutoffs	
Primary screen	z</= -2.5
Exogenous Hh Test	FL<0.75, SD<0.15
Wnt Test	0.9<FL/RL>1.1
Cross library Test	FL<0.75, SD<0.15

Library Information			Primary Screen	Exogenous Shh Test		Wnt Test		Cross Library Test		Category
LIBRARY	GENE NAME	GENE ID	FL z	L AVG	L SD	L/R AVG	L/R SD	AVG L	SD L	
DHARMACON	4932416A15	244694	-2.7	0.63	0.05	1.10	0.12	0.54	0.08	Genes identified by low-throughput testing format, Hh Activator
DHARMACON	CAR4	12351	-2.6	0.59	0.03	1.02	0.23	0.58	0.13	Genes identified by low-throughput testing format, Hh Activator
DHARMACON	STK22B	22115	-2.1	0.52	0.13	1.01	0.18	0.60	0.14	Genes identified by low-throughput testing format, Hh Activator
DHARMACON	GPRK2L	14772	-2.1	0.71	0.06	1.03	0.17	0.62	0.08	Genes identified by low-throughput testing format, Hh Activator
DHARMACON	RHOD	11854	-2.6	0.50	0.09	0.95	0.15	0.67	0.04	Genes identified by low-throughput testing format, Hh Activator
QIAGEN	MGI:2387006	209047	-2.0	0.67	0.11	1.06	0.23	0.70	0.01	Genes identified by low-throughput testing format, Hh Activator
QIAGEN	Aaas	223921	-3.4	0.53	0.10	1.02	0.15	0.71	0.07	Genes identified by low-throughput testing format, Hh Activator
DHARMACON	GATA6	14465	-2.0	0.66	0.12	1.03	0.18	0.73	0.06	Genes identified by low-throughput testing format, Hh Activator
DHARMACON	CSNK1G3	70425	-2.2	0.51	0.06	1.07	0.10	0.73	0.05	Genes identified by low-throughput testing format, Hh Activator
DHARMACON	GPR73	58182	-2.1	0.70	0.03	1.02	0.12	0.75	0.08	Genes identified by low-throughput testing format, Hh Activator
QIAGEN	Arf2	11841	-2.4	0.53	0.05	0.94	0.20	0.76	0.07	Dedicated Hh Activator
QIAGEN	Abca7	27403	-2.0	0.64	0.09	1.03	0.18	0.77	0.02	Dedicated Hh Activator
DHARMACON	CRYBA2	12958	-2.0	0.58	0.11	0.99	0.00	0.78	0.10	Dedicated Hh Activator
QIAGEN	B230104P22Rik	77976	-3.3	0.62	0.04	0.95	0.07	0.78	0.17	Dedicated Hh Activator
QIAGEN	Emp2	13731	-2.2	0.68	0.02	1.08	0.15	0.80	0.10	Dedicated Hh Activator
DHARMACON	GFRA2	14586	-2.0	0.71	0.13	1.00	0.08	0.81	0.07	Dedicated Hh Activator
DHARMACON	GPR119	236781	-2.2	0.59	0.08	1.05	0.12	0.82	0.07	Dedicated Hh Activator
DHARMACON	C6	12274	-2.0	0.73	0.10	0.94	0.17	0.82	0.06	Dedicated Hh Activator
QIAGEN	Dguok	27369	-2.0	0.66	0.04	1.06	0.07	0.82	0.11	Dedicated Hh Activator
QIAGEN	Epb4.1l2	13822	-2.0	0.53	0.04	1.07	0.20	0.83	0.10	Dedicated Hh Activator
DHARMACON	VTI1A	53611	-2.4	0.60	0.04	0.97	0.18	0.83	0.07	Dedicated Hh Activator
QIAGEN	Gm337	240672	-2.0	0.53	0.06	1.02	0.10	0.84	0.04	Dedicated Hh Activator
DHARMACON	SIN3B	20467	-3.4	0.64	0.07	0.91	0.14	0.85	0.06	Dedicated Hh Activator

QIAGEN	Coro1b	23789	-2.3	0.49	0.06	0.93	0.23	0.85	0.11	Dedicated Hh Activator
DHARMACON	FGF2	14173	-3.0	0.66	0.09	0.99	0.06	0.85	0.02	Dedicated Hh Activator
QIAGEN	Rasa4	54153	-2.3	0.65	0.05	0.95	0.07	0.86	0.06	Dedicated Hh Activator
DHARMACON	MMP2	17390	-2.1	0.45	0.09	0.90	0.07	0.86	0.27	Dedicated Hh Activator
DHARMACON	CD69	12515	-3.9	0.48	0.00	0.96	0.17	0.87	0.08	Dedicated Hh Activator
QIAGEN	Car7	12354	-2.6	0.72	0.10	1.01	0.13	0.87	0.07	Dedicated Hh Activator
DHARMACON	B430119L13RIK	320974	-2.5	0.55	0.09	0.93	0.18	0.87	0.01	Dedicated Hh Activator
DHARMACON	A730013G03RIK	320952	-2.5	0.41	0.08	0.91	0.13	0.87	0.09	Dedicated Hh Activator
DHARMACON	GHRH	14601	-2.7	0.46	0.02	0.98	0.11	0.88	0.02	Dedicated Hh Activator
QIAGEN	Nphp3	74025	-2.0	0.72	0.12	1.03	0.17	0.88	0.06	Dedicated Hh Activator
QIAGEN	Wisp2	22403	-2.7	0.46	0.06	1.00	0.19	0.88	0.04	Dedicated Hh Activator
QIAGEN	5730439E10Rik	102632	-2.4	0.69	0.03	1.00	0.17	0.89	0.06	Dedicated Hh Activator
DHARMACON	SLC9A8	77031	-2.1	0.70	0.03	0.96	0.20	0.89	0.00	Dedicated Hh Activator
DHARMACON	CTSR	56835	-2.3	0.64	0.12	1.09	0.07	0.89	0.02	Dedicated Hh Activator
DHARMACON	D12ERTD604E	380752	-4.0	0.56	0.09	0.95	0.03	0.90	0.20	Dedicated Hh Activator
DHARMACON	INCENP	16319	-2.4	0.69	0.11	0.93	0.15	0.91	0.07	Dedicated Hh Activator
DHARMACON	8430420C20RIK	233806	-2.0	0.61	0.03	1.09	0.12	0.92	0.05	Dedicated Hh Activator
QIAGEN	Olfr1494	258992	-2.1	0.57	0.05	0.99	0.17	0.93	0.02	Dedicated Hh Activator
DHARMACON	5730436H21RIK	107071	-3.0	0.56	0.07	1.00	0.26	0.95	0.26	Dedicated Hh Activator
QIAGEN	AU040576	101772	-2.3	0.74	0.03	1.07	0.05	0.95	0.03	Dedicated Hh Activator
DHARMACON	LOC213439	213439	-2.0	0.68	0.04	0.93	0.17	0.97	0.08	Dedicated Hh Activator
QIAGEN	Gm979	381304	-2.5	0.65	0.10	1.10	0.13	NT	NT	Dedicated Hh Activator
QIAGEN	LOC435634	435634	-2.0	0.64	0.05	1.08	0.22	NT	NT	Dedicated Hh Activator
QIAGEN	LOC331528	331528	-2.0	0.52	0.05	1.07	0.03	NT	NT	Dedicated Hh Activator
QIAGEN	Gm550	225852	-2.6	0.57	0.06	1.06	0.18	NT	NT	Dedicated Hh Activator
QIAGEN	Scn1a	20265	-2.0	0.48	0.09	1.05	0.24	NT	NT	Dedicated Hh Activator
DHARMACON	LOC381832	381832	-2.2	0.61	0.07	1.00	0.20	NT	NT	Dedicated Hh Activator
QIAGEN	Dnahc10	56087	-2.3	0.60	0.07	0.99	0.05	NT	NT	Dedicated Hh Activator
QIAGEN	LOC269389	269389	-3.0	0.67	0.12	0.97	0.03	NT	NT	Dedicated Hh Activator
QIAGEN	1700007E06Rik	75459	-2.8	0.46	0.03	0.97	0.12	NT	NT	Dedicated Hh Activator
QIAGEN	A530080P10	329858	-2.3	0.60	0.04	0.96	0.02	NT	NT	Dedicated Hh Activator
QIAGEN	Lrdd	57913	-2.0	0.63	0.01	0.95	0.11	NT	NT	Dedicated Hh Activator
QIAGEN	1110033I14Rik	68701	-2.8	0.58	0.01	0.94	0.15	NT	NT	Dedicated Hh Activator
QIAGEN	LOC384757	384757	-2.7	0.56	0.09	0.93	0.10	NT	NT	Dedicated Hh Activator
QIAGEN	Gm250	216880	-3.1	0.51	0.07	0.93	0.20	NT	NT	Dedicated Hh Activator
QIAGEN	Gm256	212855	-2.1	0.62	0.05	0.92	0.10	NT	NT	Dedicated Hh Activator
QIAGEN	Gm972	381259	-2.3	0.71	0.08	0.92	0.06	NT	NT	Dedicated Hh Activator
QIAGEN	1190003J15Rik	76974	-2.6	0.51	0.03	0.92	0.13	NT	NT	Dedicated Hh Activator
QIAGEN	Htra4	330723	-3.8	0.57	0.12	0.92	0.13	NT	NT	Dedicated Hh Activator

QIAGEN	Sf3b1	81898	-2.1	0.34	0.11	3.80	1.15			Hh Activator / Wnt Suppressor
DHARMACON	HIST1H2BG	319181	-2.2	0.43	0.02	3.19	0.85			Hh Activator / Wnt Suppressor
QIAGEN	Gm340	381224	-3.0	0.51	0.08	2.55	0.17			Hh Activator / Wnt Suppressor
QIAGEN	Mcl1	17210	-2.0	0.61	0.13	2.38	0.15			Hh Activator / Wnt Suppressor
DHARMACON	REG1	19692	-2.4	0.56	0.02	2.28	0.36			Hh Activator / Wnt Suppressor
QIAGEN	LOC545261	545261	-2.9	0.59	0.06	2.04	0.16			Hh Activator / Wnt Suppressor
DHARMACON	ROBO2	268902	-2.0	0.70	0.03	2.01	0.17			Hh Activator / Wnt Suppressor
QIAGEN	Mbd3l1	73503	-2.1	0.67	0.07	1.97	0.05			Hh Activator / Wnt Suppressor
DHARMACON	D11LGP1E	80860	-2.9	0.64	0.06	1.96	0.40			Hh Activator / Wnt Suppressor
DHARMACON	FGF18	14172	-2.1	0.57	0.09	1.94	0.05			Hh Activator / Wnt Suppressor
QIAGEN	Mei1	74369	-2.9	0.39	0.07	1.92	0.03			Hh Activator / Wnt Suppressor
DHARMACON	MSX1	17701	-2.7	0.64	0.12	1.87	0.23			Hh Activator / Wnt Suppressor
DHARMACON	BTG1	12226	-2.0	0.64	0.02	1.86	0.05			Hh Activator / Wnt Suppressor
DHARMACON	C030035D04RIK	77532	-2.7	0.72	0.06	1.78	0.11			Hh Activator / Wnt Suppressor
QIAGEN	Cldn18	56492	-3.4	0.58	0.04	1.75	0.49			Hh Activator / Wnt Suppressor
QIAGEN	Oip5	70645	-2.3	0.66	0.03	1.74	0.25			Hh Activator / Wnt Suppressor
QIAGEN	Hk3	212032	-2.7	0.71	0.03	1.69	0.08			Hh Activator / Wnt Suppressor
QIAGEN	1110031M08Rik	68693	-2.0	0.71	0.05	1.68	0.15			Hh Activator / Wnt Suppressor
DHARMACON	Ihpk3	271424	-3.6	0.55	0.10	1.66	0.19			Hh Activator / Wnt Suppressor
DHARMACON	AA517853	353190	-2.2	0.73	0.11	1.64	0.05			Hh Activator / Wnt Suppressor
DHARMACON	Ptafr	19204	-2.0	0.65	0.09	1.64	0.09			Hh Activator / Wnt Suppressor
QIAGEN	Gm1305	383592	-3.1	0.75	0.09	1.62	0.06			Hh Activator / Wnt Suppressor
QIAGEN	Esrrbl1	73916	-2.1	0.64	0.10	1.58	0.07			Hh Activator / Wnt Suppressor
DHARMACON	HTR2A	15558	-2.2	0.74	0.06	1.57	0.09			Hh Activator / Wnt Suppressor
QIAGEN	Gnaz	14687	-2.1	0.68	0.02	1.57	0.07			Hh Activator / Wnt Suppressor
QIAGEN	1700109H08Rik	77036	-2.1	0.69	0.09	1.56	0.18			Hh Activator / Wnt Suppressor
QIAGEN	Gm1206	382867	-2.4	0.55	0.06	1.56	0.20			Hh Activator / Wnt Suppressor
DHARMACON	PRKAR1A	19084	-2.3	0.37	0.03	1.54	0.22			Hh Activator / Wnt Suppressor
QIAGEN	Preb	50907	-2.4	0.74	0.10	1.53	0.13			Hh Activator / Wnt Suppressor
DHARMACON	CSF3	12985	-2.0	0.51	0.06	1.52	0.07			Hh Activator / Wnt Suppressor
QIAGEN	Fstl3	83554	-2.8	0.55	0.03	1.52	0.34			Hh Activator / Wnt Suppressor
QIAGEN	4922501K12Rik	105511	-2.4	0.57	0.03	1.51	0.21			Hh Activator / Wnt Suppressor
QIAGEN	Gm1911	382510	-2.2	0.74	0.05	1.51	0.18			Hh Activator / Wnt Suppressor
DHARMACON	B230114J08RIK	77975	-2.9	0.63	0.07	1.51	0.20			Hh Activator / Wnt Suppressor
QIAGEN	Gm725	277899	-2.0	0.56	0.04	1.50	0.28			Hh Activator / Wnt Suppressor
QIAGEN	Plxnb2	140570	-2.4	0.57	0.02	1.48	0.77			Hh Activator / Wnt Suppressor
DHARMACON	SMO	319757	-3.2	0.53	0.04	1.48	0.07	0.81	0.07	Hh Activator / Wnt Suppressor
DHARMACON	STK11	20869	-2.2	0.54	0.04	1.47	0.11			Hh Activator / Wnt Suppressor
QIAGEN	Zfp251	71591	-2.1	0.69	0.09	1.47	0.16			Hh Activator / Wnt Suppressor

DHARMACON	GPC1	14733	-2.9	0.63	0.09	1.46	0.24			Hh Activator / Wnt Suppressor
QIAGEN	Unc13b	22249	-2.1	0.66	0.08	1.46	0.19			Hh Activator / Wnt Suppressor
QIAGEN	Drd5	13492	-2.8	0.71	0.08	1.46	0.24			Hh Activator / Wnt Suppressor
DHARMACON	B130017I01RIK	214137	-2.1	0.44	0.13	1.43	0.18			Hh Activator / Wnt Suppressor
QIAGEN	A730092B10	328953	-2.2	0.64	0.03	1.43	0.09			Hh Activator / Wnt Suppressor
QIAGEN	D030056L22	225995	-2.0	0.70	0.08	1.42	0.12			Hh Activator / Wnt Suppressor
DHARMACON	BC028265	268670	-2.8	0.51	0.07	1.41	0.18			Hh Activator / Wnt Suppressor
DHARMACON	BC027344	233057	-2.0	0.48	0.12	1.40	0.16			Hh Activator / Wnt Suppressor
QIAGEN	NM_146680	258675	-3.3	0.61	0.01	1.40	0.19			Hh Activator / Wnt Suppressor
DHARMACON	PDZRN3	55983	-2.1	0.63	0.05	1.39	0.12			Hh Activator / Wnt Suppressor
QIAGEN	Arl6ip5	65106	-2.3	0.65	0.10	1.39	0.12			Hh Activator / Wnt Suppressor
QIAGEN	Olfr1428	258673	-2.7	0.70	0.07	1.37	0.07			Hh Activator / Wnt Suppressor
DHARMACON	RDHE2	242285	-2.1	0.62	0.08	1.34	0.11			Hh Activator / Wnt Suppressor
DHARMACON	1190002A17RIK	68870	-3.1	0.59	0.06	1.34	0.14			Hh Activator / Wnt Suppressor
QIAGEN	1700123J19Rik	73614	-2.0	0.66	0.05	1.32	0.34			Hh Activator / Wnt Suppressor
DHARMACON	GOT1	14718	-2.0	0.65	0.02	1.32	0.20			Hh Activator / Wnt Suppressor
QIAGEN	Farp2	227377	-2.1	0.64	0.02	1.32	0.20			Hh Activator / Wnt Suppressor
DHARMACON	TNFRSF14	230979	-2.3	0.47	0.09	1.30	0.29			Hh Activator / Wnt Suppressor
DHARMACON	SNX4	69150	-2.2	0.68	0.03	1.30	0.22			Hh Activator / Wnt Suppressor
QIAGEN	1300018I17Rik	72325	-2.4	0.53	0.04	1.30	0.11			Hh Activator / Wnt Suppressor
QIAGEN	Lrrc10	237560	-2.3	0.61	0.08	1.28	0.10			Hh Activator / Wnt Suppressor
DHARMACON	CHRNA3	110834	-2.2	0.46	0.06	1.28	0.07			Hh Activator / Wnt Suppressor
DHARMACON	5330439C02RIK	217143	-4.1	0.56	0.06	1.26	0.03			Hh Activator / Wnt Suppressor
DHARMACON	V1RH4	171247	-2.2	0.60	0.05	1.26	0.14			Hh Activator / Wnt Suppressor
QIAGEN	MGC67181	242747	-2.0	0.64	0.09	1.25	0.29			Hh Activator / Wnt Suppressor
QIAGEN	C430042M11Rik	320021	-2.2	0.70	0.05	1.25	0.26			Hh Activator / Wnt Suppressor
DHARMACON	FN1	14268	-3.0	0.52	0.12	1.24	0.36			Hh Activator / Wnt Suppressor
DHARMACON	DDX6	13209	-2.4	0.58	0.08	1.24	0.19			Hh Activator / Wnt Suppressor
DHARMACON	IFNG	15978	-2.0	0.59	0.05	1.24	0.16			Hh Activator / Wnt Suppressor
DHARMACON	V2R12	22303	-2.5	0.68	0.08	1.23	0.14			Hh Activator / Wnt Suppressor
QIAGEN	Cd2	12481	-3.1	0.72	0.08	1.23	0.14			Hh Activator / Wnt Suppressor
QIAGEN	Ttc10	21821	-2.0	0.66	0.06	1.22	0.20	0.76	0.04	Hh Activator / Wnt Suppressor
QIAGEN	Dgkq	110524	-2.7	0.69	0.13	1.21	0.39			Hh Activator / Wnt Suppressor
DHARMACON	DEFB37	353320	-2.2	0.44	0.05	1.21	0.23			Hh Activator / Wnt Suppressor
QIAGEN	Fcer1a	14125	-2.8	0.67	0.02	1.21	0.19			Hh Activator / Wnt Suppressor
DHARMACON	OPN4	30044	-3.1	0.61	0.06	1.20	0.31			Hh Activator / Wnt Suppressor
DHARMACON	SIRT5	68346	-2.7	0.65	0.04	1.20	0.09			Hh Activator / Wnt Suppressor
DHARMACON	BCL2L1	12048	-4.1	0.31	0.06	1.20	0.18			Hh Activator / Wnt Suppressor
DHARMACON	INPP5B	16330	-3.0	0.50	0.12	1.20	0.05			Hh Activator / Wnt Suppressor

QIAGEN	Gm261	238321	-3.0	0.53	0.10	1.19	0.17		Hh Activator / Wnt Suppressor
DHARMACON	CNBP1	12785	-2.0	0.68	0.12	1.19	0.09		Hh Activator / Wnt Suppressor
QIAGEN	Pkig	18769	-2.4	0.42	0.03	1.19	0.16		Hh Activator / Wnt Suppressor
QIAGEN	Klhl11	217194	-2.3	0.66	0.05	1.18	0.17		Hh Activator / Wnt Suppressor
QIAGEN	Fabp9	21884	-2.7	0.66	0.04	1.17	0.15		Hh Activator / Wnt Suppressor
QIAGEN	1810062O14Rik	108995	-2.0	0.66	0.09	1.16	0.13		Hh Activator / Wnt Suppressor
DHARMACON	EFNA2	13637	-2.5	0.63	0.07	1.15	0.10		Hh Activator / Wnt Suppressor
QIAGEN	Atp6v0d1	11972	-2.0	0.68	0.08	1.15	0.16		Hh Activator / Wnt Suppressor
QIAGEN	Gm359	228966	-2.0	0.68	0.10	1.14	0.37		Hh Activator / Wnt Suppressor
QIAGEN	Cnot3	232791	-2.8	0.52	0.04	1.14	0.05		Hh Activator / Wnt Suppressor
DHARMACON	AV006891	65964	-2.9	0.46	0.05	1.14	0.09		Hh Activator / Wnt Suppressor
QIAGEN	2700069A02Rik	75553	-2.1	0.48	0.14	1.13	0.07		Hh Activator / Wnt Suppressor
QIAGEN	NM_146703	258698	-2.0	0.59	0.06	1.13	0.07		Hh Activator / Wnt Suppressor
DHARMACON	RLBP1	19771	-2.2	0.61	0.13	1.11	0.14		Hh Activator / Wnt Suppressor
DHARMACON	CALM3	12315	-2.8	0.75	0.05	1.11	0.06		Hh Activator / Wnt Suppressor
QIAGEN	Cspg5	29873	-2.1	0.68	0.04	0.89	0.16		Hh Activator / Wnt Activator
QIAGEN	Gm505	244666	-2.5	0.73	0.04	0.89	0.13		Hh Activator / Wnt Activator
DHARMACON	DEFB19	246700	-2.6	0.49	0.08	0.89	0.08		Hh Activator / Wnt Activator
DHARMACON	NFATC2	18019	-2.0	0.68	0.14	0.88	0.05		Hh Activator / Wnt Activator
DHARMACON	C030039L03RIK	112415	-2.6	0.49	0.02	0.88	0.11		Hh Activator / Wnt Activator
DHARMACON	DUSP6	67603	-2.2	0.71	0.07	0.87	0.09		Hh Activator / Wnt Activator
DHARMACON	KIF21A	16564	-2.0	0.71	0.08	0.87	0.15		Hh Activator / Wnt Activator
DHARMACON	MP4	114600	-2.5	0.64	0.07	0.87	0.11		Hh Activator / Wnt Activator
QIAGEN	Rtdr1	71236	-2.1	0.68	0.06	0.87	0.05		Hh Activator / Wnt Activator
QIAGEN	2610304F09Rik	269003	-2.8	0.71	0.10	0.87	0.17		Hh Activator / Wnt Activator
DHARMACON	KCNE1L	66240	-2.4	0.46	0.13	0.86	0.12		Hh Activator / Wnt Activator
QIAGEN	4930545L08Rik	78028	-2.1	0.59	0.07	0.86	0.06		Hh Activator / Wnt Activator
QIAGEN	Copz1	56447	-2.3	0.65	0.11	0.86	0.12		Hh Activator / Wnt Activator
DHARMACON	FADS2	56473	-2.1	0.57	0.05	0.86	0.25		Hh Activator / Wnt Activator
DHARMACON	4930547C10RIK	68274	-2.1	0.75	0.02	0.85	0.16		Hh Activator / Wnt Activator
QIAGEN	Fxyd6	59095	-2.2	0.58	0.03	0.85	0.22		Hh Activator / Wnt Activator
DHARMACON	ANKRD3	72388	-2.7	0.51	0.03	0.85	0.29		Hh Activator / Wnt Activator
DHARMACON	D830007F02RIK	213435	-2.4	0.56	0.12	0.85	0.02		Hh Activator / Wnt Activator
QIAGEN	Gm630	268949	-4.0	0.65	0.06	0.85	0.12		Hh Activator / Wnt Activator
QIAGEN	MGI:1914755	67505	-2.1	0.74	0.12	0.85	0.18		Hh Activator / Wnt Activator
QIAGEN	2210415F13Rik	70163	-2.0	0.60	0.13	0.85	0.08		Hh Activator / Wnt Activator
QIAGEN	RIPK1	19766	-2.1	0.59	0.07	0.85	0.13		Hh Activator / Wnt Activator
QIAGEN	Matn2	17181	-2.9	0.69	0.02	0.84	0.13		Hh Activator / Wnt Activator
DHARMACON	Dyrk2	69181	-2.7	0.66	0.07	0.84	0.09		Hh Activator / Wnt Activator

DHARMACON	BSND	140475	-2.3	0.58	0.04	0.84	0.08		Hh Activator / Wnt Activator
QIAGEN	1110007F05Rik	71787	-2.5	0.69	0.07	0.83	0.19		Hh Activator / Wnt Activator
QIAGEN	Gm1078	381835	-2.3	0.58	0.04	0.83	0.27		Hh Activator / Wnt Activator
DHARMACON	6720456B07RIK	101314	-2.3	0.65	0.05	0.83	0.07		Hh Activator / Wnt Activator
QIAGEN	9430022A14	214547	-2.2	0.73	0.08	0.83	0.18		Hh Activator / Wnt Activator
QIAGEN	Gm508	235086	-2.5	0.70	0.08	0.83	0.02		Hh Activator / Wnt Activator
DHARMACON	SLC7A13	74087	-2.1	0.70	0.05	0.82	0.12		Hh Activator / Wnt Activator
DHARMACON	CSE1L	110750	-3.0	0.58	0.07	0.82	0.14		Hh Activator / Wnt Activator
DHARMACON	BDKRB2	12062	-2.9	0.71	0.13	0.82	0.34		Hh Activator / Wnt Activator
DHARMACON	TAS1R1	110326	-2.3	0.51	0.10	0.82	0.13		Hh Activator / Wnt Activator
QIAGEN	PLK4	20873	-2.2	0.71	0.05	0.82	0.02		Hh Activator / Wnt Activator
QIAGEN	Gm817	329207	-2.2	0.60	0.02	0.81	0.24		Hh Activator / Wnt Activator
QIAGEN	Arl11	219144	-2.5	0.71	0.08	0.81	0.10		Hh Activator / Wnt Activator
QIAGEN	Gm665	268473	-3.1	0.62	0.08	0.81	0.10		Hh Activator / Wnt Activator
QIAGEN	4930500O05Rik	242409	-2.3	0.67	0.04	0.81	0.04		Hh Activator / Wnt Activator
DHARMACON	A730012O14RIK	330301	-2.3	0.71	0.08	0.81	0.18		Hh Activator / Wnt Activator
QIAGEN	Zfp313	81018	-2.3	0.62	0.07	0.80	0.11		Hh Activator / Wnt Activator
QIAGEN	Obscn	380698	-2.6	0.70	0.02	0.80	0.09		Hh Activator / Wnt Activator
QIAGEN	Rasl10b	276952	-2.6	0.60	0.05	0.80	0.10		Hh Activator / Wnt Activator
QIAGEN	Rcvrn	19674	-3.4	0.53	0.12	0.80	0.08		Hh Activator / Wnt Activator
DHARMACON	RBP1	19659	-2.0	0.73	0.03	0.79	0.14		Hh Activator / Wnt Activator
QIAGEN	Mapk13	26415	-2.1	0.62	0.06	0.79	0.13		Hh Activator / Wnt Activator
DHARMACON	GPR18	110168	-2.6	0.51	0.05	0.79	0.15		Hh Activator / Wnt Activator
DHARMACON	9130422G05RIK	66819	-2.2	0.73	0.07	0.79	0.09		Hh Activator / Wnt Activator
DHARMACON	SMAD7	17131	-2.0	0.59	0.04	0.79	0.12		Hh Activator / Wnt Activator
DHARMACON	4921537J05RIK	70938	-2.2	0.66	0.09	0.79	0.11		Hh Activator / Wnt Activator
QIAGEN	Map1lc3b	67443	-2.3	0.66	0.06	0.79	0.04		Hh Activator / Wnt Activator
DHARMACON	COPB1	70349	-2.2	0.48	0.04	0.79	0.10		Hh Activator / Wnt Activator
QIAGEN	Gm8	194744	-2.3	0.47	0.04	0.78	0.07		Hh Activator / Wnt Activator
QIAGEN	Gm484	243967	-2.0	0.68	0.03	0.78	0.12		Hh Activator / Wnt Activator
DHARMACON	4933411K20RIK	66756	-2.2	0.54	0.11	0.78	0.19		Hh Activator / Wnt Activator
QIAGEN	Gm980	381311	-2.5	0.64	0.02	0.78	0.10		Hh Activator / Wnt Activator
QIAGEN	Pcdhgb5	93702	-2.8	0.70	0.04	0.77	0.06		Hh Activator / Wnt Activator
DHARMACON	CARHSP1	52502	-2.8	0.73	0.08	0.77	0.14		Hh Activator / Wnt Activator
QIAGEN	Mospd4	72076	-2.8	0.57	0.06	0.77	0.05		Hh Activator / Wnt Activator
DHARMACON	BC003331	226499	-2.2	0.66	0.09	0.77	0.12		Hh Activator / Wnt Activator
DHARMACON	KLHL1	93688	-2.6	0.52	0.03	0.77	0.13		Hh Activator / Wnt Activator
DHARMACON	CD151	12476	-2.2	0.58	0.08	0.76	0.15		Hh Activator / Wnt Activator
DHARMACON	E2F1	13555	-2.0	0.67	0.06	0.76	0.06		Hh Activator / Wnt Activator

QIAGEN	Irx1	16371	-2.0	0.53	0.03	0.76	0.02		Hh Activator / Wnt Activator
QIAGEN	Iqsec2	245666	-2.3	0.58	0.04	0.76	0.18		Hh Activator / Wnt Activator
DHARMACON	GATA2	14461	-2.4	0.56	0.09	0.76	0.08		Hh Activator / Wnt Activator
QIAGEN	Xpr1	19775	-3.2	0.70	0.06	0.75	0.12		Hh Activator / Wnt Activator
DHARMACON	BC021917	225913	-3.0	0.47	0.03	0.75	0.11		Hh Activator / Wnt Activator
DHARMACON	KCNA7	16495	-2.9	0.68	0.12	0.75	0.16		Hh Activator / Wnt Activator
DHARMACON	BC027309	243371	-2.0	0.50	0.09	0.75	0.06		Hh Activator / Wnt Activator
QIAGEN	Nme4	56520	-2.1	0.58	0.12	0.74	0.14		Hh Activator / Wnt Activator
DHARMACON	ESRRG	26381	-2.2	0.69	0.02	0.74	0.08		Hh Activator / Wnt Activator
QIAGEN	Gpr39	71111	-2.8	0.55	0.10	0.74	0.05		Hh Activator / Wnt Activator
QIAGEN	TSSK1	22114	-2.2	0.72	0.10	0.74	0.14		Hh Activator / Wnt Activator
QIAGEN	4930521I23Rik	74716	-2.5	0.51	0.06	0.73	0.03		Hh Activator / Wnt Activator
DHARMACON	EDN2	13615	-2.3	0.47	0.09	0.73	0.08		Hh Activator / Wnt Activator
DHARMACON	CDKN1C	12577	-4.0	0.55	0.03	0.73	0.11		Hh Activator / Wnt Activator
DHARMACON	SLC10A3	214601	-3.5	0.42	0.05	0.73	0.06		Hh Activator / Wnt Activator
DHARMACON	VDAC2	22334	-2.2	0.53	0.07	0.73	0.08		Hh Activator / Wnt Activator
QIAGEN	4930448N21Rik	384817	-2.1	0.65	0.04	0.73	0.09		Hh Activator / Wnt Activator
DHARMACON	5630401M14RIK	75746	-2.3	0.55	0.10	0.73	0.05		Hh Activator / Wnt Activator
DHARMACON	CHRNE	11448	-2.1	0.68	0.11	0.72	0.01		Hh Activator / Wnt Activator
QIAGEN	Hsf2bp	74377	-4.1	0.62	0.12	0.72	0.09		Hh Activator / Wnt Activator
DHARMACON	4930438D12RIK	74868	-3.9	0.57	0.12	0.72	0.05		Hh Activator / Wnt Activator
QIAGEN	BC064011	407790	-2.2	0.65	0.07	0.72	0.04		Hh Activator / Wnt Activator
QIAGEN	Gm207	240879	-3.9	0.57	0.05	0.71	0.12		Hh Activator / Wnt Activator
DHARMACON	2700050C12RIK	72585	-2.0	0.66	0.04	0.71	0.09		Hh Activator / Wnt Activator
DHARMACON	4732463G12RIK	338364	-2.2	0.75	0.10	0.71	0.11		Hh Activator / Wnt Activator
DHARMACON	4930463G05RIK	70806	-3.3	0.54	0.05	0.71	0.04		Hh Activator / Wnt Activator
QIAGEN	1810054O13Rik	67893	-2.2	0.63	0.08	0.71	0.12		Hh Activator / Wnt Activator
DHARMACON	A530088H08RIK	193003	-2.1	0.66	0.13	0.71	0.09		Hh Activator / Wnt Activator
QIAGEN	Fkbpl	56299	-2.5	0.73	0.03	0.70	0.14		Hh Activator / Wnt Activator
DHARMACON	CCNI	12453	-2.7	0.56	0.09	0.70	0.11		Hh Activator / Wnt Activator
DHARMACON	OPRL	18389	-2.0	0.63	0.06	0.70	0.04		Hh Activator / Wnt Activator
QIAGEN	Prkca	18750	-2.4	0.69	0.03	0.70	0.04		Hh Activator / Wnt Activator
DHARMACON	IL1F5	54450	-2.0	0.73	0.06	0.69	0.02		Hh Activator / Wnt Activator
QIAGEN	Tlm	21893	-2.5	0.72	0.03	0.69	0.20		Hh Activator / Wnt Activator
DHARMACON	IL22	50929	-2.4	0.62	0.12	0.69	0.11		Hh Activator / Wnt Activator
QIAGEN	Fndc5	384061	-2.3	0.58	0.02	0.69	0.06		Hh Activator / Wnt Activator
DHARMACON	CNN2	12798	-2.1	0.73	0.05	0.69	0.04		Hh Activator / Wnt Activator
DHARMACON	CAPZA3	12344	-2.8	0.75	0.06	0.68	0.02		Hh Activator / Wnt Activator
DHARMACON	4930451F05RIK	74673	-3.0	0.58	0.06	0.68	0.00		Hh Activator / Wnt Activator

DHARMACON	GORASP1	74498	-2.0	0.61	0.02	0.68	0.18		Hh Activator / Wnt Activator
DHARMACON	St6galnac2	20446	-2.1	0.43	0.04	0.68	0.07		Hh Activator / Wnt Activator
DHARMACON	IL11RA1	16157	-2.3	0.59	0.06	0.68	0.13		Hh Activator / Wnt Activator
QIAGEN	2310038E17Rik	71903	-2.6	0.75	0.04	0.68	0.06		Hh Activator / Wnt Activator
QIAGEN	Mt3	17751	-2.0	0.68	0.10	0.67	0.09		Hh Activator / Wnt Activator
DHARMACON	SEC8L1	20336	-3.1	0.61	0.06	0.67	0.13		Hh Activator / Wnt Activator
QIAGEN	Noxa1	241275	-2.1	0.61	0.07	0.67	0.12		Hh Activator / Wnt Activator
DHARMACON	TTBK1	140810	-2.4	0.49	0.10	0.67	0.11		Hh Activator / Wnt Activator
QIAGEN	Gm24	195236	-2.6	0.74	0.04	0.67	0.06		Hh Activator / Wnt Activator
QIAGEN	C230098I05Rik	269994	-2.2	0.56	0.07	0.67	0.13		Hh Activator / Wnt Activator
QIAGEN	Ldb3	24131	-2.7	0.51	0.04	0.67	0.16		Hh Activator / Wnt Activator
DHARMACON	CDK3	69681	-3.5	0.65	0.11	0.66	0.12		Hh Activator / Wnt Activator
DHARMACON	ARMCX2	67416	-2.0	0.66	0.08	0.66	0.15		Hh Activator / Wnt Activator
DHARMACON	CASP2	12366	-2.3	0.60	0.12	0.66	0.08		Hh Activator / Wnt Activator
DHARMACON	CHRNA4	11438	-2.3	0.51	0.05	0.66	0.12		Hh Activator / Wnt Activator
QIAGEN	Myst3	244349	-2.1	0.53	0.03	0.65	0.17		Hh Activator / Wnt Activator
DHARMACON	OLFR1370	258528	-2.0	0.64	0.05	0.64	0.06		Hh Activator / Wnt Activator
DHARMACON	BC030440	210035	-2.6	0.58	0.06	0.64	0.08		Hh Activator / Wnt Activator
QIAGEN	LOC384405	384405	-2.1	0.62	0.07	0.64	0.05		Hh Activator / Wnt Activator
DHARMACON	4930579J09RIK	67752	-2.5	0.70	0.05	0.63	0.09		Hh Activator / Wnt Activator
QIAGEN	6530402A20	328479	-2.3	0.72	0.04	0.63	0.13		Hh Activator / Wnt Activator
QIAGEN	Clec2f	435921	-2.4	0.63	0.08	0.63	0.16		Hh Activator / Wnt Activator
QIAGEN	Gap43	14432	-2.3	0.66	0.07	0.63	0.12		Hh Activator / Wnt Activator
DHARMACON	ZFY2	22768	-2.0	0.67	0.07	0.63	0.17		Hh Activator / Wnt Activator
DHARMACON	A430079E08	232537	-2.2	0.43	0.06	0.63	0.05		Hh Activator / Wnt Activator
DHARMACON	KLK11	16613	-2.1	0.70	0.02	0.63	0.09		Hh Activator / Wnt Activator
QIAGEN	2010012F05Rik	75608	-3.1	0.34	0.06	0.63	0.09		Hh Activator / Wnt Activator
DHARMACON	CLDN9	56863	-2.5	0.54	0.08	0.62	0.18		Hh Activator / Wnt Activator
DHARMACON	NKX1-2	20231	-2.4	0.66	0.07	0.62	0.09		Hh Activator / Wnt Activator
DHARMACON	SERPINB1C	380839	-2.1	0.57	0.05	0.61	0.06		Hh Activator / Wnt Activator
DHARMACON	5730410E15RIK	319613	-3.6	0.75	0.08	0.60	0.06		Hh Activator / Wnt Activator
DHARMACON	A530099J19RIK	319293	-2.4	0.60	0.09	0.60	0.06		Hh Activator / Wnt Activator
QIAGEN	Fbxo11	225055	-2.7	0.52	0.11	0.60	0.06		Hh Activator / Wnt Activator
QIAGEN	1700026P10Rik	70069	-4.1	0.67	0.13	0.60	0.27		Hh Activator / Wnt Activator
DHARMACON	ITPKB	320404	-2.2	0.57	0.08	0.60	0.10		Hh Activator / Wnt Activator
DHARMACON	AW212607	241732	-2.2	0.64	0.10	0.60	0.19		Hh Activator / Wnt Activator
QIAGEN	Og9x	18292	-3.2	0.64	0.12	0.60	0.05		Hh Activator / Wnt Activator
DHARMACON	CLIC6	209195	-3.0	0.62	0.06	0.60	0.11		Hh Activator / Wnt Activator
DHARMACON	WARS2	70560	-2.5	0.61	0.04	0.59	0.15		Hh Activator / Wnt Activator

DHARMACON	CDV3	321022	-3.0	0.72	0.10	0.59	0.13		Hh Activator / Wnt Activator
DHARMACON	RBP2	19660	-3.1	0.65	0.10	0.59	0.20		Hh Activator / Wnt Activator
DHARMACON	A230103N10RIK	104625	-2.8	0.49	0.07	0.58	0.11		Hh Activator / Wnt Activator
DHARMACON	ADARB2	94191	-2.0	0.67	0.14	0.57	0.06		Hh Activator / Wnt Activator
QIAGEN	2610029G23Rik	67683	-2.4	0.68	0.09	0.57	0.08		Hh Activator / Wnt Activator
DHARMACON	A930001N09RIK	77128	-2.0	0.63	0.06	0.56	0.04		Hh Activator / Wnt Activator
DHARMACON	BTN1A1	12231	-2.1	0.60	0.13	0.56	0.02		Hh Activator / Wnt Activator
QIAGEN	2610028H24Rik	76964	-2.0	0.57	0.08	0.55	0.12		Hh Activator / Wnt Activator
QIAGEN	Fmnl3	22379	-2.5	0.68	0.03	0.55	0.08		Hh Activator / Wnt Activator
DHARMACON	MAP3K5	26408	-3.0	0.70	0.11	0.54	0.05		Hh Activator / Wnt Activator
DHARMACON	BC021891	234878	-2.5	0.74	0.05	0.54	0.17		Hh Activator / Wnt Activator
DHARMACON	CACNA2D2	56808	-4.7	0.52	0.06	0.54	0.09		Hh Activator / Wnt Activator
DHARMACON	CALML3	70405	-4.0	0.44	0.03	0.54	0.11		Hh Activator / Wnt Activator
DHARMACON	AU040829	216831	-2.2	0.55	0.04	0.53	0.13		Hh Activator / Wnt Activator
DHARMACON	BC026744	330192	-2.0	0.56	0.11	0.53	0.09		Hh Activator / Wnt Activator
QIAGEN	Foxr1	382074	-2.5	0.62	0.05	0.52	0.12		Hh Activator / Wnt Activator
DHARMACON	NKTR	18087	-2.0	0.59	0.05	0.51	0.08		Hh Activator / Wnt Activator
DHARMACON	4833432M17RIK	381318	-2.0	0.39	0.05	0.50	0.11		Hh Activator / Wnt Activator
DHARMACON	2900075G08RIK	72978	-2.2	0.58	0.04	0.49	0.03		Hh Activator / Wnt Activator
DHARMACON	FAU	14109	-2.8	0.58	0.11	0.49	0.06		Hh Activator / Wnt Activator
DHARMACON	9230106L14RIK	192201	-2.8	0.50	0.07	0.49	0.03		Hh Activator / Wnt Activator
QIAGEN	LOC432958	432958	-3.1	0.53	0.13	0.48	0.03		Hh Activator / Wnt Activator
DHARMACON	BC031353	235493	-2.8	0.56	0.04	0.48	0.04		Hh Activator / Wnt Activator
DHARMACON	HADHSC	15107	-3.2	0.55	0.09	0.48	0.04		Hh Activator / Wnt Activator
QIAGEN	Copb2	50797	-2.3	0.48	0.09	0.47	0.08		Hh Activator / Wnt Activator
DHARMACON	CLDN16	114141	-2.1	0.61	0.13	0.47	0.08		Hh Activator / Wnt Activator
DHARMACON	BMP8A	12163	-2.8	0.74	0.07	0.46	0.03		Hh Activator / Wnt Activator
DHARMACON	CRSP7	70625	-4.3	0.40	0.01	0.46	0.06		Hh Activator / Wnt Activator
DHARMACON	FOXM1	14235	-3.2	0.56	0.14	0.46	0.17		Hh Activator / Wnt Activator
DHARMACON	CTSH	13036	-2.3	0.57	0.11	0.45	0.05		Hh Activator / Wnt Activator
DHARMACON	CASP4	12363	-2.5	0.71	0.10	0.44	0.11		Hh Activator / Wnt Activator
DHARMACON	CIZ1	68379	-2.8	0.49	0.07	0.44	0.16		Hh Activator / Wnt Activator
QIAGEN	Hspa5	14828	-3.1	0.65	0.05	0.44	0.06		Hh Activator / Wnt Activator
DHARMACON	BC035291	208043	-2.7	0.62	0.10	0.43	0.07		Hh Activator / Wnt Activator
DHARMACON	D11ERTD498E	52639	-3.1	0.59	0.07	0.43	0.08		Hh Activator / Wnt Activator
DHARMACON	A930039G15RIK	338366	-2.0	0.62	0.09	0.42	0.08		Hh Activator / Wnt Activator
DHARMACON	5730405M13RIK	66627	-2.4	0.43	0.09	0.41	0.16		Hh Activator / Wnt Activator
DHARMACON	PSMB8	16913	-2.5	0.53	0.02	0.41	0.15		Hh Activator / Wnt Activator
DHARMACON	NR1D1	217166	-2.0	0.43	0.11	0.40	0.05		Hh Activator / Wnt Activator

DHARMACON	AURKC	20871	-2.3	0.59	0.04	0.40	0.15		Hh Activator / Wnt Activator
QIAGEN	Gm967	381217	-2.8	0.73	0.03	0.39	0.13		Hh Activator / Wnt Activator
DHARMACON	LOC381810	381810	-2.1	0.55	0.06	0.38	0.04		Hh Activator / Wnt Activator
DHARMACON	ADARB1	110532	-2.0	0.68	0.14	0.35	0.08		Hh Activator / Wnt Activator
DHARMACON	4432406C05RIK	66690	-2.1	0.62	0.09	0.35	0.05		Hh Activator / Wnt Activator
QIAGEN	Pura	19290	-2.3	0.72	0.11	0.31	0.02		Hh Activator / Wnt Activator
QIAGEN	Camta2	216874	-2.0	0.83	0.05				Failed to pass Secondary Screening
QIAGEN	Adamts16	271127	-2.0	0.77	0.04				Failed to pass Secondary Screening
DHARMACON	PKIB	18768	-2.0	0.72	0.19				Failed to pass Secondary Screening
QIAGEN	Gm264	217738	-2.0	0.77	0.08				Failed to pass Secondary Screening
QIAGEN	Snta1	20648	-2.0	0.52	0.18				Failed to pass Secondary Screening
QIAGEN	Kcnab1	16497	-2.0	0.89	0.32				Failed to pass Secondary Screening
QIAGEN	Parp6	67287	-2.0	0.78	0.05				Failed to pass Secondary Screening
DHARMACON	MRTF-B	239719	-2.0	0.57	0.17				Failed to pass Secondary Screening
QIAGEN	Ugt1a2	22236	-2.0	0.86	0.09				Failed to pass Secondary Screening
DHARMACON	WDR10	81896	-2.0	0.84	0.04				Failed to pass Secondary Screening
DHARMACON	BGLAP1	12096	-2.0	1.07	0.02				Failed to pass Secondary Screening
QIAGEN	Mrpl13	68537	-2.0	0.79	0.16				Failed to pass Secondary Screening
QIAGEN	Ccnb1	268697	-2.0	0.81	0.11				Failed to pass Secondary Screening
DHARMACON	9230110J10	329958	-2.0	0.71	0.15				Failed to pass Secondary Screening
DHARMACON	GPLD1	14756	-2.0	0.86	0.08				Failed to pass Secondary Screening
QIAGEN	Ube2c	68612	-2.0	0.82	0.02				Failed to pass Secondary Screening
DHARMACON	GPATC2	67769	-2.0	0.97	0.13				Failed to pass Secondary Screening
DHARMACON	TAGLN	21345	-2.0	0.93	0.12				Failed to pass Secondary Screening
QIAGEN	Kctd7	212919	-2.0	0.76	0.03				Failed to pass Secondary Screening
QIAGEN	Drd1a	13488	-2.0	0.87	0.09				Failed to pass Secondary Screening
DHARMACON	MLP	17357	-2.0	0.57	0.22				Failed to pass Secondary Screening
QIAGEN	LOC432713	432713	-2.0	0.77	0.04				Failed to pass Secondary Screening
DHARMACON	NME5	75533	-2.0	0.74	0.16				Failed to pass Secondary Screening
DHARMACON	PDK2	18604	-2.0	0.77	0.07				Failed to pass Secondary Screening
DHARMACON	NR2F2	11819	-2.0	0.62	0.21				Failed to pass Secondary Screening
QIAGEN	2700049P18Rik	108900	-2.0	0.90	0.07				Failed to pass Secondary Screening
DHARMACON	4932411N23	237029	-2.0	0.92	0.05				Failed to pass Secondary Screening
DHARMACON	SREBF1	20787	-2.0	1.12	0.30				Failed to pass Secondary Screening
DHARMACON	C130032F08RIK	243372	-2.1	0.90	0.08				Failed to pass Secondary Screening
DHARMACON	4921536K21RIK	67430	-2.1	0.96	0.17				Failed to pass Secondary Screening
QIAGEN	Gan	209239	-2.1	0.82	0.10				Failed to pass Secondary Screening
DHARMACON	ARRB2	216869	-2.1	0.89	0.07				Failed to pass Secondary Screening
DHARMACON	A630042L21RIK	106894	-2.1	0.75	0.18				Failed to pass Secondary Screening

DHARMACON	4933425K02RIK	74446	-2.1	0.76	0.07			Failed to pass Secondary Screening
DHARMACON	MXD4	17122	-2.1	0.76	0.20			Failed to pass Secondary Screening
QIAGEN	2410018G23Rik	69742	-2.1	0.84	0.05			Failed to pass Secondary Screening
DHARMACON	SLC12A2	20496	-2.1	0.75	0.27			Failed to pass Secondary Screening
QIAGEN	4921511K06Rik	232664	-2.1	0.40	0.34			Failed to pass Secondary Screening
DHARMACON	YWHAZ	22631	-2.1	0.97	0.28			Failed to pass Secondary Screening
DHARMACON	C920006C10RIK	76740	-2.1	1.19	0.02			Failed to pass Secondary Screening
DHARMACON	WHSC2	24116	-2.1	1.13	0.10			Failed to pass Secondary Screening
QIAGEN	Stxbp6	217517	-2.1	0.83	0.19			Failed to pass Secondary Screening
DHARMACON	FGF4	14175	-2.1	0.79	0.18			Failed to pass Secondary Screening
DHARMACON	PROX1	19130	-2.1	1.79	0.52			Failed to pass Secondary Screening
DHARMACON	TERF2	21750	-2.1	0.80	0.26			Failed to pass Secondary Screening
QIAGEN	2610016F04Rik	66923	-2.1	0.77	0.21			Failed to pass Secondary Screening
DHARMACON	BOP1	12181	-2.1	0.92	0.02			Failed to pass Secondary Screening
QIAGEN	Apln	30878	-2.1	0.83	0.08			Failed to pass Secondary Screening
DHARMACON	PTPRF	19268	-2.1	0.74	0.32			Failed to pass Secondary Screening
DHARMACON	NUCB	18220	-2.1	0.82	0.24			Failed to pass Secondary Screening
QIAGEN	Ngfa	18048	-2.2	0.80	0.07			Failed to pass Secondary Screening
QIAGEN	B4galt2	53418	-2.2	0.79	0.03			Failed to pass Secondary Screening
DHARMACON	IVD	56357	-2.2	0.78	0.12			Failed to pass Secondary Screening
QIAGEN	Usp15	14479	-2.2	0.73	0.15			Failed to pass Secondary Screening
QIAGEN	Ces5	234673	-2.2	0.76	0.22			Failed to pass Secondary Screening
DHARMACON	MPZL1	68481	-2.2	0.79	0.21			Failed to pass Secondary Screening
DHARMACON	1810020G14RIK	66272	-2.2	0.82	0.06			Failed to pass Secondary Screening
QIAGEN	Galgt2	14422	-2.2	0.77	0.05			Failed to pass Secondary Screening
DHARMACON	4930506D23RIK	75099	-2.2	0.77	0.15			Failed to pass Secondary Screening
QIAGEN	Prpf3	70767	-2.2	0.85	0.12			Failed to pass Secondary Screening
QIAGEN	Mlze	83492	-2.2	0.76	0.04			Failed to pass Secondary Screening
DHARMACON	AVP	11998	-2.2	0.56	0.22			Failed to pass Secondary Screening
QIAGEN	4631426E05Rik	66696	-2.2	0.50	0.15			Failed to pass Secondary Screening
DHARMACON	DICER1	192119	-2.2	0.77	0.12			Failed to pass Secondary Screening
QIAGEN	Atp1b3	11933	-2.2	0.80	0.02			Failed to pass Secondary Screening
DHARMACON	9530053H22	328919	-2.2	0.54	0.15			Failed to pass Secondary Screening
QIAGEN	0610038D11Rik	67674	-2.3	0.88	0.06			Failed to pass Secondary Screening
DHARMACON	RAPGEF2	76089	-2.3	1.09	0.18			Failed to pass Secondary Screening
DHARMACON	DAPK2	13143	-2.3	0.88	0.08			Failed to pass Secondary Screening
DHARMACON	SSPN	16651	-2.3	0.62	0.19			Failed to pass Secondary Screening
DHARMACON	ITPKC	233011	-2.3	0.79	0.09			Failed to pass Secondary Screening
QIAGEN	Lrp10	65107	-2.3	0.55	0.38			Failed to pass Secondary Screening

DHARMACON	MBD2	17191	-2.3	1.32	0.44			Failed to pass Secondary Screening
DHARMACON	IFI35	70110	-2.3	0.82	0.13			Failed to pass Secondary Screening
QIAGEN	Nudt14	66174	-2.3	0.79	0.05			Failed to pass Secondary Screening
QIAGEN	BC022651	330460	-2.3	0.77	0.08			Failed to pass Secondary Screening
DHARMACON	BC026432	233890	-2.3	0.68	0.15			Failed to pass Secondary Screening
DHARMACON	6330503K22RIK	101565	-2.3	1.36	0.13			Failed to pass Secondary Screening
QIAGEN	Sox17	20671	-2.3	0.56	0.17			Failed to pass Secondary Screening
DHARMACON	BIRC2	11797	-2.3	0.97	0.15			Failed to pass Secondary Screening
QIAGEN	Gmeb1	56809	-2.3	0.83	0.11			Failed to pass Secondary Screening
QIAGEN	B3galt3	26879	-2.3	0.82	0.06			Failed to pass Secondary Screening
QIAGEN	Glp1r	14652	-2.3	0.77	0.11			Failed to pass Secondary Screening
QIAGEN	Cct2	12461	-2.3	0.78	0.10			Failed to pass Secondary Screening
DHARMACON	CCM2	216527	-2.4	0.92	0.16			Failed to pass Secondary Screening
DHARMACON	AB041803	232685	-2.4	0.62	0.16			Failed to pass Secondary Screening
DHARMACON	SRRM2	75956	-2.4	0.80	0.17			Failed to pass Secondary Screening
DHARMACON	CABP5	29865	-2.4	1.03	0.21			Failed to pass Secondary Screening
QIAGEN	1700052I22Rik	67340	-2.4	0.91	0.10			Failed to pass Secondary Screening
DHARMACON	Stat6	20852	-2.4	0.79	0.22			Failed to pass Secondary Screening
DHARMACON	PARVB	170736	-2.4	0.80	0.03			Failed to pass Secondary Screening
DHARMACON	ITK	16428	-2.4	1.01	0.16			Failed to pass Secondary Screening
DHARMACON	SLIT2	20563	-2.4	0.80	0.26			Failed to pass Secondary Screening
DHARMACON	6230417E10RIK	271849	-2.4	0.94	0.04			Failed to pass Secondary Screening
DHARMACON	NFE2L1	18023	-2.4	0.89	0.12			Failed to pass Secondary Screening
DHARMACON	MCM3AP	54387	-2.4	1.10	0.17			Failed to pass Secondary Screening
DHARMACON	RHOE	74194	-2.4	0.74	0.31			Failed to pass Secondary Screening
QIAGEN	Mfap1	67532	-2.4	0.76	0.07			Failed to pass Secondary Screening
DHARMACON	WNT3	22415	-2.5	1.04	0.06			Failed to pass Secondary Screening
QIAGEN	Mrgprd	211578	-2.5	0.88	0.03			Failed to pass Secondary Screening
DHARMACON	VDR	22337	-2.5	1.20	0.40			Failed to pass Secondary Screening
DHARMACON	TXK	22165	-2.5	0.68	0.15			Failed to pass Secondary Screening
DHARMACON	OGG1	18294	-2.5	0.68	0.30			Failed to pass Secondary Screening
DHARMACON	GM1395	231637	-2.5	0.64	0.18			Failed to pass Secondary Screening
DHARMACON	AATF	56321	-2.5	0.69	0.28			Failed to pass Secondary Screening
DHARMACON	IRF3	54131	-2.5	0.82	0.16			Failed to pass Secondary Screening
DHARMACON	GM711	279029	-2.5	0.83	0.04			Failed to pass Secondary Screening
DHARMACON	CTSK	13038	-2.5	0.82	0.06			Failed to pass Secondary Screening
DHARMACON	CACNA2D3	12294	-2.5	0.89	0.14			Failed to pass Secondary Screening
DHARMACON	XEDAR	245527	-2.5	0.93	0.23			Failed to pass Secondary Screening
DHARMACON	SYNCRIP	56403	-2.5	1.12	0.17			Failed to pass Secondary Screening

DHARMACON	BAX	12028	-2.6	0.86	0.48			Failed to pass Secondary Screening
DHARMACON	Tcf12	21406	-2.6	1.43	0.49			Failed to pass Secondary Screening
DHARMACON	ICAM1	15894	-2.6	0.95	0.16			Failed to pass Secondary Screening
QIAGEN	2610027O18Rik	76357	-2.6	0.76	0.08			Failed to pass Secondary Screening
DHARMACON	CPLX1	12889	-2.6	0.91	0.18			Failed to pass Secondary Screening
QIAGEN	Olfr1457	258568	-2.6	0.80	0.06			Failed to pass Secondary Screening
QIAGEN	Gm943	381122	-2.6	0.84	0.09			Failed to pass Secondary Screening
DHARMACON	KCNAB1	16497	-2.6	0.93	0.16			Failed to pass Secondary Screening
QIAGEN	Chst7	60322	-2.6	0.82	0.05			Failed to pass Secondary Screening
DHARMACON	TNFRSF13B	57916	-2.6	0.81	0.30			Failed to pass Secondary Screening
DHARMACON	CTGF	14219	-2.6	0.77	0.07			Failed to pass Secondary Screening
DHARMACON	6330408A02RIK	321008	-2.7	1.55	0.02			Failed to pass Secondary Screening
DHARMACON	DAB2	13132	-2.7	0.80	0.10			Failed to pass Secondary Screening
QIAGEN	Olfr1134	259032	-2.7	0.79	0.07			Failed to pass Secondary Screening
DHARMACON	Stat4	20849	-2.7	0.83	0.20			Failed to pass Secondary Screening
DHARMACON	EDAR	13608	-2.7	1.17	0.28			Failed to pass Secondary Screening
DHARMACON	CAPN9	73647	-2.7	0.85	0.03			Failed to pass Secondary Screening
QIAGEN	Neu1	18010	-2.7	0.82	0.06			Failed to pass Secondary Screening
QIAGEN	Olfr1076	258401	-2.7	0.91	0.03			Failed to pass Secondary Screening
DHARMACON	6030410K14	329628	-2.7	0.38	0.22			Failed to pass Secondary Screening
DHARMACON	CMYA1	22437	-2.8	0.84	0.09			Failed to pass Secondary Screening
DHARMACON	ITGA9	104099	-2.8	0.87	0.15			Failed to pass Secondary Screening
DHARMACON	SIAT8E	225742	-2.8	1.16	0.09			Failed to pass Secondary Screening
DHARMACON	MRC2	17534	-2.8	0.80	0.22			Failed to pass Secondary Screening
DHARMACON	PAPSS2	23972	-2.8	1.05	0.31			Failed to pass Secondary Screening
DHARMACON	BHLHB2	20893	-2.9	0.82	0.25			Failed to pass Secondary Screening
DHARMACON	B230114P05RIK	207596	-2.9	0.46	0.16			Failed to pass Secondary Screening
DHARMACON	SPRY1	24063	-2.9	1.09	0.19			Failed to pass Secondary Screening
DHARMACON	NUBP2	26426	-2.9	0.66	0.16			Failed to pass Secondary Screening
DHARMACON	B3GNT1	53625	-2.9	1.04	0.15			Failed to pass Secondary Screening
DHARMACON	EFNA5	13640	-2.9	0.72	0.19			Failed to pass Secondary Screening
DHARMACON	B230205M03	232430	-3.0	0.67	0.27			Failed to pass Secondary Screening
DHARMACON	BTBD6	399566	-3.0	0.90	0.13			Failed to pass Secondary Screening
DHARMACON	AY147207	378429	-3.0	0.83	0.15			Failed to pass Secondary Screening
DHARMACON	TAF7L	74469	-3.1	0.72	0.16			Failed to pass Secondary Screening
QIAGEN	Abpe	381970	-3.1	0.76	0.09			Failed to pass Secondary Screening
DHARMACON	FZR1	56371	-3.1	0.72	0.19			Failed to pass Secondary Screening
DHARMACON	VIM	22352	-3.1	1.11	0.39			Failed to pass Secondary Screening
QIAGEN	Glp2r	93896	-3.1	0.76	0.11			Failed to pass Secondary Screening

DHARMACON	6330530A05RIK	230678	-3.1	0.76	0.06			Failed to pass Secondary Screening
DHARMACON	IL2RA	16184	-3.2	0.84	0.18			Failed to pass Secondary Screening
DHARMACON	PPM1A	19042	-3.2	0.72	0.35			Failed to pass Secondary Screening
DHARMACON	ATIC	108147	-3.3	0.82	0.30			Failed to pass Secondary Screening
DHARMACON	YWHAG	22628	-3.3	0.62	0.18			Failed to pass Secondary Screening
QIAGEN	Fmr1nb	207854	-3.3	0.82	0.02			Failed to pass Secondary Screening
DHARMACON	Idb1	15901	-3.3	1.25	0.33			Failed to pass Secondary Screening
DHARMACON	5730437N04RIK	70544	-3.3	0.77	0.05			Failed to pass Secondary Screening
QIAGEN	1100001G20Rik	66107	-3.4	0.79	0.08			Failed to pass Secondary Screening
QIAGEN	Madcam1	17123	-3.4	0.70	0.15			Failed to pass Secondary Screening
DHARMACON	APLP1	11803	-3.4	1.20	0.60			Failed to pass Secondary Screening
DHARMACON	4933425L11RIK	66767	-3.5	0.80	0.17			Failed to pass Secondary Screening
DHARMACON	CARD10	105844	-3.5	0.92	0.10			Failed to pass Secondary Screening
QIAGEN	Ube2v2	70620	-3.5	0.86	0.08			Failed to pass Secondary Screening
QIAGEN	Fubp1	51886	-3.5	0.81	0.05			Failed to pass Secondary Screening
DHARMACON	LOC381406	381406	-3.6	0.72	0.17			Failed to pass Secondary Screening
QIAGEN	Kin	16588	-3.6	0.42	0.20			Failed to pass Secondary Screening
DHARMACON	PRSS25	64704	-3.7	1.56	0.41			Failed to pass Secondary Screening
DHARMACON	BC062109	231503	-3.8	0.80	0.09			Failed to pass Secondary Screening
DHARMACON	BRI3	55950	-3.8	1.25	0.08			Failed to pass Secondary Screening
DHARMACON	BC061212	381724	-3.9	1.20	0.07			Failed to pass Secondary Screening
DHARMACON	IGFBP3	16009	-3.9	0.85	0.13			Failed to pass Secondary Screening
DHARMACON	SH3BP1	20401	-3.9	0.87	0.06			Failed to pass Secondary Screening
DHARMACON	NPNT	114249	-3.9	0.99	0.15			Failed to pass Secondary Screening
DHARMACON	5730406I15RIK	66624	-4.0	0.88	0.12			Failed to pass Secondary Screening
DHARMACON	C920025J10	218444	-4.2	0.89	0.05			Failed to pass Secondary Screening
QIAGEN	1110001A12Rik	100087	-4.3	0.83	0.07			Failed to pass Secondary Screening
DHARMACON	NRAP	18175	-4.4	1.42	0.21			Failed to pass Secondary Screening
DHARMACON	CASP3	12367	-4.4	0.77	0.11			Failed to pass Secondary Screening
DHARMACON	BC062185	215112	-4.4	1.01	0.12			Failed to pass Secondary Screening
DHARMACON	BTBD3	228662	-4.7	0.88	0.03			Failed to pass Secondary Screening
DHARMACON	CABLES1	63955	-4.9	0.83	0.11			Failed to pass Secondary Screening
DHARMACON	BMF	171543	-5.1	1.08	0.15			Failed to pass Secondary Screening
DHARMACON	DAO1	13142	-5.6	1.11	0.05			Failed to pass Secondary Screening

APPENDIX D

siRNA sequences targeting disease genes

Gene	Library	siRNA sequence
Gli2	Qiagen	CACCTGCATGCTAGAGGCAAA
		CTGCAGCAATATGGCAGCCAA
		CTCGCTGGTAGCTTACATCAA
		ACCATCATGAATGGCCATCAA
	Dharmacon	GGAGGGAAGGUACCAUUAU
		CAUCAAGGCUCACACCGGU
		GCAUCACGAUUCUCUAGUC
		GAUCAGAACACGCUAUACU
Stk22B/Tssk2	Qiagen	CAAGTTCAATGTGGCAGTCAA
		AAGATCATAGACCGAAAGAAA
		CCGTTCCATCATTAAGACCTA
		CAGGTAGGAGCTGAAGAAGCA
	Dharmacon	GAACCUAACUGGUGAGUGC
		GGCAAGGGCUCCUACGCAA
		AACCACCGUUCCAUCAUUA
		GCUGAUUGCAAGUUGGAUA
Dgkq	Qiagen	CAAGATTGTTCAGATGAATAA
		CACAAGCAGGTTCCACAACAA
		CAGTTTGGGCTTAACATACTA
		CAGCAGGATTATGACACGTAT
Gpc1	Dharmacon	GAUCAUGACCAACCGUUUA
		GGGCCAACCUGCACCUUGA
		UACCAGAGGUGAUGGGUGA
		GAAGCGUCGCCGUGGCAAA
Rlbp1	Dharmacon	CAAGUAUGGUCGAGUGGUU
		GGUCUUUGUUCACGGAGAU
		GAUGAGAUCUUACAGGCAU
		CAAAUCAACGGCUUCUGUA
Aaas	Qiagen	CAGATCTTTCTGAGACAACAA
		CACCCTGTATGAGCACAATAA
		AAGAAGTGTTTGAGTGGGTAA
		CACCGTCTGCAGCGAAATGTA
	Dharmacon	CGACUGCUGUUCACUGUAU
		GAUCAAUCUUCCUGUCCUA
		UAUGGGACGUUUCAACAGA
		GCGCCCAGGUGUUGUCUCA
Ift57/Hippi	Qiagen	TACAATGAATATAGTATTTAA
		CACGATTAGGACTGACAATAA
		CAGGTGAAATCTAGTATTTGA

		CAGCAATTGGCTTCTATTAAA
Smo	Dharmacon	CCAAUUGGCCUGGUGCUUA
		GAGCCCACCUCCAGUGAGA
		GGGCAAGACAUCCUAUUUC
		GAGGGUGGCCUGACUUUCU
Prkar1a	Dharmacon	GAAAUUGCCCUGCUGAUGA
		CGAGACAGCUACCGAAGAA
		GAUGCUGCCUCCUACGUUA
		CGAAGAAUUUGUUGAAGUG
Stk11/Lkb1	Dharmacon	CCAAUGGACUGGACACCUU
		GCGCCAAGCUCAUCGGCAA
		GGUCACACUUUACAACAUC
		GUGAUGGAGUACUGCGUAU

BIBLIOGRAPHY

Aberle, H., Bauer, A., Stappert, J., Kispert, A., and Kemler, R. (1997). beta-catenin is a target for the ubiquitin-proteasome pathway. EMBO J *16*, 3797-3804.

Akita, K., Francis-West, P., and Vargesson, N. (1996). The ectodermal control in chick limb development: Wnt-7a, Shh, Bmp-2 and Bmp-4 expression and the effect of FGF-4 on gene expression. Mech Dev *60*, 127-137.

Alcedo, J., Ayzenzon, M., Von Ohlen, T., Noll, M., and Hooper, J.E. (1996). The Drosophila smoothened gene encodes a seven-pass membrane protein, a putative receptor for the hedgehog signal. Cell *86*, 221-232.

Alexandre, C., Jacinto, A., and Ingham, P.W. (1996). Transcriptional activation of hedgehog target genes in Drosophila is mediated directly by the cubitus interruptus protein, a member of the GLI family of zinc finger DNA-binding proteins. Genes Dev *10*, 2003-2013.

Alieva, I.B., Gorgidze, L.A., Komarova, Y.A., Chernobelskaya, O.A., and Vorobjev, I.A. (1999). Experimental model for studying the primary cilia in tissue culture cells. Membr Cell Biol *12*, 895-905.

Alvarez-Medina, R., Cayuso, J., Okubo, T., Takada, S., and Martí, E. (2008). Wnt canonical pathway restricts graded Shh/Gli patterning activity through the regulation of Gli3 expression. Development *135*, 237-247.

Amieux, P.S., and McKnight, G.S. (2002). The essential role of RI alpha in the maintenance of regulated PKA activity. Ann N Y Acad Sci *968*, 75-95.

Amit, S., Hatzubai, A., Birman, Y., Andersen, J.S., Ben-Shushan, E., Mann, M., Ben-Neriah, Y., and Alkalay, I. (2002). Axin-mediated CKI phosphorylation of beta-catenin at Ser 45: a molecular switch for the Wnt pathway. Genes Dev *16*, 1066-1076.

Aza-Blanc, P., Ramírez-Weber, F.A., Laget, M.P., Schwartz, C., and Kornberg, T.B. (1997). Proteolysis that is inhibited by hedgehog targets Cubitus interruptus protein to the nucleus and converts it to a repressor. Cell *89*, 1043-1053.

Bai, C.B., and Joyner, A.L. (2001). Gli1 can rescue the in vivo function of Gli2. Development *128*, 5161-5172.

Baker, N. (1988). Embryonic and imaginal requirements for wingless, a segment-polarity gene in Drosophila. Dev Biol *125*, 96-108.

Balordi, F., and Fishell, G. (2007a). Hedgehog signaling in the subventricular zone is required for both the maintenance of stem cells and the migration of newborn neurons. J Neurosci *27*, 5936-5947.

Balordi, F., and Fishell, G. (2007b). Mosaic removal of hedgehog signaling in the adult SVZ reveals that the residual wild-type stem cells have a limited capacity for self-renewal. J Neurosci *27*, 14248-14259.

Barakat, M.T., Humke, E.W., and Scott, M.P. (2010). Learning from Jekyll to control Hyde: Hedgehog signaling in development and cancer. Trends Mol Med *16*, 337-348.

Bardeesy, N., Sinha, M., Hezel, A.F., Signoretti, S., Hathaway, N.A., Sharpless, N.E., Loda, M., Carrasco, D.R., and DePinho, R.A. (2002). Loss of the Lkb1 tumour suppressor provokes intestinal polyposis but resistance to transformation. Nature *419*, 162-167.

Barker, N., and Clevers, H. (2006). Mining the Wnt pathway for cancer therapeutics. Nat Rev Drug Discov *5*, 997-1014.

Barton, G.M., and Medzhitov, R. (2002). Retroviral delivery of small interfering RNA into primary cells. Proc Natl Acad Sci U S A *99*, 14943-14945.

Barzi, M., Berenguer, J., Menendez, A., Alvarez-Rodriguez, R., and Pons, S. (2010). Sonic-hedgehog-mediated proliferation requires the localization of PKA to the cilium base. J Cell Sci *123*, 62-69.

Beachy, P.A., Karhadkar, S.S., and Berman, D.M. (2004). Tissue repair and stem cell renewal in carcinogenesis. Nature *432*, 324-331.

Behrens, J., Jerchow, B.A., Würtele, M., Grimm, J., Asbrand, C., Wirtz, R., Kühl, M., Wedlich, D., and Birchmeier, W. (1998). Functional interaction of an axin homolog, conductin, with beta-catenin, APC, and GSK3beta. Science *280*, 596-599.

Behrens, J., von Kries, J.P., Kühl, M., Bruhn, L., Wedlich, D., Grosschedl, R., and Birchmeier, W. (1996). Functional interaction of beta-catenin with the transcription factor LEF-1. Nature *382*, 638-642.

Belloni, E., Muenke, M., Roessler, E., Traverso, G., Siegel-Bartelt, J., Frumkin, A., Mitchell, H.F., Donis-Keller, H., Helms, C., Hing, A.V.*, et al.* (1996). Identification of Sonic hedgehog as a candidate gene responsible for holoprosencephaly. Nat Genet *14*, 353-356.

Bennett, C.N., Longo, K.A., Wright, W.S., Suva, L.J., Lane, T.F., Hankenson, K.D., and MacDougald, O.A. (2005). Regulation of osteoblastogenesis and bone mass by Wnt10b. Proc Natl Acad Sci U S A *102*, 3324-3329.

Bernstein, E., Caudy, A.A., Hammond, S.M., and Hannon, G.J. (2001). Role for a bidentate ribonuclease in the initiation step of RNA interference. Nature *409*, 363-366.

Bhanot, P., Brink, M., Samos, C.H., Hsieh, J.C., Wang, Y., Macke, J.P., Andrew, D., Nathans, J., and Nusse, R. (1996). A new member of the frizzled family from Drosophila functions as a Wingless receptor. Nature *382*, 225-230.

Bijlsma, M.F., Spek, C.A., Zivkovic, D., van de Water, S., Rezaee, F., and Peppelenbosch, M.P. (2006). Repression of smoothened by patched-dependent (pro-)vitamin D3 secretion. PLoS Biol *4*, e232.

Bilic, J., Huang, Y.L., Davidson, G., Zimmermann, T., Cruciat, C.M., Bienz, M., and Niehrs, C. (2007). Wnt induces LRP6 signalosomes and promotes dishevelled-dependent LRP6 phosphorylation. Science *316*, 1619-1622.

Birmingham, A., Selfors, L.M., Forster, T., Wrobel, D., Kennedy, C.J., Shanks, E., Santoyo-Lopez, J., Dunican, D.J., Long, A., Kelleher, D.*, et al.* (2009). Statistical methods for analysis of high-throughput RNA interference screens. Nat Methods *6*, 569-575.

Bitgood, M.J., and McMahon, A.P. (1995). Hedgehog and Bmp genes are coexpressed at many diverse sites of cell-cell interaction in the mouse embryo. Dev Biol *172*, 126-138.

Bitgood, M.J., Shen, L., and McMahon, A.P. (1996). Sertoli cell signaling by Desert hedgehog regulates the male germline. Curr Biol *6*, 298-304.

Boutros, M., and Ahringer, J. (2008). The art and design of genetic screens: RNA interference. Nat Rev Genet *9*, 554-566.

Briscoe, J., Sussel, L., Serup, P., Hartigan-O'Connor, D., Jessell, T.M., Rubenstein, J.L., and Ericson, J. (1999). Homeobox gene Nkx2.2 and specification of neuronal identity by graded Sonic hedgehog signalling. Nature *398*, 622-627.

Brisken, C., Heineman, A., Chavarria, T., Elenbaas, B., Tan, J., Dey, S.K., McMahon, J.A., McMahon, A.P., and Weinberg, R.A. (2000). Essential function of Wnt-4 in mammary gland development downstream of progesterone signaling. Genes Dev *14*, 650-654.

Brunner, E., Peter, O., Schweizer, L., and Basler, K. (1997). pangolin encodes a Lef-1 homologue that acts downstream of Armadillo to transduce the Wingless signal in Drosophila. Nature *385*, 829-833.

Bryja, V., Schulte, G., Rawal, N., Grahn, A., and Arenas, E. (2007). Wnt-5a induces Dishevelled phosphorylation and dopaminergic differentiation via a CK1-dependent mechanism. J Cell Sci *120*, 586-595.

Burke, R., Nellen, D., Bellotto, M., Hafen, E., Senti, K.A., Dickson, B.J., and Basler, K. (1999). Dispatched, a novel sterol-sensing domain protein dedicated to the release of cholesterol-modified hedgehog from signaling cells. Cell *99*, 803-815.

Byrd, N., Becker, S., Maye, P., Narasimhaiah, R., St-Jacques, B., Zhang, X., McMahon, J., McMahon, A., and Grabel, L. (2002). Hedgehog is required for murine yolk sac angiogenesis. Development *129*, 361-372.

Carey, N., and La Thangue, N.B. (2006). Histone deacetylase inhibitors: gathering pace. Curr Opin Pharmacol *6*, 369-375.

Carretero, J., Shimamura, T., Rikova, K., Jackson, A.L., Wilkerson, M.D., Borgman, C.L., Buttarazzi, M.S., Sanofsky, B.A., McNamara, K.L., Brandstetter, K.A.*, et al.* (2010). Integrative genomic and proteomic analyses identify targets for Lkb1-deficient metastatic lung tumors. Cancer Cell *17*, 547-559.

Carroll, T.J., Park, J.S., Hayashi, S., Majumdar, A., and McMahon, A.P. (2005). Wnt9b plays a central role in the regulation of mesenchymal to epithelial transitions underlying organogenesis of the mammalian urogenital system. Dev Cell *9*, 283-292.

Carthew, R.W., and Sontheimer, E.J. (2009). Origins and Mechanisms of miRNAs and siRNAs. Cell *136*, 642-655.

Caspary, T., Larkins, C.E., and Anderson, K.V. (2007). The graded response to Sonic Hedgehog depends on cilia architecture. Dev Cell *12*, 767-778.

Cavallo, R.A., Cox, R.T., Moline, M.M., Roose, J., Polevoy, G.A., Clevers, H., Peifer, M., and Bejsovec, A. (1998). Drosophila Tcf and Groucho interact to repress Wingless signalling activity. Nature *395*, 604-608.

Chamoun, Z., Mann, R.K., Nellen, D., von Kessler, D.P., Bellotto, M., Beachy, P.A., and Basler, K. (2001). Skinny hedgehog, an acyltransferase required for palmitoylation and activity of the hedgehog signal. Science *293*, 2080-2084.

Chang, D.T., López, A., von Kessler, D.P., Chiang, C., Simandl, B.K., Zhao, R., Seldin, M.F., Fallon, J.F., and Beachy, P.A. (1994). Products, genetic linkage and limb patterning activity of a murine hedgehog gene. Development *120*, 3339-3353.

Chen, B., Dodge, M.E., Tang, W., Lu, J., Ma, Z., Fan, C.W., Wei, S., Hao, W., Kilgore, J., Williams, N.S.*, et al.* (2009). Small molecule-mediated disruption of Wnt-dependent signaling in tissue regeneration and cancer. Nat Chem Biol *5*, 100-107.

Chen, C.M., and Struhl, G. (1999). Wingless transduction by the Frizzled and Frizzled2 proteins of Drosophila. Development *126*, 5441-5452.

Chen, J.K., Taipale, J., Cooper, M.K., and Beachy, P.A. (2002). Inhibition of Hedgehog signaling by direct binding of cyclopamine to Smoothened. Genes Dev *16*, 2743-2748.

Chen, Y., Gallaher, N., Goodman, R.H., and Smolik, S.M. (1998). Protein kinase A directly regulates the activity and proteolysis of cubitus interruptus. Proc Natl Acad Sci U S A *95*, 2349-2354.

Chen, Y., and Struhl, G. (1996). Dual roles for patched in sequestering and transducing Hedgehog. Cell *87*, 553-563.

Chiang, C., Swan, R.Z., Grachtchouk, M., Bolinger, M., Litingtung, Y., Robertson, E.K., Cooper, M.K., Gaffield, W., Westphal, H., Beachy, P.A*., et al.* (1999). Essential role for Sonic hedgehog during hair follicle morphogenesis. Dev Biol *205*, 1-9.

Chien, A.J., Conrad, W.H., and Moon, R.T. (2009). A Wnt survival guide: from flies to human disease. J Invest Dermatol *129*, 1614-1627.

Clevers, H. (2006). Wnt/beta-catenin signaling in development and disease. Cell *127*, 469-480.

Cliffe, A., Hamada, F., and Bienz, M. (2003). A role of Dishevelled in relocating Axin to the plasma membrane during wingless signaling. Curr Biol *13*, 960-966.

Contreras, C.M., Akbay, E.A., Gallardo, T.D., Haynie, J.M., Sharma, S., Tagao, O., Bardeesy, N., Takahashi, M., Settleman, J., Wong, K.K*., et al.* (2010). Lkb1 inactivation is sufficient to drive endometrial cancers that are aggressive yet highly responsive to mTOR inhibitor monotherapy. Dis Model Mech *3*, 181-193.

Contreras, C.M., Gurumurthy, S., Haynie, J.M., Shirley, L.J., Akbay, E.A., Wingo, S.N., Schorge, J.O., Broaddus, R.R., Wong, K.K., Bardeesy, N*., et al.* (2008). Loss of Lkb1 provokes highly invasive endometrial adenocarcinomas. Cancer Res *68*, 759-766.

Corbit, K.C., Aanstad, P., Singla, V., Norman, A.R., Stainier, D.Y., and Reiter, J.F. (2005). Vertebrate Smoothened functions at the primary cilium. Nature *437*, 1018-1021.

Corcoran, R.B., and Scott, M.P. (2006). Oxysterols stimulate Sonic hedgehog signal transduction and proliferation of medulloblastoma cells. Proc Natl Acad Sci U S A *103*, 8408-8413.

Cronshaw, J.M., Krutchinsky, A.N., Zhang, W., Chait, B.T., and Matunis, M.J. (2002). Proteomic analysis of the mammalian nuclear pore complex. J Cell Biol *158*, 915-927.

DasGupta, R., Kaykas, A., Moon, R.T., and Perrimon, N. (2005). Functional genomic analysis of the Wnt-wingless signaling pathway. Science *308*, 826-833.

Denef, N., Neubüser, D., Perez, L., and Cohen, S.M. (2000). Hedgehog induces opposite changes in turnover and subcellular localization of patched and smoothened. Cell *102*, 521-531.

Devroe, E., and Silver, P.A. (2002). Retrovirus-delivered siRNA. BMC Biotechnol *2*, 15.
Ding, S., Wu, X., Li, G., Han, M., Zhuang, Y., and Xu, T. (2005). Efficient transposition of the piggyBac (PB) transposon in mammalian cells and mice. Cell *122*, 473-483.

Dissanayake, S.K., Wade, M., Johnson, C.E., O'Connell, M.P., Leotlela, P.D., French, A.D., Shah, K.V., Hewitt, K.J., Rosenthal, D.T., Indig, F.E.*, et al.* (2007). The Wnt5A/protein kinase C pathway mediates motility in melanoma cells via the inhibition of metastasis suppressors and initiation of an epithelial to mesenchymal transition. J Biol Chem *282*, 17259-17271.

Dodge, M.E., and Lum, L. (2011). Drugging the cancer stem cell compartment: lessons learned from the hedgehog and Wnt signal transduction pathways. Annu Rev Pharmacol Toxicol *51*, 289-310.

Dwyer, J.R., Sever, N., Carlson, M., Nelson, S.F., Beachy, P.A., and Parhami, F. (2007). Oxysterols are novel activators of the hedgehog signaling pathway in pluripotent mesenchymal cells. J Biol Chem *282*, 8959-8968.

Echelard, Y., Epstein, D.J., St-Jacques, B., Shen, L., Mohler, J., McMahon, J.A., and McMahon, A.P. (1993). Sonic hedgehog, a member of a family of putative signaling molecules, is implicated in the regulation of CNS polarity. Cell *75*, 1417-1430.

Echeverri, C.J., Beachy, P.A., Baum, B., Boutros, M., Buchholz, F., Chanda, S.K., Downward, J., Ellenberg, J., Fraser, A.G., Hacohen, N.*, et al.* (2006). Minimizing the risk of reporting false positives in large-scale RNAi screens. Nat Methods *3*, 777-779.

Elbashir, S.M., Harborth, J., Lendeckel, W., Yalcin, A., Weber, K., and Tuschl, T. (2001a). Duplexes of 21-nucleotide RNAs mediate RNA interference in cultured mammalian cells. Nature *411*, 494-498.

Elbashir, S.M., Lendeckel, W., and Tuschl, T. (2001b). RNA interference is mediated by 21- and 22-nucleotide RNAs. Genes Dev *15*, 188-200.

Elbashir, S.M., Martinez, J., Patkaniowska, A., Lendeckel, W., and Tuschl, T. (2001c). Functional anatomy of siRNAs for mediating efficient RNAi in Drosophila melanogaster embryo lysate. EMBO J *20*, 6877-6888.

Ericson, J., Rashbass, P., Schedl, A., Brenner-Morton, S., Kawakami, A., van Heyningen, V., Jessell, T.M., and Briscoe, J. (1997). Pax6 controls progenitor cell identity and neuronal fate in response to graded Shh signaling. Cell *90*, 169-180.

Evangelista, M., Lim, T.Y., Lee, J., Parker, L., Ashique, A., Peterson, A.S., Ye, W., Davis, D.P., and de Sauvage, F.J. (2008). Kinome siRNA screen identifies regulators of ciliogenesis and hedgehog signal transduction. Sci Signal *1*, ra7.

Finnin, M.S., Donigian, J.R., Cohen, A., Richon, V.M., Rifkind, R.A., Marks, P.A., Breslow, R., and Pavletich, N.P. (1999). Structures of a histone deacetylase homologue bound to the TSA and SAHA inhibitors. Nature *401*, 188-193.

Fire, A., Xu, S., Montgomery, M.K., Kostas, S.A., Driver, S.E., and Mello, C.C. (1998). Potent and specific genetic interference by double-stranded RNA in Caenorhabditis elegans. Nature *391*, 806-811.

Gailani, M.R., Ståhle-Bäckdahl, M., Leffell, D.J., Glynn, M., Zaphiropoulos, P.G., Pressman, C., Undén, A.B., Dean, M., Brash, D.E., Bale, A.E.*, et al.* (1996). The role of the human homologue of Drosophila patched in sporadic basal cell carcinomas. Nat Genet *14*, 78-81.

Gao, C., and Chen, Y.G. (2010). Dishevelled: The hub of Wnt signaling. Cell Signal *22*, 717-727.

Goodrich, L.V., Milenković, L., Higgins, K.M., and Scott, M.P. (1997). Altered neural cell fates and medulloblastoma in mouse patched mutants. Science *277*, 1109-1113.

Goyal, S., Vanden Heuvel, G., and Aronson, P.S. (2003). Renal expression of novel Na+/H+ exchanger isoform NHE8. Am J Physiol Renal Physiol *284*, F467-473.

Grumolato, L., Liu, G., Mong, P., Mudbhary, R., Biswas, R., Arroyave, R., Vijayakumar, S., Economides, A.N., and Aaronson, S.A. (2010). Canonical and noncanonical Wnts use a common mechanism to activate completely unrelated coreceptors. Genes Dev *24*, 2517-2530.

Haegel, H., Larue, L., Ohsugi, M., Fedorov, L., Herrenknecht, K., and Kemler, R. (1995). Lack of beta-catenin affects mouse development at gastrulation. Development *121*, 3529-3537.

Hahn, H., Wicking, C., Zaphiropoulous, P.G., Gailani, M.R., Shanley, S., Chidambaram, A., Vorechovsky, I., Holmberg, E., Unden, A.B., Gillies, S.*, et al.* (1996). Mutations of the human homolog of Drosophila patched in the nevoid basal cell carcinoma syndrome. Cell *85*, 841-851.

Halvorson, D.L., and McCune, S.A. (1984). Inhibition of fatty acid synthesis in isolated adipocytes by 5-(tetradecyloxy)-2-furoic acid. Lipids *19*, 851-856.

Hamada, F., Tomoyasu, Y., Takatsu, Y., Nakamura, M., Nagai, S., Suzuki, A., Fujita, F., Shibuya, H., Toyoshima, K., Ueno, N.*, et al.* (1999). Negative regulation of Wingless signaling by D-axin, a Drosophila homolog of axin. Science *283*, 1739-1742.

Hammond, S.M., Bernstein, E., Beach, D., and Hannon, G.J. (2000). An RNA-directed nuclease mediates post-transcriptional gene silencing in Drosophila cells. Nature *404*, 293-296.

Hannon, G.J. (2002). RNA interference. Nature *418*, 244-251.

Haycraft, C.J., Banizs, B., Aydin-Son, Y., Zhang, Q., Michaud, E.J., and Yoder, B.K. (2005). Gli2 and Gli3 localize to cilia and require the intraflagellar transport protein polaris for processing and function. PLoS Genet *1*, e53.

He, T.C., Sparks, A.B., Rago, C., Hermeking, H., Zawel, L., da Costa, L.T., Morin, P.J., Vogelstein, B., and Kinzler, K.W. (1998). Identification of c-MYC as a target of the APC pathway. Science *281*, 1509-1512.

Heisenberg, C.P., Tada, M., Rauch, G.J., Saúde, L., Concha, M.L., Geisler, R., Stemple, D.L., Smith, J.C., and Wilson, S.W. (2000). Silberblick/Wnt11 mediates convergent extension movements during zebrafish gastrulation. Nature *405*, 76-81.

Hemminki, A., Tomlinson, I., Markie, D., Järvinen, H., Sistonen, P., Björkqvist, A.M., Knuutila, S., Salovaara, R., Bodmer, W., Shibata, D.*, et al.* (1997). Localization of a susceptibility locus for Peutz-Jeghers syndrome to 19p using comparative genomic hybridization and targeted linkage analysis. Nat Genet *15*, 87-90.

Heydeck, W., Zeng, H., and Liu, A. (2009). Planar cell polarity effector gene Fuzzy regulates cilia formation and Hedgehog signal transduction in mouse. Dev Dyn *238*, 3035-3042.

Hezel, A.F., and Bardeesy, N. (2008). LKB1; linking cell structure and tumor suppression. Oncogene *27*, 6908-6919.

Holmen, S.L., Zylstra, C.R., Mukherjee, A., Sigler, R.E., Faugere, M.C., Bouxsein, M.L., Deng, L., Clemens, T.L., and Williams, B.O. (2005). Essential role of beta-catenin in postnatal bone acquisition. J Biol Chem *280*, 21162-21168.

Hooper, J.E. (2003). Smoothened translates Hedgehog levels into distinct responses. Development *130*, 3951-3963.

Houssa, B., Schaap, D., van der Wal, J., Goto, K., Kondo, H., Yamakawa, A., Shibata, M., Takenawa, T., and van Blitterswijk, W.J. (1997). Cloning of a novel human diacylglycerol kinase (DGKtheta) containing three cysteine-rich domains, a proline-rich region, and a pleckstrin homology domain with an overlapping Ras-associating domain. J Biol Chem *272*, 10422-10428.

Huang, L., Pu, Y., Hu, W.Y., Birch, L., Luccio-Camelo, D., Yamaguchi, T., and Prins, G.S. (2009a). The role of Wnt5a in prostate gland development. Dev Biol *328*, 188-199.

Huang, S.M., Mishina, Y.M., Liu, S., Cheung, A., Stegmeier, F., Michaud, G.A., Charlat, O., Wiellette, E., Zhang, Y., Wiessner, S.*, et al.* (2009b). Tankyrase inhibition stabilizes axin and antagonizes Wnt signalling. Nature *461*, 614-620.

Huangfu, D., and Anderson, K.V. (2005). Cilia and Hedgehog responsiveness in the mouse. Proc Natl Acad Sci U S A *102*, 11325-11330.

Huangfu, D., and Anderson, K.V. (2006). Signaling from Smo to Ci/Gli: conservation and divergence of Hedgehog pathways from Drosophila to vertebrates. Development *133*, 3-14.

Huangfu, D., Liu, A., Rakeman, A.S., Murcia, N.S., Niswander, L., and Anderson, K.V. (2003). Hedgehog signalling in the mouse requires intraflagellar transport proteins. Nature *426*, 83-87.

Huber, O., Korn, R., McLaughlin, J., Ohsugi, M., Herrmann, B.G., and Kemler, R. (1996). Nuclear localization of beta-catenin by interaction with transcription factor LEF-1. Mech Dev *59*, 3-10.

Hui, C.C., and Joyner, A.L. (1993). A mouse model of greig cephalopolysyndactyly syndrome: the extra-toesJ mutation contains an intragenic deletion of the Gli3 gene. Nat Genet *3*, 241-246.

Humke, E.W., Dorn, K.V., Milenkovic, L., Scott, M.P., and Rohatgi, R. (2010). The output of Hedgehog signaling is controlled by the dynamic association between Suppressor of Fused and the Gli proteins. Genes Dev *24*, 670-682.

Huntzicker, E.G., Estay, I.S., Zhen, H., Lokteva, L.A., Jackson, P.K., and Oro, A.E. (2006). Dual degradation signals control Gli protein stability and tumor formation. Genes Dev *20*, 276-281.

Itoh, K., Krupnik, V.E., and Sokol, S.Y. (1998). Axis determination in Xenopus involves biochemical interactions of axin, glycogen synthase kinase 3 and beta-catenin. Curr Biol *8*, 591-594.

Jackson, A.L., Bartz, S.R., Schelter, J., Kobayashi, S.V., Burchard, J., Mao, M., Li, B., Cavet, G., and Linsley, P.S. (2003). Expression profiling reveals off-target gene regulation by RNAi. Nat Biotechnol *21*, 635-637.

Jackson, A.L., Burchard, J., Schelter, J., Chau, B.N., Cleary, M., Lim, L., and Linsley, P.S. (2006). Widespread siRNA "off-target" transcript silencing mediated by seed region sequence complementarity. RNA *12*, 1179-1187.

Jacob, L., and Lum, L. (2007a). Hedgehog signaling pathway in Drosophila. Sci STKE *2007*, cm7.

Jacob, L., and Lum, L. (2007b). Hedgehog signaling pathway. Sci STKE *2007*, cm6.

Jaks, V., Barker, N., Kasper, M., van Es, J.H., Snippert, H.J., Clevers, H., and Toftgård, R. (2008). Lgr5 marks cycling, yet long-lived, hair follicle stem cells. Nat Genet *40*, 1291-1299.

Jeghers H, M.V., Katz KH. (1949). Generalized intestinal polyposis and melanin spots of the oral mucosa, lips and digits; a syndrome of diagnostic significance. N Engl J Med *241*, 1031-1036.

Jessell, T.M. (2000). Neuronal specification in the spinal cord: inductive signals and transcriptional codes. Nat Rev Genet *1*, 20-29.

Jho, E.H., Zhang, T., Domon, C., Joo, C.K., Freund, J.N., and Costantini, F. (2002). Wnt/beta-catenin/Tcf signaling induces the transcription of Axin2, a negative regulator of the signaling pathway. Mol Cell Biol *22*, 1172-1183.

Ji, H., Ramsey, M.R., Hayes, D.N., Fan, C., McNamara, K., Kozlowski, P., Torrice, C., Wu, M.C., Shimamura, T., Perera, S.A.*, et al.* (2007). LKB1 modulates lung cancer differentiation and metastasis. Nature *448*, 807-810.

Jia, J., Amanai, K., Wang, G., Tang, J., Wang, B., and Jiang, J. (2002). Shaggy/GSK3 antagonizes Hedgehog signalling by regulating Cubitus interruptus. Nature *416*, 548-552.
Jia, J., Tong, C., and Jiang, J. (2003). Smoothened transduces Hedgehog signal by physically interacting with Costal2/Fused complex through its C-terminal tail. Genes Dev *17*, 2709-2720.

Jia, J., Tong, C., Wang, B., Luo, L., and Jiang, J. (2004). Hedgehog signalling activity of Smoothened requires phosphorylation by protein kinase A and casein kinase I. Nature *432*, 1045-1050.

Jia, J., Zhang, L., Zhang, Q., Tong, C., Wang, B., Hou, F., Amanai, K., and Jiang, J. (2005). Phosphorylation by double-time/CKIepsilon and CKIalpha targets cubitus interruptus for Slimb/beta-TRCP-mediated proteolytic processing. Dev Cell *9*, 819-830.

Jiang, J., and Struhl, G. (1998). Regulation of the Hedgehog and Wingless signalling pathways by the F-box/WD40-repeat protein Slimb. Nature *391*, 493-496.

Johnson, R.L., Rothman, A.L., Xie, J., Goodrich, L.V., Bare, J.W., Bonifas, J.M., Quinn, A.G., Myers, R.M., Cox, D.R., Epstein, E.H.*, et al.* (1996). Human homolog of patched, a candidate gene for the basal cell nevus syndrome. Science *272*, 1668-1671.

Kadowaki, T., Wilder, E., Klingensmith, J., Zachary, K., and Perrimon, N. (1996). The segment polarity gene porcupine encodes a putative multitransmembrane protein involved in Wingless processing. Genes Dev *10*, 3116-3128.

Kasarskis, A., Manova, K., and Anderson, K.V. (1998). A phenotype-based screen for embryonic lethal mutations in the mouse. Proc Natl Acad Sci U S A *95*, 7485-7490.

Kato, M., Patel, M.S., Levasseur, R., Lobov, I., Chang, B.H., Glass, D.A., Hartmann, C., Li, L., Hwang, T.H., Brayton, C.F.*, et al.* (2002). Cbfa1-independent decrease in osteoblast proliferation, osteopenia, and persistent embryonic eye vascularization in mice deficient in Lrp5, a Wnt coreceptor. J Cell Biol *157*, 303-314.

Kawakami, Y., Wada, N., Nishimatsu, S., Komaguchi, C., Noji, S., and Nohno, T. (2000a). Identification of chick frizzled-10 expressed in the developing limb and the central nervous system. Mech Dev *91*, 375-378.

Kawakami, Y., Wada, N., Nishimatsu, S., and Nohno, T. (2000b). Involvement of frizzled-10 in Wnt-7a signaling during chick limb development. Dev Growth Differ *42*, 561-569.

Ketting, R.F., Fischer, S.E., Bernstein, E., Sijen, T., Hannon, G.J., and Plasterk, R.H. (2001). Dicer functions in RNA interference and in synthesis of small RNA involved in developmental timing in C. elegans. Genes Dev *15*, 2654-2659.

Khadilkar, A., Iannuzzi, P., and Orlowski, J. (2001). Identification of sites in the second exomembrane loop and ninth transmembrane helix of the mammalian Na+/H+ exchanger important for drug recognition and cation translocation. J Biol Chem *276*, 43792-43800.
Khvorova, A., Reynolds, A., and Jayasena, S.D. (2003). Functional siRNAs and miRNAs exhibit strand bias. Cell *115*, 209-216.

Kibler, K.V., Shors, T., Perkins, K.B., Zeman, C.C., Banaszak, M.P., Biesterfeldt, J., Langland, J.O., and Jacobs, B.L. (1997). Double-stranded RNA is a trigger for apoptosis in vaccinia virus-infected cells. J Virol *71*, 1992-2003.

Kile, B.T., and Hilton, D.J. (2005). The art and design of genetic screens: mouse. Nat Rev Genet *6*, 557-567.

Kim, J., Kato, M., and Beachy, P.A. (2009a). Gli2 trafficking links Hedgehog-dependent activation of Smoothened in the primary cilium to transcriptional activation in the nucleus. Proc Natl Acad Sci U S A *106*, 21666-21671.

Kim, V.N., Han, J., and Siomi, M.C. (2009b). Biogenesis of small RNAs in animals. Nat Rev Mol Cell Biol *10*, 126-139.

Kinzler, K.W., Bigner, S.H., Bigner, D.D., Trent, J.M., Law, M.L., O'Brien, S.J., Wong, A.J., and Vogelstein, B. (1987). Identification of an amplified, highly expressed gene in a human glioma. Science *236*, 70-73.

Kinzler, K.W., Ruppert, J.M., Bigner, S.H., and Vogelstein, B. (1988). The GLI gene is a member of the Kruppel family of zinc finger proteins. Nature *332*, 371-374.

Knight, S.W., and Bass, B.L. (2001). A role for the RNase III enzyme DCR-1 in RNA interference and germ line development in Caenorhabditis elegans. Science *293*, 2269-2271.

Komekado, H., Yamamoto, H., Chiba, T., and Kikuchi, A. (2007). Glycosylation and palmitoylation of Wnt-3a are coupled to produce an active form of Wnt-3a. Genes Cells *12*, 521-534.

Korinek, V., Barker, N., Morin, P.J., van Wichen, D., de Weger, R., Kinzler, K.W., Vogelstein, B., and Clevers, H. (1997). Constitutive transcriptional activation by a beta-catenin-Tcf complex in APC-/- colon carcinoma. Science *275*, 1784-1787.

Krock, B.L., and Perkins, B.D. (2008). The intraflagellar transport protein IFT57 is required for cilia maintenance and regulates IFT-particle-kinesin-II dissociation in vertebrate photoreceptors. J Cell Sci *121*, 1907-1915.

Krol, J., Sobczak, K., Wilczynska, U., Drath, M., Jasinska, A., Kaczynska, D., and Krzyzosiak, W.J. (2004). Structural features of microRNA (miRNA) precursors and their relevance to miRNA biogenesis and small interfering RNA/short hairpin RNA design. J Biol Chem *279*, 42230-42239.

Kurayoshi, M., Yamamoto, H., Izumi, S., and Kikuchi, A. (2007). Post-translational palmitoylation and glycosylation of Wnt-5a are necessary for its signalling. Biochem J *402*, 515-523.

Lanske, B., Karaplis, A.C., Lee, K., Luz, A., Vortkamp, A., Pirro, A., Karperien, M., Defize, L.H., Ho, C., Mulligan, R.C.*, et al.* (1996). PTH/PTHrP receptor in early development and Indian hedgehog-regulated bone growth. Science *273*, 663-666.

Lee, J.J., Ekker, S.C., von Kessler, D.P., Porter, J.A., Sun, B.I., and Beachy, P.A. (1994). Autoproteolysis in hedgehog protein biogenesis. Science *266*, 1528-1537.

Lettice, L.A., Heaney, S.J., Purdie, L.A., Li, L., de Beer, P., Oostra, B.A., Goode, D., Elgar, G., Hill, R.E., and de Graaff, E. (2003). A long-range Shh enhancer regulates expression in the developing limb and fin and is associated with preaxial polydactyly. Hum Mol Genet *12*, 1725-1735.

Lewis, K.E., Currie, P.D., Roy, S., Schauerte, H., Haffter, P., and Ingham, P.W. (1999). Control of muscle cell-type specification in the zebrafish embryo by Hedgehog signalling. Dev Biol *216*, 469-480.

Li, C., Xiao, J., Hormi, K., Borok, Z., and Minoo, P. (2002). Wnt5a participates in distal lung morphogenesis. Dev Biol *248*, 68-81.

Litingtung, Y., and Chiang, C. (2000). Specification of ventral neuron types is mediated by an antagonistic interaction between Shh and Gli3. Nat Neurosci *3*, 979-985.

Liu, A., Wang, B., and Niswander, L.A. (2005). Mouse intraflagellar transport proteins regulate both the activator and repressor functions of Gli transcription factors. Development *132*, 3103-3111.

Liu, C., Li, Y., Semenov, M., Han, C., Baeg, G.H., Tan, Y., Zhang, Z., Lin, X., and He, X. (2002). Control of beta-catenin phosphorylation/degradation by a dual-kinase mechanism. Cell *108*, 837-847.

Liu, P., Wakamiya, M., Shea, M.J., Albrecht, U., Behringer, R.R., and Bradley, A. (1999). Requirement for Wnt3 in vertebrate axis formation. Nat Genet *22*, 361-365.

Liu, T.H., Raval, A., Chen, S.S., Matkovic, J.J., Byrd, J.C., and Plass, C. (2006). CpG island methylation and expression of the secreted frizzled-related protein gene family in chronic lymphocytic leukemia. Cancer Res *66*, 653-658.

Lum, L., Yao, S., Mozer, B., Rovescalli, A., Von Kessler, D., Nirenberg, M., and Beachy, P.A. (2003a). Identification of Hedgehog pathway components by RNAi in Drosophila cultured cells. Science *299*, 2039-2045.

Lum, L., Zhang, C., Oh, S., Mann, R., von Kessler, D., Taipale, J., Weis-Garcia, F., Gong, R., Wang, B., and Beachy, P. (2003b). Hedgehog signal transduction via Smoothened association with a cytoplasmic complex scaffolded by the atypical kinesin, Costal-2. Mol Cell *12*, 1261-1274.

Ma, Y., Erkner, A., Gong, R., Yao, S., Taipale, J., Basler, K., and Beachy, P.A. (2002). Hedgehog-mediated patterning of the mammalian embryo requires transporter-like function of dispatched. Cell *111*, 63-75.

MacDonald, B.T., Tamai, K., and He, X. (2009). Wnt/beta-catenin signaling: components, mechanisms, and diseases. Dev Cell *17*, 9-26.

MacRae, I.J., Ma, E., Zhou, M., Robinson, C.V., and Doudna, J.A. (2008). In vitro reconstitution of the human RISC-loading complex. Proc Natl Acad Sci U S A *105*, 512-517.

Majumdar, A., Vainio, S., Kispert, A., McMahon, J., and McMahon, A.P. (2003). Wnt11 and Ret/Gdnf pathways cooperate in regulating ureteric branching during metanephric kidney development. Development *130*, 3175-3185.

Mandel, H., Shemer, R., Borochowitz, Z.U., Okopnik, M., Knopf, C., Indelman, M., Drugan, A., Tiosano, D., Gershoni-Baruch, R., Choder, M.*, et al.* (2008). SERKAL syndrome: an autosomal-recessive disorder caused by a loss-of-function mutation in WNT4. Am J Hum Genet *82*, 39-47.

Mao, J., Wang, J., Liu, B., Pan, W., Farr, G.H., Flynn, C., Yuan, H., Takada, S., Kimelman, D., Li, L.*, et al.* (2001). Low-density lipoprotein receptor-related protein-5 binds to Axin and regulates the canonical Wnt signaling pathway. Mol Cell *7*, 801-809.

Marigo, V., Davey, R.A., Zuo, Y., Cunningham, J.M., and Tabin, C.J. (1996). Biochemical evidence that patched is the Hedgehog receptor. Nature *384*, 176-179.

Marigo, V., Roberts, D.J., Lee, S.M., Tsukurov, O., Levi, T., Gastier, J.M., Epstein, D.J., Gilbert, D.J., Copeland, N.G., and Seidman, C.E. (1995). Cloning, expression, and chromosomal location of SHH and IHH: two human homologues of the Drosophila segment polarity gene hedgehog. Genomics *28*, 44-51.

Marikawa, Y., and Elinson, R.P. (1998). beta-TrCP is a negative regulator of Wnt/beta-catenin signaling pathway and dorsal axis formation in Xenopus embryos. Mech Dev *77*, 75-80.

Marlow, F., Gonzalez, E.M., Yin, C., Rojo, C., and Solnica-Krezel, L. (2004). No tail co-operates with non-canonical Wnt signaling to regulate posterior body morphogenesis in zebrafish. Development *131*, 203-216.

Matranga, C., Tomari, Y., Shin, C., Bartel, D.P., and Zamore, P.D. (2005). Passenger-strand cleavage facilitates assembly of siRNA into Ago2-containing RNAi enzyme complexes. Cell *123*, 607-620.

Maw, M.A., Kennedy, B., Knight, A., Bridges, R., Roth, K.E., Mani, E.J., Mukkadan, J.K., Nancarrow, D., Crabb, J.W., and Denton, M.J. (1997). Mutation of the gene encoding cellular retinaldehyde-binding protein in autosomal recessive retinitis pigmentosa. Nat Genet *17*, 198-200.

May, S.R., Ashique, A.M., Karlen, M., Wang, B., Shen, Y., Zarbalis, K., Reiter, J., Ericson, J., and Peterson, A.S. (2005). Loss of the retrograde motor for IFT disrupts localization of Smo to cilia and prevents the expression of both activator and repressor functions of Gli. Dev Biol *287*, 378-389.

Mazieres, J., You, L., He, B., Xu, Z., Lee, A.Y., Mikami, I., McCormick, F., and Jablons, D.M. (2005). Inhibition of Wnt16 in human acute lymphoblastoid leukemia cells containing the t(1;19) translocation induces apoptosis. Oncogene *24*, 5396-5400.

McCune, S.A., and Harris, R.A. (1979). Mechanism responsible for 5-(tetradecyloxy)-2-furoic acid inhibition of hepatic lipogenesis. J Biol Chem *254*, 10095-10101.
McLellan, J.S., Yao, S., Zheng, X., Geisbrecht, B.V., Ghirlando, R., Beachy, P.A., and Leahy, D.J. (2006). Structure of a heparin-dependent complex of Hedgehog and Ihog. Proc Natl Acad Sci U S A *103*, 17208-17213.

Miller, B.W., Lau, G., Grouios, C., Mollica, E., Barrios-Rodiles, M., Liu, Y., Datti, A., Morris, Q., Wrana, J.L., and Attisano, L. (2009). Application of an integrated physical and functional screening approach to identify inhibitors of the Wnt pathway. Mol Syst Biol *5*, 315.

Miyoshi, K., Tsukumo, H., Nagami, T., Siomi, H., and Siomi, M.C. (2005). Slicer function of Drosophila Argonautes and its involvement in RISC formation. Genes Dev *19*, 2837-2848.

Mo, R., Freer, A.M., Zinyk, D.L., Crackower, M.A., Michaud, J., Heng, H.H., Chik, K.W., Shi, X.M., Tsui, L.C., Cheng, S.H.*, et al.* (1997). Specific and redundant functions of Gli2 and Gli3 zinc finger genes in skeletal patterning and development. Development *124*, 113-123.

Mohler, J. (1988). Requirements for hedgehog, a segmental polarity gene, in patterning larval and adult cuticle of Drosophila. Genetics *120*, 1061-1072.

Mohr, S., Bakal, C., and Perrimon, N. (2010). Genomic screening with RNAi: results and challenges. Annu Rev Biochem *79*, 37-64.

Molenaar, M., van de Wetering, M., Oosterwegel, M., Peterson-Maduro, J., Godsave, S., Korinek, V., Roose, J., Destrée, O., and Clevers, H. (1996). XTcf-3 transcription factor mediates beta-catenin-induced axis formation in Xenopus embryos. Cell *86*, 391-399.

Monnier, V., Dussillol, F., Alves, G., Lamour-Isnard, C., and Plessis, A. (1998). Suppressor of fused links fused and Cubitus interruptus on the hedgehog signalling pathway. Curr Biol *8*, 583-586.

Méthot, N., and Basler, K. (2000). Suppressor of fused opposes hedgehog signal transduction by impeding nuclear accumulation of the activator form of Cubitus interruptus. Development *127*, 4001-4010.

Müller, B., and Basler, K. (2000). The repressor and activator forms of Cubitus interruptus control Hedgehog target genes through common generic gli-binding sites. Development *127*, 2999-3007.

Niemann, S., Zhao, C., Pascu, F., Stahl, U., Aulepp, U., Niswander, L., Weber, J.L., and Müller, U. (2004). Homozygous WNT3 mutation causes tetra-amelia in a large consanguineous family. Am J Hum Genet *74*, 558-563.

Nusse, R., and Varmus, H.E. (1982). Many tumors induced by the mouse mammary tumor virus contain a provirus integrated in the same region of the host genome. Cell *31*, 99-109.

Nykänen, A., Haley, B., and Zamore, P.D. (2001). ATP requirements and small interfering RNA structure in the RNA interference pathway. Cell *107*, 309-321.

Nüsslein-Volhard, C., and Wieschaus, E. (1980). Mutations affecting segment number and polarity in Drosophila. Nature *287*, 795-801.

Ogden, S.K., Ascano, M., Stegman, M.A., Suber, L.M., Hooper, J.E., and Robbins, D.J. (2003). Identification of a functional interaction between the transmembrane protein Smoothened and the kinesin-related protein Costal2. Curr Biol *13*, 1998-2003.

Ohlmeyer, J.T., and Kalderon, D. (1998). Hedgehog stimulates maturation of Cubitus interruptus into a labile transcriptional activator. Nature *396*, 749-753.

Okino, K., Nagai, H., Hatta, M., Nagahata, T., Yoneyama, K., Ohta, Y., Jin, E., Kawanami, O., Araki, T., and Emi, M. (2003). Up-regulation and overproduction of DVL-1, the human counterpart of the Drosophila dishevelled gene, in cervical squamous cell carcinoma. Oncol Rep *10*, 1219-1223.

Orban, T.I., and Izaurralde, E. (2005). Decay of mRNAs targeted by RISC requires XRN1, the Ski complex, and the exosome. RNA *11*, 459-469.

Paddison, P.J., Caudy, A.A., Bernstein, E., Hannon, G.J., and Conklin, D.S. (2002). Short hairpin RNAs (shRNAs) induce sequence-specific silencing in mammalian cells. Genes Dev *16*, 948-958.

Pan, Y., Bai, C.B., Joyner, A.L., and Wang, B. (2006). Sonic hedgehog signaling regulates Gli2 transcriptional activity by suppressing its processing and degradation. Mol Cell Biol *26*, 3365-3377.

Pandur, P., Läsche, M., Eisenberg, L.M., and Kühl, M. (2002). Wnt-11 activation of a non-canonical Wnt signalling pathway is required for cardiogenesis. Nature *418*, 636-641.

Panáková, D., Sprong, H., Marois, E., Thiele, C., and Eaton, S. (2005). Lipoprotein particles are required for Hedgehog and Wingless signalling. Nature *435*, 58-65.

Park, H.L., Bai, C., Platt, K.A., Matise, M.P., Beeghly, A., Hui, C.C., Nakashima, M., and Joyner, A.L. (2000). Mouse Gli1 mutants are viable but have defects in SHH signaling in combination with a Gli2 mutation. Development *127*, 1593-1605.

Park, T.J., Mitchell, B.J., Abitua, P.B., Kintner, C., and Wallingford, J.B. (2008). Dishevelled controls apical docking and planar polarization of basal bodies in ciliated epithelial cells. Nat Genet *40*, 871-879.

Parr, B.A., and McMahon, A.P. (1995). Dorsalizing signal Wnt-7a required for normal polarity of D-V and A-P axes of mouse limb. Nature *374*, 350-353.

Pepinsky, R.B., Zeng, C., Wen, D., Rayhorn, P., Baker, D.P., Williams, K.P., Bixler, S.A., Ambrose, C.M., Garber, E.A., Miatkowski, K.*, et al.* (1998). Identification of a palmitic acid-modified form of human Sonic hedgehog. J Biol Chem *273*, 14037-14045.

Perrimon, N., and Mathey-Prevot, B. (2007). Applications of high-throughput RNA interference screens to problems in cell and developmental biology. Genetics *175*, 7-16.

Pinson, K.I., Brennan, J., Monkley, S., Avery, B.J., and Skarnes, W.C. (2000). An LDL-receptor-related protein mediates Wnt signalling in mice. Nature *407*, 535-538.

Porter, J.A., Ekker, S.C., Park, W.J., von Kessler, D.P., Young, K.E., Chen, C.H., Ma, Y., Woods, A.S., Cotter, R.J., Koonin, E.V.*, et al.* (1996). Hedgehog patterning activity: role of a lipophilic modification mediated by the carboxy-terminal autoprocessing domain. Cell *86*, 21-34.

Price, M.A., and Kalderon, D. (1999). Proteolysis of cubitus interruptus in Drosophila requires phosphorylation by protein kinase A. Development *126*, 4331-4339.

Price, M.A., and Kalderon, D. (2002). Proteolysis of the Hedgehog signaling effector Cubitus interruptus requires phosphorylation by Glycogen Synthase Kinase 3 and Casein Kinase 1. Cell *108*, 823-835.

Préat, T. (1992). Characterization of Suppressor of fused, a complete suppressor of the fused segment polarity gene of Drosophila melanogaster. Genetics *132*, 725-736.

Pugacheva, E.N., Jablonski, S.A., Hartman, T.R., Henske, E.P., and Golemis, E.A. (2007). HEF1-dependent Aurora A activation induces disassembly of the primary cilium. Cell *129*, 1351-1363.

Rad, R., Rad, L., Wang, W., Cadinanos, J., Vassiliou, G., Rice, S., Campos, L.S., Yusa, K., Banerjee, R., Li, M.A., *et al.* (2010). PiggyBac transposon mutagenesis: a tool for cancer gene discovery in mice. Science *330*, 1104-1107.

Rand, T.A., Petersen, S., Du, F., and Wang, X. (2005). Argonaute2 cleaves the anti-guide strand of siRNA during RISC activation. Cell *123*, 621-629.

Richon, V.M., Emiliani, S., Verdin, E., Webb, Y., Breslow, R., Rifkind, R.A., and Marks, P.A. (1998). A class of hybrid polar inducers of transformed cell differentiation inhibits histone deacetylases. Proc Natl Acad Sci U S A *95*, 3003-3007.

Riddle, R.D., Johnson, R.L., Laufer, E., and Tabin, C. (1993). Sonic hedgehog mediates the polarizing activity of the ZPA. Cell *75*, 1401-1416.

Riese, J., Yu, X., Munnerlyn, A., Eresh, S., Hsu, S.C., Grosschedl, R., and Bienz, M. (1997). LEF-1, a nuclear factor coordinating signaling inputs from wingless and decapentaplegic. Cell *88*, 777-787.

Rijsewijk, F., Schuermann, M., Wagenaar, E., Parren, P., Weigel, D., and Nusse, R. (1987). The Drosophila homolog of the mouse mammary oncogene int-1 is identical to the segment polarity gene wingless. Cell *50*, 649-657.

Roarty, K., and Serra, R. (2007). Wnt5a is required for proper mammary gland development and TGF-beta-mediated inhibition of ductal growth. Development *134*, 3929-3939.

Robbins, D.J., Nybakken, K.E., Kobayashi, R., Sisson, J.C., Bishop, J.M., and Thérond, P.P. (1997). Hedgehog elicits signal transduction by means of a large complex containing the kinesin-related protein costal2. Cell *90*, 225-234.

Roelink, H., Augsburger, A., Heemskerk, J., Korzh, V., Norlin, S., Ruiz i Altaba, A., Tanabe, Y., Placzek, M., Edlund, T., and Jessell, T.M. (1994). Floor plate and motor neuron induction by vhh-1, a vertebrate homolog of hedgehog expressed by the notochord. Cell *76*, 761-775.

Roessler, E., Belloni, E., Gaudenz, K., Jay, P., Berta, P., Scherer, S.W., Tsui, L.C., and Muenke, M. (1996). Mutations in the human Sonic Hedgehog gene cause holoprosencephaly. Nat Genet *14*, 357-360.

Rohatgi, R., Milenkovic, L., and Scott, M.P. (2007). Patched1 regulates hedgehog signaling at the primary cilium. Science *317*, 372-376.

Rominger, C.M., Bee, W.L., Copeland, R.A., Davenport, E.A., Gilmartin, A., Gontarek, R., Hornberger, K.R., Kallal, L.A., Lai, Z., Lawrie, K.*, et al.* (2009). Evidence for allosteric interactions of antagonist binding to the smoothened receptor. J Pharmacol Exp Ther *329*, 995-1005.

Roose, J., Molenaar, M., Peterson, J., Hurenkamp, J., Brantjes, H., Moerer, P., van de Wetering, M., Destrée, O., and Clevers, H. (1998). The Xenopus Wnt effector XTcf-3 interacts with Groucho-related transcriptional repressors. Nature *395*, 608-612.

Ruel, L., Rodriguez, R., Gallet, A., Lavenant-Staccini, L., and Thérond, P.P. (2003). Stability and association of Smoothened, Costal2 and Fused with Cubitus interruptus are regulated by Hedgehog. Nat Cell Biol *5*, 907-913.

Rulifson, E.J., Wu, C.H., and Nusse, R. (2000). Pathway specificity by the bifunctional receptor frizzled is determined by affinity for wingless. Mol Cell *6*, 117-126.

Sanchez-Cespedes, M., Parrella, P., Esteller, M., Nomoto, S., Trink, B., Engles, J.M., Westra, W.H., Herman, J.G., and Sidransky, D. (2002). Inactivation of LKB1/STK11 is a common event in adenocarcinomas of the lung. Cancer Res *62*, 3659-3662.

Sasaki, H., Hui, C., Nakafuku, M., and Kondoh, H. (1997). A binding site for Gli proteins is essential for HNF-3beta floor plate enhancer activity in transgenics and can respond to Shh in vitro. Development *124*, 1313-1322.

Schwarz, D.S., Hutvágner, G., Du, T., Xu, Z., Aronin, N., and Zamore, P.D. (2003). Asymmetry in the assembly of the RNAi enzyme complex. Cell *115*, 199-208.

Schwarz-Romond, T., Fiedler, M., Shibata, N., Butler, P.J., Kikuchi, A., Higuchi, Y., and Bienz, M. (2007a). The DIX domain of Dishevelled confers Wnt signaling by dynamic polymerization. Nat Struct Mol Biol *14*, 484-492.

Schwarz-Romond, T., Metcalfe, C., and Bienz, M. (2007b). Dynamic recruitment of axin by Dishevelled protein assemblies. J Cell Sci *120*, 2402-2412.

Shaw, R.J., Bardeesy, N., Manning, B.D., Lopez, L., Kosmatka, M., DePinho, R.A., and Cantley, L.C. (2004a). The LKB1 tumor suppressor negatively regulates mTOR signaling. Cancer Cell *6*, 91-99.

Shaw, R.J., Kosmatka, M., Bardeesy, N., Hurley, R.L., Witters, L.A., DePinho, R.A., and Cantley, L.C. (2004b). The tumor suppressor LKB1 kinase directly activates AMP-activated kinase and regulates apoptosis in response to energy stress. Proc Natl Acad Sci U S A *101*, 3329-3335.

Shu, W., Jiang, Y.Q., Lu, M.M., and Morrisey, E.E. (2002). Wnt7b regulates mesenchymal proliferation and vascular development in the lung. Development *129*, 4831-4842.

Sisson, J.C., Ho, K.S., Suyama, K., and Scott, M.P. (1997). Costal2, a novel kinesin-related protein in the Hedgehog signaling pathway. Cell *90*, 235-245.

Sjöblom, T., Jones, S., Wood, L.D., Parsons, D.W., Lin, J., Barber, T.D., Mandelker, D., Leary, R.J., Ptak, J., Silliman, N.*, et al.* (2006). The consensus coding sequences of human breast and colorectal cancers. Science *314*, 268-274.

St-Jacques, B., Dassule, H.R., Karavanova, I., Botchkarev, V.A., Li, J., Danielian, P.S., McMahon, J.A., Lewis, P.M., Paus, R., and McMahon, A.P. (1998). Sonic hedgehog signaling is essential for hair development. Curr Biol *8*, 1058-1068.

St-Jacques, B., Hammerschmidt, M., and McMahon, A.P. (1999). Indian hedgehog signaling regulates proliferation and differentiation of chondrocytes and is essential for bone formation. Genes Dev *13*, 2072-2086.

Stark, K., Vainio, S., Vassileva, G., and McMahon, A.P. (1994). Epithelial transformation of metanephric mesenchyme in the developing kidney regulated by Wnt-4. Nature *372*, 679-683.

Strigini, M., and Cohen, S.M. (1997). A Hedgehog activity gradient contributes to AP axial patterning of the Drosophila wing. Development *124*, 4697-4705.

Sui, G., Soohoo, C., Affar, e.B., Gay, F., Shi, Y., and Forrester, W.C. (2002). A DNA vector-based RNAi technology to suppress gene expression in mammalian cells. Proc Natl Acad Sci U S A *99*, 5515-5520.

Svärd, J., Heby-Henricson, K., Henricson, K.H., Persson-Lek, M., Rozell, B., Lauth, M., Bergström, A., Ericson, J., Toftgård, R., and Teglund, S. (2006). Genetic elimination of Suppressor of fused reveals an essential repressor function in the mammalian Hedgehog signaling pathway. Dev Cell *10*, 187-197.

Taipale, J., Chen, J.K., Cooper, M.K., Wang, B., Mann, R.K., Milenkovic, L., Scott, M.P., and Beachy, P.A. (2000). Effects of oncogenic mutations in Smoothened and Patched can be reversed by cyclopamine. Nature *406*, 1005-1009.

Taipale, J., Cooper, M.K., Maiti, T., and Beachy, P.A. (2002). Patched acts catalytically to suppress the activity of Smoothened. Nature *418*, 892-897.

Takada, R., Satomi, Y., Kurata, T., Ueno, N., Norioka, S., Kondoh, H., Takao, T., and Takada, S. (2006). Monounsaturated fatty acid modification of Wnt protein: its role in Wnt secretion. Dev Cell *11*, 791-801.

Tang, W., Dodge, M., Gundapaneni, D., Michnoff, C., Roth, M., and Lum, L. (2008). A genome-wide RNAi screen for Wnt/beta-catenin pathway components identifies unexpected roles for TCF transcription factors in cancer. Proc Natl Acad Sci U S A *105*, 9697-9702.

Tate, G., Satoh, H., Endo, Y., and Mitsuya, T. (2000). Assignment of desert hedgehog (DHH) to human chromosome bands 12q12-->q13.1 by in situ hybridization. Cytogenet Cell Genet *88*, 93-94.

Tenzen, T., Allen, B.L., Cole, F., Kang, J.S., Krauss, R.S., and McMahon, A.P. (2006). The cell surface membrane proteins Cdo and Boc are components and targets of the Hedgehog signaling pathway and feedback network in mice. Dev Cell *10*, 647-656.

Theodosiou, N.A., Zhang, S., Wang, W.Y., and Xu, T. (1998). slimb coordinates wg and dpp expression in the dorsal-ventral and anterior-posterior axes during limb development. Development *125*, 3411-3416.

Tran, P.V., Haycraft, C.J., Besschetnova, T.Y., Turbe-Doan, A., Stottmann, R.W., Herron, B.J., Chesebro, A.L., Qiu, H., Scherz, P.J., Shah, J.V.*, et al.* (2008). THM1 negatively modulates mouse sonic hedgehog signal transduction and affects retrograde intraflagellar transport in cilia. Nat Genet *40*, 403-410.

Uematsu, K., He, B., You, L., Xu, Z., McCormick, F., and Jablons, D.M. (2003). Activation of the Wnt pathway in non small cell lung cancer: evidence of dishevelled overexpression. Oncogene *22*, 7218-7221.

van Amerongen, R., and Berns, A. (2006). Knockout mouse models to study Wnt signal transduction. Trends Genet *22*, 678-689.

van Amerongen, R., and Nusse, R. (2009). Towards an integrated view of Wnt signaling in development. Development *136*, 3205-3214.

van Blitterswijk, W.J., and Houssa, B. (2000). Properties and functions of diacylglycerol kinases. Cell Signal *12*, 595-605.

van de Wetering, M., Cavallo, R., Dooijes, D., van Beest, M., van Es, J., Loureiro, J., Ypma, A., Hursh, D., Jones, T., Bejsovec, A.*, et al.* (1997). Armadillo coactivates transcription driven by the product of the Drosophila segment polarity gene dTCF. Cell *88*, 789-799.

van den Brink, G.R., Bleuming, S.A., Hardwick, J.C., Schepman, B.L., Offerhaus, G.J., Keller, J.J., Nielsen, C., Gaffield, W., van Deventer, S.J., Roberts, D.J.*, et al.* (2004). Indian Hedgehog is an antagonist of Wnt signaling in colonic epithelial cell differentiation. Nat Genet *36*, 277-282.

Varjosalo, M., Björklund, M., Cheng, F., Syvänen, H., Kivioja, T., Kilpinen, S., Sun, Z., Kallioniemi, O., Stunnenberg, H.G., He, W.W., *et al.* (2008). Application of active and kinase-deficient kinome collection for identification of kinases regulating hedgehog signaling. Cell *133*, 537-548.

Varjosalo, M., Li, S.P., and Taipale, J. (2006). Divergence of hedgehog signal transduction mechanism between Drosophila and mammals. Dev Cell *10*, 177-186.
Varjosalo, M., and Taipale, J. (2008). Hedgehog: functions and mechanisms. Genes Dev *22*, 2454-2472.

Von Hoff, D.D., LoRusso, P.M., Rudin, C.M., Reddy, J.C., Yauch, R.L., Tibes, R., Weiss, G.J., Borad, M.J., Hann, C.L., Brahmer, J.R., *et al.* (2009). Inhibition of the hedgehog pathway in advanced basal-cell carcinoma. N Engl J Med *361*, 1164-1172.

Wallingford, J.B., and Habas, R. (2005). The developmental biology of Dishevelled: an enigmatic protein governing cell fate and cell polarity. Development *132*, 4421-4436.

Waltzer, L., and Bienz, M. (1998). Drosophila CBP represses the transcription factor TCF to antagonize Wingless signalling. Nature *395*, 521-525.

Wang, G., Amanai, K., Wang, B., and Jiang, J. (2000). Interactions with Costal2 and suppressor of fused regulate nuclear translocation and activity of cubitus interruptus. Genes Dev *14*, 2893-2905.

Weeraratna, A.T., Becker, D., Carr, K.M., Duray, P.H., Rosenblatt, K.P., Yang, S., Chen, Y., Bittner, M., Strausberg, R.L., Riggins, G.J., *et al.* (2004). Generation and analysis of melanoma SAGE libraries: SAGE advice on the melanoma transcriptome. Oncogene *23*, 2264-2274.

Wehrli, M., Dougan, S.T., Caldwell, K., O'Keefe, L., Schwartz, S., Vaizel-Ohayon, D., Schejter, E., Tomlinson, A., and DiNardo, S. (2000). arrow encodes an LDL-receptor-related protein essential for Wingless signalling. Nature *407*, 527-530.

Wen, X., Lai, C.K., Evangelista, M., Hongo, J.A., de Sauvage, F.J., and Scales, S.J. (2010). Kinetics of hedgehog-dependent full-length Gli3 accumulation in primary cilia and subsequent degradation. Mol Cell Biol *30*, 1910-1922.

Wijgerde, M., McMahon, J.A., Rule, M., and McMahon, A.P. (2002). A direct requirement for Hedgehog signaling for normal specification of all ventral progenitor domains in the presumptive mammalian spinal cord. Genes Dev *16*, 2849-2864.

Willert, K., Brown, J.D., Danenberg, E., Duncan, A.W., Weissman, I.L., Reya, T., Yates, J.R., and Nusse, R. (2003). Wnt proteins are lipid-modified and can act as stem cell growth factors. Nature *423*, 448-452.

Wingo, S.N., Gallardo, T.D., Akbay, E.A., Liang, M.C., Contreras, C.M., Boren, T., Shimamura, T., Miller, D.S., Sharpless, N.E., Bardeesy, N.*, et al.* (2009). Somatic LKB1 mutations promote cervical cancer progression. PLoS One *4*, e5137.

Wolff, C., Roy, S., and Ingham, P.W. (2003). Multiple muscle cell identities induced by distinct levels and timing of hedgehog activity in the zebrafish embryo. Curr Biol *13*, 1169-1181.

Wu, S., Ying, G., Wu, Q., and Capecchi, M.R. (2007). Toward simpler and faster genome-wide mutagenesis in mice. Nat Genet *39*, 922-930.

Yamada, T., Placzek, M., Tanaka, H., Dodd, J., and Jessell, T.M. (1991). Control of cell pattern in the developing nervous system: polarizing activity of the floor plate and notochord. Cell *64*, 635-647.

Yanagawa, S., Matsuda, Y., Lee, J.S., Matsubayashi, H., Sese, S., Kadowaki, T., and Ishimoto, A. (2002). Casein kinase I phosphorylates the Armadillo protein and induces its degradation in Drosophila. EMBO J *21*, 1733-1742.

Yang, D., Buchholz, F., Huang, Z., Goga, A., Chen, C.Y., Brodsky, F.M., and Bishop, J.M. (2002). Short RNA duplexes produced by hydrolysis with Escherichia coli RNase III mediate effective RNA interference in mammalian cells. Proc Natl Acad Sci U S A *99*, 9942-9947.

Yang, Y., Topol, L., Lee, H., and Wu, J. (2003). Wnt5a and Wnt5b exhibit distinct activities in coordinating chondrocyte proliferation and differentiation. Development *130*, 1003-1015.

Yao, S., Lum, L., and Beachy, P. (2006). The ihog cell-surface proteins bind Hedgehog and mediate pathway activation. Cell *125*, 343-357.

Zamore, P.D., Tuschl, T., Sharp, P.A., and Bartel, D.P. (2000). RNAi: double-stranded RNA directs the ATP-dependent cleavage of mRNA at 21 to 23 nucleotide intervals. Cell *101*, 25-33.

Zeng, X., Huang, H., Tamai, K., Zhang, X., Harada, Y., Yokota, C., Almeida, K., Wang, J., Doble, B., Woodgett, J.*, et al.* (2008). Initiation of Wnt signaling: control of Wnt coreceptor Lrp6 phosphorylation/activation via frizzled, dishevelled and axin functions. Development *135*, 367-375.

Zeng, X., Tamai, K., Doble, B., Li, S., Huang, H., Habas, R., Okamura, H., Woodgett, J., and He, X. (2005). A dual-kinase mechanism for Wnt co-receptor phosphorylation and activation. Nature *438*, 873-877.

Zhang, C., Williams, E.H., Guo, Y., Lum, L., and Beachy, P.A. (2004). Extensive phosphorylation of Smoothened in Hedgehog pathway activation. Proc Natl Acad Sci U S A *101*, 17900-17907.

Zhang, J., Bobulescu, I.A., Goyal, S., Aronson, P.S., Baum, M.G., and Moe, O.W. (2007). Characterization of Na+/H+ exchanger NHE8 in cultured renal epithelial cells. Am J Physiol Renal Physiol *293*, F761-766.

Zhang, J.H., Chung, T.D., and Oldenburg, K.R. (1999). A Simple Statistical Parameter for Use in Evaluation and Validation of High Throughput Screening Assays. J Biomol Screen *4*, 67-73.

Zhang, W., Zhao, Y., Tong, C., Wang, G., Wang, B., Jia, J., and Jiang, J. (2005). Hedgehog-regulated Costal2-kinase complexes control phosphorylation and proteolytic processing of Cubitus interruptus. Dev Cell *8*, 267-278.

Zhang, X.D. (2007). A pair of new statistical parameters for quality control in RNA interference high-throughput screening assays. Genomics *89*, 552-561.

Zhao, Y., Tong, C., and Jiang, J. (2007). Hedgehog regulates smoothened activity by inducing a conformational switch. Nature *450*, 252-258.

Zhao, Y., Yang, Z.Q., Wang, Y., Miao, Y., Liu, Y., Dai, S.D., Han, Y., and Wang, E.H. (2010). Dishevelled-1 and dishevelled-3 affect cell invasion mainly through canonical and noncanonical Wnt pathway, respectively, and associate with poor prognosis in nonsmall cell lung cancer. Mol Carcinog *49*, 760-770.